

# UC San Diego

## UC San Diego Previously Published Works

### Title

Energy geostructures: A review of analysis approaches, in situ testing and model scale experiments

### Permalink

<https://escholarship.org/uc/item/60q7n0h5>

### Authors

Loveridge, Fleur  
McCartney, John S  
Narsilio, Guillermo A  
[et al.](#)

### Publication Date

2020-05-01

### DOI

10.1016/j.gete.2019.100173

Peer reviewed

## Manuscript Details

<b>Manuscript number</b>	GETE_2018_43_R1
<b>Title</b>	Energy geostructures: a review of analysis approaches, in situ testing and model scale experiments
<b>Article type</b>	Research Paper

### Abstract

This position paper was developed by members of the task force on “Energy Geostructures” of the International Society of Soil Mechanics and Geotechnical Engineering (ISSMGE) Technical Committee TC308 on ‘Energy Geotechnics’. The article includes a summary and review of some of the most recent analysis approaches, in situ testing, full scale testing and model scale experiments with a focus on energy piles and other energy geostructures. The geotechnics literature in these topics has increased rapidly in the last five years suggesting a surge in this emerging research area. Here complementary lines of research can be distinguished, one focusing on thermal analysis and another focusing on thermo-geomechanical analysis. Limitations, shortcomings and knowledge gaps are identified and needs for further research and development within the geotechnical community are highlighted.

<b>Keywords</b>	geothermal, ground source heat pumps, ground heat exchangers, energy piles, review, state of the art
<b>Corresponding Author</b>	Marcelo Sanchez
<b>Corresponding Author's Institution</b>	Texas A&M University - College Station
<b>Order of Authors</b>	Fleur Loveridge, John McCartney, Guillermo Narsilio, Marcelo Sanchez
<b>Suggested reviewers</b>	Laloui Lyesse, abdelmalek bouazza

## Submission Files Included in this PDF

### File Name [File Type]

cover letter.doc [Cover Letter]

Comments from the guest editor.docx [Response to Reviewers]

highlights.pdf [Highlights]

2019-05-31 - TC308 - Energy Geostructures Position Paper - Rev.docx [Manuscript File]

declaration-of-competing-interests.docx [Conflict of Interest]

Author questionnaire.pdf [Author Agreement]

To view all the submission files, including those not included in the PDF, click on the manuscript title on your EVISE Homepage, then click 'Download zip file'.

## Research Data Related to this Submission

There are no linked research data sets for this submission. The following reason is given:  
No data was used for the research described in the article

1  
2  
3  
4  
5  
6  
7  
8  
9  
10  
11  
12  
13  
14  
15  
16  
17  
18  
19  
20  
21  
22  
23  
24  
25  
26  
27  
28  
29  
30

**Title:**

**Energy geostructures: a review of analysis approaches, in situ testing and model scale experiments**

**AUTHORS:**

**Fleur Loveridge<sup>1</sup>, John S. McCartney<sup>2</sup>, Guillermo A. Narsilio<sup>3</sup>, Marcelo Sanchez<sup>4</sup>**

**AFFILIATION:**

<sup>1</sup>**Fleur Loveridge**, Ph.D., CEng MICE, FGS CGeol, University Academic Fellow. University of Leeds, UK

<sup>2</sup>**John S. McCartney**, Ph.D., P.E., F.ASCE, Professor and Chair, Department of Structural Engineering, University of California San Diego. USA.

<sup>3</sup>**Guillermo A. Narsilio** Ph.D., Associate Professor, Melbourne School of Engineering, The University of Melbourne, Australia.

<sup>4</sup>**Marcelo Sanchez**, Ph.D., Professor, Zachry Department of Civil Engineering, Texas A&M University, College Station, USA

**Corresponding Author:**

Marcelo Sanchez, Ph.D.  
Professor  
Zachry Department of Civil Engineering  
Texas A&M University  
201 Dwight Look Engineering Building  
College Station, TX 77843-3136  
Phone: 979-862-6604  
<https://ceprofs.civil.tamu.edu/msanchez/>

31 **Abstract**

32 This position paper was developed by members of the task force on “Energy Geostructures” of the  
33 International Society of Soil Mechanics and Geotechnical Engineering (ISSMGE) Technical Committee  
34 TC308 on ‘Energy Geotechnics’. The article includes a summary and review of some of the most recent  
35 analysis approaches, in situ testing, full scale testing and model scale experiments with a focus on  
36 energy piles and other energy geostructures. The geotechnics literature in these topics has increased  
37 rapidly in the last five years suggesting a surge in this emerging research area. Here complementary  
38 lines of research can be distinguished, one focusing on thermal analysis and another focusing on  
39 thermo-geomechanical analysis. Limitations, shortcomings and knowledge gaps are identified and  
40 needs for further research and development within the geotechnical community are highlighted.

41 **Keywords:** geothermal, ground source heat pumps, ground heat exchangers, energy piles, review,  
42 state of the art

43

44 **Table of Contents**

45 April 4, 2019 ..... 1  
46 Title:..... 1  
47 1 Introduction..... 4  
48 2 Analysis of Energy Geostructures ..... 5  
49 2.1 Thermal Analysis..... 5  
50 2.1.1 Overview ..... 5  
51 2.1.1.1 Thermal Loads..... 5  
52 2.1.1.2 Temperature Limits..... 6  
53 2.1.1.3 Mechanical Design ..... 6  
54 2.1.2 Piles..... 6  
55 2.1.2.1 Classical G-functions ..... 7  
56 2.1.2.2 Pile Specific G-functions..... 9  
57 2.1.2.3 Thermal Resistances ..... 11  
58 2.1.2.4 Transient Pile Models ..... 12  
59 2.1.2.5 Numerical Simulations ..... 12  
60 2.1.2.6 Hybrid Models ..... 14  
61 2.1.2.7 Pipe Arrangements and Pile Geometry ..... 15  
62 2.1.3 Energy Walls ..... 16  
63 2.1.3.1 Overview ..... 16  
64 2.1.3.2 The Excavation Space..... 16  
65 2.1.3.3 Numerical Simulations ..... 17  
66 2.1.3.4 Analytical Methods ..... 17  
67 2.1.3.5 Pipe Arrangements ..... 18  
68 2.1.4 Energy Tunnels..... 19  
69 2.1.4.1 Overview ..... 19  
70 2.1.4.2 The Tunnel Space ..... 20  
71 2.1.4.3 Analytical Methods ..... 21  
72 2.1.4.4 Pipe Arrangements ..... 21  
73 2.1.5 Other Geotechnical Structures ..... 22  
74 2.2 Geomechanical and Structural Analysis..... 23  
75 2.2.1 Overview ..... 23

76	2.2.2	Piles.....	23
77	2.2.3	Other Energy Geostructures.....	26
78	3	Full Scale Field Scale Testing.....	26
79	3.1	Pile Thermal Tests.....	26
80	3.1.1	Thermal Performance Tests.....	26
81	3.1.1.1	Short Term Tests.....	27
82	3.1.1.2	Long Term Tests and Operation.....	29
83	3.1.2	Thermal Response Tests.....	30
84	3.1.2.1	Case Studies.....	31
85	3.1.2.2	Recommendations.....	33
86	3.2	Pile Geomechanical Tests.....	33
87	3.2.1	Single Piles.....	33
88	3.2.2	Pile Groups.....	34
89	3.3	Energy Walls.....	34
90	3.4	Energy Tunnels.....	38
91	3.4.1	Geomechanical Aspects.....	<b>Error! Bookmark not defined.</b>
92	3.4.2	Thermal Aspects.....	<b>Error! Bookmark not defined.</b>
93	3.5	Other Energy Geostructures.....	43
94	4	Model Scale Testing.....	43
95	4.1	Model Test on Piles.....	44
96	4.1.1	Laboratory Scale Tests (1-g).....	44
97	4.1.1.1	Overview.....	44
98	4.1.1.2	Evaluation of Heat Transfer in Laboratory-scale Tests.....	44
99	4.1.1.3	Evaluation of Soil-structure Interaction in Laboratory-scale Tests.....	45
100	4.1.2	Centrifuge Tests on Energy Piles (N-g).....	47
101	4.1.2.1	Overview.....	47
102	4.1.2.2	Evaluation of Heat Transfer and Water Flow in Centrifuge-scale Tests.....	48
103	4.1.2.3	Evaluation of Soil-Structure Interaction in Centrifuge-Scale Tests.....	50
104	4.2	Model Scale Tests on Other Energy Geostructures.....	52
105	5	Discussion.....	53
106	6	Summary.....	54
107		References.....	55
108			

## 110 **1 Introduction**

111 There is an inexorable increase in global energy demand driven by world population growth and the  
112 global pursuit of a higher 'quality' of life. As a result, the annual per capita energy consumption has  
113 grown exponentially for a century (Glassley 2010). This growing demand may be satisfied by increasing  
114 energy supply, for example by finding new ways to exploit oil and gas reservoirs that were previously  
115 deemed uneconomical to exploit. However, the long term and more sustainable solution relies on  
116 both reducing global energy demand and the use of fossil fuels and increasing the use of energy from  
117 renewable sources. Geo-professionals can contribute to the development of a number of different  
118 renewable energy sources with low greenhouse gas emissions (Arulrajah et al. 2015, McCartney et al.  
119 2016, Sanchez et al. 2017).

120 Shallow geothermal energy or ground source heat pump (GSHP) technology can contribute to  
121 lowering or flattening peak energy demand through efficient heating and cooling of residential,  
122 commercial and industrial buildings (Brandl 2006; Olgun and McCartney 2014; Sanchez et al. 2017). A  
123 GSHP system is inherently more efficient than alternative Heating Ventilation and Air Conditioning  
124 (HVAC) systems as it exchanges heat with a more stable source/sink: the ground temperature in the  
125 upper tens of meters is typically close to the mean atmospheric temperature for a given location year-  
126 round. Energy geostructures are foundations or other buried geotechnical structures which have been  
127 equipped with heat transfer pipes so that they may act as the ground heat exchanger (GHE) part of a  
128 GSHP system. Therefore, energy geostructures remove the need for construction of special purpose  
129 GHEs, offering opportunities to reduce capital costs for shallow geothermal energy (CIBSE, 2013; Park  
130 et al. 2015; Lu and Narsilio 2019; Akrouch et al. 2018).

131 Piles are the most common type of energy geostructure, having been first constructed in northern  
132 Europe in the 1980's (Brandl 2006). Their application has expanded in the subsequent decades (e.g.  
133 Amis & Loveridge, 2014), but their numbers are still minor compared to the total GSHP installations  
134 worldwide. Demonstration projects using slabs, walls and tunnels as ground heat exchangers soon  
135 followed the first pile installations (Adam & Markiewicz 2009). However, these types of energy  
136 geostructures are rarer, for several reasons. First, piles clearly have the potential to offer reduced  
137 capital costs compared to traditional vertical GHEs (CIBSE, 2013) such as boreholes. Second, as piles  
138 have a superficial resemblance to boreholes, there are available thermal design methods which can  
139 be adapted for use with piles (e.g., Eskilson 1987; Pahud 2007). There remain limitations of such  
140 approaches (Loveridge & Powrie 2013a), but they are readily available. Additional approaches for the  
141 geotechnical design of piles subject to thermal changes are under development (e.g. Mimouni & Laloui  
142 2015; Rotta Loria & Laloui 2016a). By contrast, for other structures there are no standard design and  
143 analysis approaches and every project must proceed very much on a case by case basis. The  
144 development of infrastructure schemes for shallow geothermal utilisation also comes with additional  
145 challenges regarding users for the stored thermal energy. While piled foundations are typically  
146 constructed to support a building which is then well placed to use the renewable heating/cooling  
147 provided, for retaining walls and tunnels the user of the thermal energy may be a third party which  
148 places additional logistical and bureaucratic barriers in place for adoption of the technology.

149 The application of energy geostructures has been summarised in Laloui & Di Donna (2013) and Soga  
150 & Rui (2016). However, research in this area has both intensified and broadened in recent years. Work  
151 has focused on two main areas. First, the geomechanical implications of using bearing structures also  
152 for heat exchange and storage (e.g., Bourne-Webb et al. 2009, Stewart & McCartney 2012). Second,

153 the development of thermal analysis approaches to assess energy performance and understand how  
154 to maximise energy efficiency (e.g. Loveridge & Powrie 2013b, Bidarmaghz et al. 2016a, 2016b,  
155 Mikhaylova et al. 2016a). Both these areas have the aim of minimising uncertainty and risk in design,  
156 facilitating reduction in capital costs and hence an increase in technology uptake.

157 This paper reviews recent research on energy geostructures in both these areas, covering analysis  
158 approaches and the field and model scale testing that have been used to inform those approaches.  
159 The topic of material parameters for energy geostructures is excluded since this is well reviewed by  
160 Vieira et al. (2017). This paper will be naturally biased towards piles since these are the most common  
161 installation and the area which has seen most research in recent years. However, energy walls in  
162 particular have seen a recent increase in interest and this is reflected in our review. The text is  
163 arranged into three main sections covering analysis and design methods (Section 2), full-scale field  
164 testing (Section 3) and model scale testing (Section 4). These will be followed by a discussion  
165 pertaining to knowledge gaps and a summary of the current state of the practice. The scope of the  
166 paper will focus mainly on the in-ground elements, where there is novelty and hence uncertainty due  
167 to the more recent adoption of energy geostructures. However, the importance of the mechanical  
168 engineering elements must not be underestimated, and some brief comments are made on these  
169 aspects in Section 2.1.

## 170 **2 Analysis of Energy Geostructures**

### 171 **2.1 Thermal Analysis**

#### 172 2.1.1 Overview

173 The thermal design of energy geostructures involves the use of analyses to estimate the amount of  
174 energy that can be readily exchanged with or stored within the ground to fully or partially satisfy the  
175 thermal energy loads of buildings. This includes consideration of the best arrangement of heat transfer  
176 pipes for energy efficiency, determining the relationship between energy exchanged and temperature  
177 changes, and selecting the heat pump and appropriately linking the source side of the energy system  
178 (the ground) to the delivery system in the building. This review focuses on the first two elements, but  
179 brief consideration of the building and mechanical engineering aspects is given below.

##### 180 2.1.1.1 *Thermal Loads*

181 The nature of the thermal loads applied to a ground source heat pump system has a large impact on  
182 its performance (CIBSE, 2013). For example, a system which is dominated by one-way heat transfer  
183 due to heat extraction will show decreasing performance over time as the ground (source side)  
184 temperature is reduced by that heat extraction. A system that is balanced between heat injection and  
185 heat extraction, on the other hand, will act as an inter-seasonal store of heat and will always operate  
186 at greater efficiency. Additionally, thermal loads that are “peaky”, displaying rapid changes in  
187 magnitude, may be most efficiently covered with a combination of a GSHP for the base thermal load  
188 and an auxiliary system for the balance.

189 Ground heat exchanger (GHE) and energy geostructure design is therefore dependent on provision of  
190 these thermal loads from the mechanical engineering team. The level of detail provided can be  
191 important and requirements will depend on the size and complexity of the heat pump scheme (GSHPA,  
192 2012). Unfortunately, reliable prediction of the heating and cooling demands of buildings is extremely

193 difficult and current approaches often lead to an underestimate of demand, leaving a so called “energy  
194 gap” (e.g. Menezes et al. 2012). To mitigate against this effect, designers can assess the risk of  
195 underestimation of thermal loads and either include a factor of safety approach to thermal loads or  
196 alternatively adopt installation and use of back up auxiliary heating and cooling systems (Garber et al.  
197 2013b; Mikhaylova et al. 2016b).

#### 198 2.1.1.2 Temperature Limits

199 It is important to ensure that the GSHP and the energy geostructures operate within acceptable  
200 temperature limits. This serves to both, protect the structure from extreme temperature changes  
201 which could impact on the geotechnical performance, and ensure that the heat pump is operating  
202 within an optimal efficiency range. While the upper bound temperature depends on the particular  
203 GSHP specifications (typically 30-40°C) and designer’s choice, the lower bound temperature is  
204 generally taken as 0°C to 2°C to avoid ground freezing (GSHPA 2002), although lower fluid  
205 temperatures can potentially be tolerated (Loveridge et al. 2012).

#### 206 2.1.1.3 Mechanical Design

207 The mechanical design aspects of a GSHP scheme are of equal importance to the GHE design.  
208 Optimisation of the heat pump and minimisation of the temperature lift are essential factors, as is the  
209 pipework and pumping design. GSHP systems are complex, extending from the ground to the heating  
210 and cooling delivery systems, via the ground heat exchangers, headers and manifolds, circulation  
211 pumps and heat pumps. All aspects need to be properly designed and executed for a system to  
212 perform well. Detailed discussion of these elements can be found in, for example, Oschner (2008).

213 Some integrated building simulation software packages allow analyses of all components of a GSHP  
214 system from the in-ground components to the delivery of heating and cooling, e.g. EnergyPlus (Fisher  
215 et al. 2006) or TRNSYS (2018). These and other applications are reviewed in Do & Haberl (2010) and  
216 are typically aimed at borehole heat exchanger design, but a standalone implementation in TRNSYS  
217 for application to energy piles is available (Pahud 2007).

#### 218 2.1.2 Piles

219 Typically, analytical solutions are used to determine the fluid temperature changes for a given thermal  
220 demand. This allows the available energy within certain temperature limits to be determined.  
221 Analytical solutions are preferable to numerical solutions since fast run times are required to process  
222 decade’s worth of thermal load input data which may vary on an hourly basis. However, closed form  
223 solutions are sometimes associated with assumptions that limit their range of application.  
224 Furthermore, some numerical tools have been implemented with sufficient computational efficiency  
225 that provide reasonable alternatives (e.g. see Section 2.1.2.6).

226 To simplify the thermal problem most analysis approaches separate the temperature change into a  
227 number of zones for which different solutions are applied, with the results then combined by  
228 superposition. Thus, the change in circulating fluid temperature,  $T_f$ , can be given by:

$$229 \Delta T_f = \Delta T_{ground} + \Delta T_{pile} + \Delta T_{pipe} \quad (1)$$

230 When analytical techniques are adopted the ground temperature change is often calculated using a  
231 transient temperature response function (G-function or  $G_g$ ) evaluated at a radial coordinate  $r=r_b$ ,  
232 where  $r_b$  is the pile radius.



233 
$$\Delta T_{ground} = \frac{q}{2\pi\lambda_g} G_g(t,r) \quad (2)$$

234 where  $\lambda_g$  is the thermal conductivity of the ground in W/(mK),  $q$  is the applied thermal power in W/m  
 235 and  $t$  is the elapsed time in seconds. The G-function can take a number of different forms (Section  
 236 2.1.2.1) as summarised in Table 1.

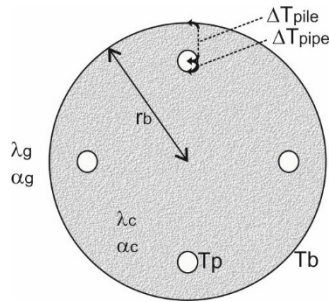
237 Traditionally  $\Delta T_{pile}$  and  $\Delta T_{pipe}$  are calculated using thermal resistances and assuming a thermal steady  
 238 state:

239 
$$\Delta T_{pile} = T_p - T_b = qR_c \quad (3)$$

240 
$$\Delta T_{pipe} = T_f - T_p = qR_p \quad (4)$$

241 where  $R$  is a lumped thermal resistance (Section 2.1.2.3) in mK/W and  $T_b$  and  $T_p$  are the average  
 242 temperatures at the pile edge and pipe edge respectively (see Figure 1).  $R_c$  is the resistance associated  
 243 with the temperature changes within the pile concrete and  $R_p$  is that associated with the pipes and  
 244 the fluid flowing within them. The latter may be further split into the conductive resistance associated  
 245 with the pipe itself and the convective resistance associated with the fluid,  $R_{p-cond}$  and  $R_{p-conv}$   
 246 respectively. Together the individual resistances make up the total resistance,  $R_b$ :

247 
$$R_b = R_c + R_{p-cond} + R_{p-conv} \quad (5)$$



248

249

**Figure 1 Typical arrangement of an energy pile**

250

251 **2.1.2.1 Classical G-functions**

252 The term G-function was originally used to describe the temperature response functions developed  
 253 for borehole heat exchangers by Eskilson (1987) using the Superposition Borehole Model (SBM), see  
 254 also Section 2.1.2.5. However, it has since been adopted more generally to describe any function  
 255 which relates the temperature change in the ground around a vertical GHE to the applied thermal  
 256 load,  $q$ . Hence the general approach is equally applicable to piles. Most typically G-functions are  
 257 expressed as a dimensionless form of Equation 2:

258 
$$\Phi = G_g(Fo, r^*) \quad (6)$$

259 where  $\Phi$  is the dimensional temperature response,  $\Phi = \frac{2\pi\lambda_g}{q} \Delta T$ ,  $Fo$  is the Fourier number or

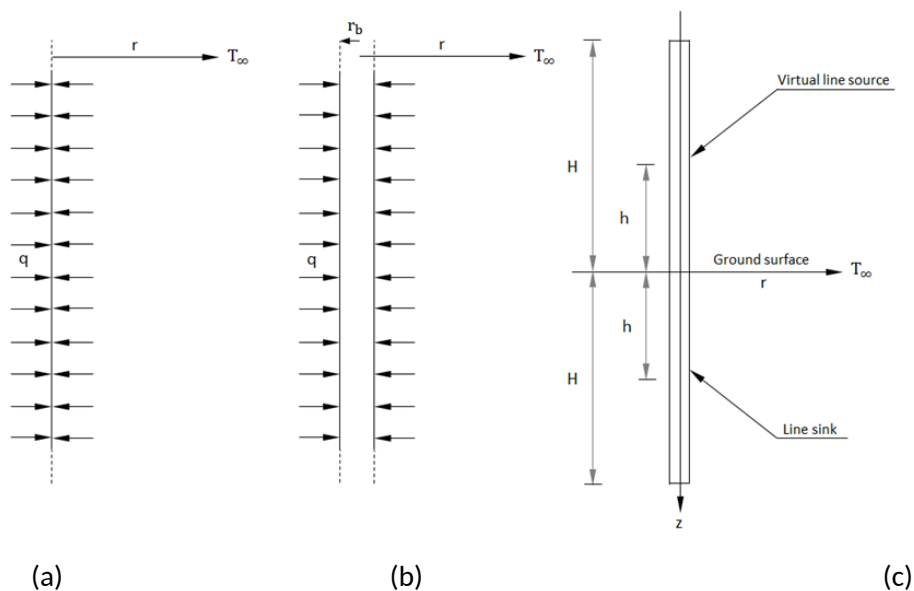
260 dimensionless time defined as  $Fo = \frac{\alpha_g t}{r_b^2}$ ,  $\alpha_g$  is the ground thermal diffusivity, and  $r_b$  the pile radius,

261 and  $r^*$  is a dimensionless geometry factor, often expressed as radial coordinate divided by heat

262 exchanger length (see Figure 1). Sometimes other non-dimensional parameter sets are used, but the  
 263 concept is the same. The classic analytical solutions of the G-functions are based on the infinite line  
 264 source (ILS), the infinite (hollow) cylindrical source, and the finite line source (FLS). These geometric  
 265 configurations used in the analytical solutions are schematically presented in Figure 2, with a summary  
 266 of these and other solutions listed in Table 1 and illustrated in Figures 3 and 4. Full details of these  
 267 solutions are not given here since they are readily available in the literature (e.g. Bourne-Webb et al.  
 268 2016a, Fadejev et al. 2017).

269 In the development of the analytical solutions, it is assumed that the ground is homogeneous and  
 270 isotropic, with no initial temperature gradient nor groundwater flow and fully saturated ground  
 271 conditions. Such factors are known to affect the temperature changes around vertical GHEs (e.g.  
 272 Signorelli et al. 2007; Bidarmaghz et al. 2016a) but are more difficult to account for by analytical  
 273 means.

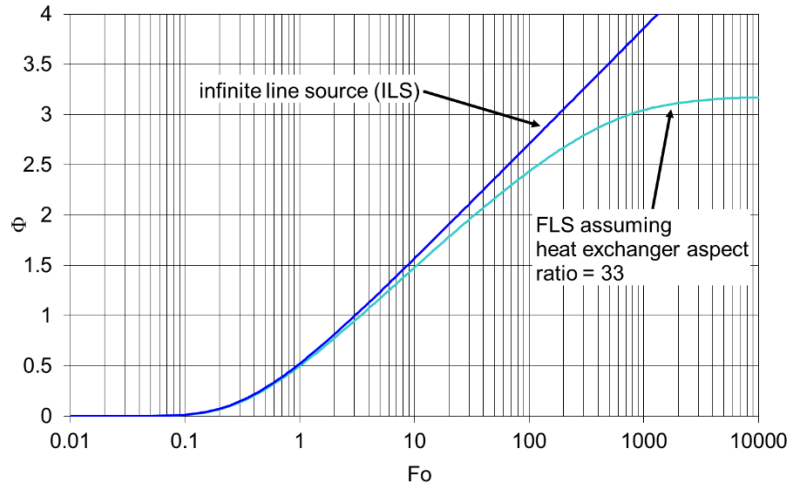
274 G-functions are normally plotted for a constant  $q$  (Figure 3 and Figure 4), but as  $q$  varies in actual  
 275 routine operation it is necessary to use some form of temporal superposition and/or load aggregation  
 276 (Claesson & Javed 2012) to determine the overall temperature change,  $\Delta T(t)$  resulting from  $q(t)$  over  
 277 the lifetime of a geo-structure.



278

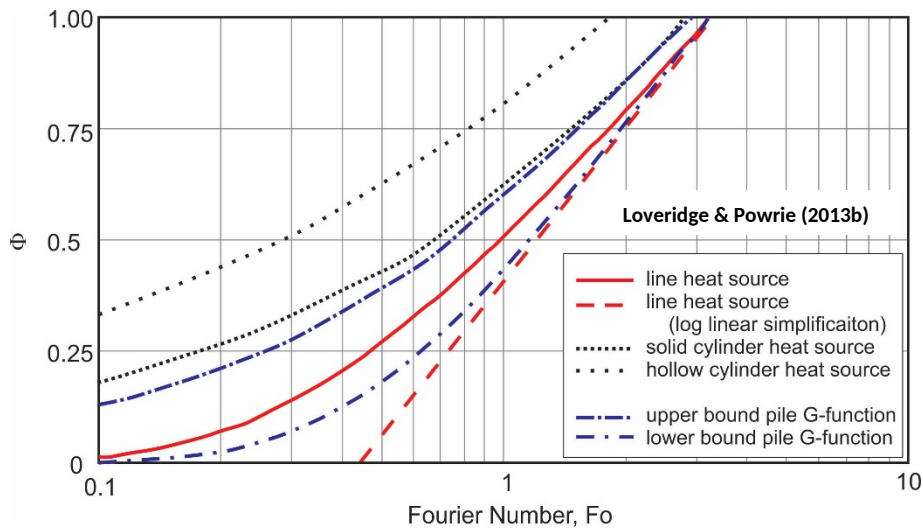
279 **Figure 2 Schematic of the classical G-function models: (a) infinite line source (ILS), (b) infinite**  
 280 **cylindrical source (ICS), (c) finite line source (FLS).  $T_\infty$ =far field temperature;  $H$ =heat exchanger**  
 281 **length;  $h$ =depth below ground surface. Adapted from Bidarmaghz 2015.**

282



283

284 **Figure 3 Example G-functions showing development of long-term steady state conditions for heat**  
 285 **exchangers of finite length. Aspect ratio = pile length / pile diameter**



286

287 **Figure 4 Different G-functions displayed at short time scales. Pile upper and lower bound G-**  
 288 **functions after Loveridge & Powrie (2013b)**

289 **2.1.2.2 Pile Specific G-functions**

290 The SBM and other FLS approaches are perhaps the most commonly adopted type of G-function, being  
 291 readily implemented in accessible borehole design software that is sometimes used for piles.  
 292 However, this type of approach is not validated for piles and may over predict temperature changes  
 293 (e.g. Wood et al. 2010a). This is due to (i) the short length of piles not being accommodated in routine  
 294 GHE software which implements these analysis methods; and (ii) the accompanying use of a steady  
 295 state resistance (see Section 2.1.2.3). However, it should be noted that such approaches remain  
 296 conservative in terms of energy assessment. This means that a design would be safe, although the  
 297 danger of over conservatism relates to increased payback times on investment.

298 The solid cylinder model has advantages for use with piles since it can capture flow of heat into the  
 299 pile as well as into the ground. Solutions have been published for both the infinite and finite heat  
 300 source scenarios (Man et al. 2010). However, this approach still requires validation, but it was

301 suggested that it may provide an upper bound for pile behaviour as shown in Figure 4 (Loveridge &  
 302 Powrie 2013b).

303 Applying a similar approach to the SBM, Loveridge & Powrie (2013b) derived upper and lower bound  
 304 G-functions based on pile geometries rather than a line source. While validated on short term thermal  
 305 response tests of small diameter piles, the approach awaits longer term validation and critical  
 306 assessment for piles with different length to diameter ratios.

307 All the finite heat source models described above are illustrated for short time periods in Figure 4. At  
 308 long time periods the temperature response will converge on that of the finite line source (Figure 3),  
 309 with the steady state value dependent on the aspect ratio. All these models also suffer some of the  
 310 same limitations which need to be appreciated. They all assume a constant surface temperature as a  
 311 boundary condition. This has two drawbacks. First, the near surface temperature distribution is not  
 312 constant, but fluctuates throughout the year. For short GHEs such as energy piles this may be  
 313 significant (e.g. Bidarmaghz et al. 2016). Second, most energy piles are buried beneath a building and  
 314 boundary conditions at the pile head may be better represented as either insulated or as a small net  
 315 flux representing heat loss from the building (Loveridge & Powrie 2013a). There are few datasets  
 316 showing pile temperatures under buildings, but initial data from Mikhaylava et al. (2016c) and Habart  
 317 et al. (2016) show fluctuations at the pile head. These temperature changes suggest some heat  
 318 exchange with the building. However, uncertainty over the most appropriate boundary conditions also  
 319 remains a barrier to further development (see also Section 3.1).

320 **Table 1 Main types of G-function for use with piles**

Model	References	Description	Comments
Infinite Line Source (ILS)	Carslaw & Jaeger (1959)	Assumes an infinitely long and thin heat source embedded in a homogeneous medium.	Infinite length means that long term steady state behaviour is neglected.
Infinite (Hollow) Cylindrical Source (ICS)	Carslaw & Jaeger (1959); Ingersol et al. (1954); Kakaç and Yener (2008); Bernier (2001)	Assumes an infinitely long hollow cylinder which acts as a heat source embedded in a homogeneous medium.	Infinite length means that long term steady state behaviour is neglected. Gives larger temperature changes than the ILS at short time periods. It is equivalent to the ILS at longer time periods.
Superposition Borehole Model (SBM)	Eskilson (1987)	Uses numerically exact calculation based on a finite line heat source, with superposition for multiple boreholes.	As calculated numerically, to be applied routinely the SBM G-functions must be pre-programmed into software codes for different combinations of multiple boreholes. This approach is widely used and well validated for borehole design (e.g. Cullin et al. 2015).
Analytical Finite Line Source (FLS)	Eskilson (1987) Zeng et al. (2002) Lamarche & Beauchamp (2007) Claesson & Javed (2011)	Using a mirrored virtual line sink approach to simulate the ground surface, these G-functions provide an analytically exact version of SBM.	Zeng et al. (2002) use the mid-depth of the heat exchanger as the reference temperature while later works use an average temperature which provides a better correlation to SBM. The more recent works concentrate on simplifying the mathematics

Model	References	Description	Comments
Solid Cylinder Model (SCM)	Man et al. (2010)	Heat flow into and out of the heat exchanger is simulated. The model has been presented in both infinite and finite forms.	Studies by Loveridge & Powrie (2013b) suggest that the SCM may provide a sensible upper bound for piles, providing the finite version of the model is used.
Pile G-Functions	Loveridge & Powrie (2013b)	Derived numerically in a similar way to SBM, these G-functions are then presented as appropriate upper and lower bound solutions to cater for the wide range of pile sizes and pipe configurations.	The functions typically fall between the SCM and the log linear simplification of the FLS (Figure 4).

321

### 322 2.1.2.3 Thermal Resistances

323 The pipe thermal resistance  $R_p$  can be readily calculated by analytical means as set out in Hellstrom  
324 (1991) and Lamarche et al. (2010). Analytical, empirical or numerically based methods can be used to  
325 calculate the resistance of the concrete part of the pile, a summary of which is given in Table 2.  
326 Claesson & Hellstrom (2011)'s multipole method for calculation of the pile resistance,  $R_c$ , has been  
327 shown to be the best solution for small diameter vertical GHEs (Lamarche et al. 2010) and is expected  
328 to also perform well with larger diameter piles. Such an approach was adopted by the SIA (2005).  
329 Additionally, numerically derived means of determining the pile resistance are proposed by Loveridge  
330 & Powrie (2014) based on the results of simulations. These correspond well to the multipole method  
331 for the two pipe cases.

332 However,  $R_c$  is a steady state parameter and a thermal steady state may not be present during  
333 operation of the pile. Except for very small diameter piles a design approach based on a steady state  
334 resistance is therefore unlikely to be a sensible assumption and would result in over prediction of the  
335 temperature changes (Loveridge & Powrie 2013b) and hence underestimation of energy availability.  
336 Consequently, transient methods are to be recommended for pile design where possible.

337 **Table 2 Methods for calculating ground heat exchanger steady state thermal resistance**

Approach	References	Description	Comments
Empirical	Paul (1996)	Shape factor approach using empirically derived values for different pipe configurations. Derived from in situ test data.	Empirical for boreholes so will not apply for larger diameter piles. Determines $R_b$
Analytical	Hellström (1991)	Direct analytical method based on line source theory. Assumes 2D heat flow.	Theoretical, therefore applicable to any geometry. Determines $R_c$
Analytical	Bennet et al. (1987); Claesson & Hellstrom (2011)	Line source method with multipole expansion correction. Assumes 2D heat flow.	Theoretical, therefore applicable to any geometry. Determines $R_c$

Analytical	Hellstrom (1991); Diao et al. (2004a)	Multipole method with correction for quasi-3D heat flow.	Theoretical, therefore applicable to any geometry. It determines $R_c$ . Not significantly different from 2D case in most scenarios.
Numerically derived	Sharqawy et al. (2009)	Empirical method based on 2D numerical simulations for boreholes	Most pile geometries will be outside range of analysis carried out to determine relationships. Determines $R_c$
Numerically derived	Loveridge & Powrie (2014)	Empirical method based on 2D numerical simulations for piles	Specific for pile geometries. Determines $R_c$

338

339 *2.1.2.4 Transient Pile Models*

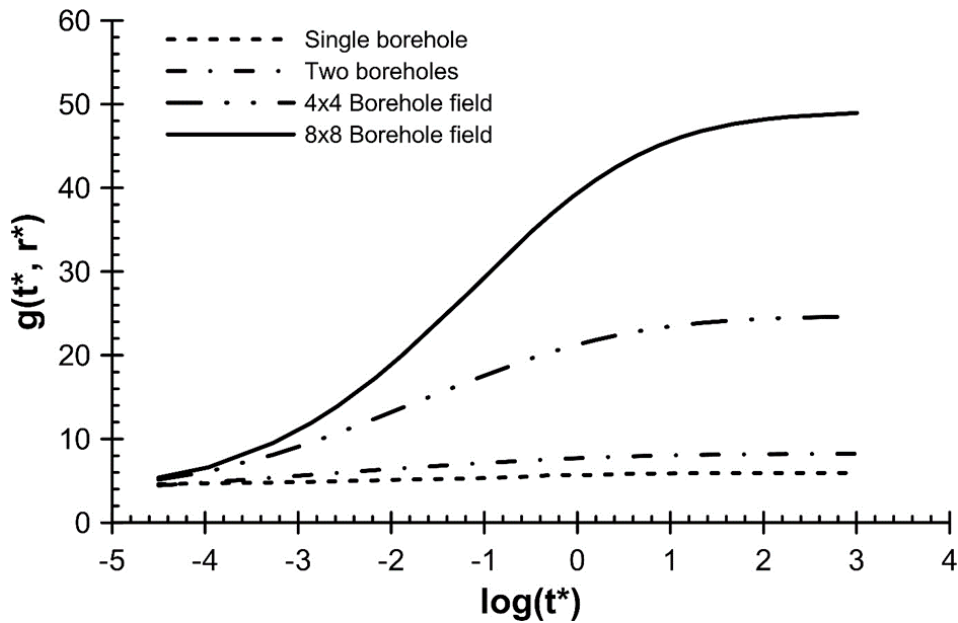
340 There are several alternatives to using a steady state pile resistance. Loveridge & Powrie (2013b)  
 341 proposed adopting temperature response functions, like G-functions, to replace the constant value of  
 342  $R_c$ . They suggested upper and lower bound functions based on a range of numerical simulations.

343 Alternative transient analysis can be carried out which considers the ground and the pile concrete in  
 344 one analysis. Li & Lai (2012) proposed composite G-functions based on superposition of several line  
 345 sources (each representing a pipe) installed in a two-material medium containing the ground and the  
 346 pile. These functions are an important step forward but would need pre-programming for a range of  
 347 likely scenarios (as is done for SBM when implemented in popular borehole software tools).

348 *2.1.2.5 Numerical Simulations*

349 Despite the fact that analytical solutions have been developed to capture the thermal performance of  
 350 GHE, most of the assumptions bring limitations. In response to these difficulties, numerical models  
 351 solving the governing heat transfer equations have surged. This includes 1D finite difference models  
 352 (e.g. Gehlin & Hellstrom 2003; Shonder & Beck 1999, 2000) and Finite Element (FE) models in 2D (e.g.  
 353 Austin, 1998; Sharqawy et al. 2009) and 3D (e.g. Bidarmaghz 2015; Ozudogru et al. 2015; Raymond et  
 354 al. 2011; Signorelli et al. 2007; Wagner et al. 2012). In the following section, selected 1D, 2D and 3D  
 355 numerical models are briefly explained, with a focus on illustrating the main approaches taken. Several  
 356 the examples have been developed for boreholes rather than piles, but the techniques used are  
 357 equally as applicable in the latter case.

358 Eskilson developed pioneering work on numerical simulation of GHEs for boreholes, which has gone  
 359 on to underpin much of current practice (Eskilson 1987; Eskilson & Claesson 1988) for both boreholes  
 360 and piles. Numerical computation on a 2D radial-axial coordinate system was used to determine the  
 361 temperature distribution around a single borehole with finite length and diameter. The mirror image  
 362 method has been used to account for the constant temperature on the ground surface, as per the  
 363 finite line source method. The temperature distribution in the ground region for a number of thermally  
 364 interacting boreholes is then obtained by superimposing the temperature response of a single  
 365 borehole in space. This is the basis of the Superposition Borehole Model (SBM) and led to the first G-  
 366 functions, examples of which are given in Figure 5. However, by neglecting the detail of the GHE, the  
 367 model is not suitable for use at short timescales.



368

369 **Figure 5 Example G-functions for different arrangements of boreholes (Bourne-Webb et al. 2016).**  
 370  **$t^*$  is the ratio of the elapsed time and time to steady state;  $r^*$  is the non-dimensional radial**  
 371 **coordinate.**

372 Based on Eskilson's  $g$ -functions, Yavuzturk et al. (1999) developed a 2D finite volume numerical model  
 373 that overcomes the short time step issues in Eskilson's model. Therefore, the thermal resistance and  
 374 capacitance effects of the heat exchanger components are considered in this model. A constant heat  
 375 flux per unit depth of the borehole was assumed for the pipe wall as the boundary condition due to  
 376 the restriction of the code used. The fluid in the pipes is not explicitly modelled. Several other 2D  
 377 models have been proposed for borehole heat exchanger fields (e.g., Muraya et al. 1996; Lazzari et al.  
 378 2010).

379 Two dimensional models have also been employed to understand pile thermal behaviour. Some of the  
 380 more notable cases include the 2D slice models of Loveridge & Powrie (2013b) and Loveridge & Powrie  
 381 (2014) who used the results of their finite element (FE) simulation to develop pile specific G-functions  
 382 and thermal resistance relationships. The models do not explicitly consider the pipes and apply a  
 383 constant heat flux at the pipe outer boundary. Similar techniques were also used by Alberdi-Pagola  
 384 et al. (2018) when interpreting thermal response tests of quadratic section energy piles.

385 Dupray et al. (2014) built a 2D model in the vertical plane to consider the potential thermal storage  
 386 available for a group of piles beneath a building. This type of simplification is unusual in GHE analysis  
 387 and reflects the adoption of plane strain for the coupled geomechanical part of the analysis. In the  
 388 model the authors used a slab of fixed temperature underlain by a low conductivity insulating layer to  
 389 represent the base of the building. The heat source was rather crudely incorporated throughout the  
 390 area of the piles within the 2D domain. However, Sailer et al. (2018a) show this 2D plane approach to  
 391 overestimate the temperature change that occurs. While this will be conservative, Sailer et al. (2018a)  
 392 go on to develop conversion factors for 2D plane analysis to improve predictions made from this  
 393 approach.

394 A transient 3D finite element model to simulate the thermal behaviour of the ground and the GHEs  
 395 was developed by Marcotte et al. (2010) and Marcotte & Pasquier (2008). The model is limited in

396 depth to the length of the GHE. The carrier fluid, the U-pipes and the grout are considered in this  
397 model, but instead of including an explicit pip bend at the base of the GHE, the pipes are simply  
398 continued to the base of the model. The fluid temperature profile is obtained after integrating the  
399 bottom horizontal face of the downward pipe, information that is then used as a boundary condition  
400 for the lower face of the upward pipe. Despite being a 3D model, axial effects related to geometry (as  
401 opposed to fluid flow) are ignored since the upper and lower boundaries are insulated. Therefore, the  
402 model is only appropriate for short timescales.

403 Bidarmaghz, Narsilio and co-workers developed a truly 3D finite element model for both boreholes  
404 and energy piles. This model explicitly considers the flow and heat transfer in the pipes embedded in  
405 the GHE. The fluid flow within the pipes is modelled either in 3D or 1D and is fully coupled to the heat  
406 diffusion in the concrete and the ground. The model has been validated against full scale experimental  
407 data covering a range of conditions and then used to investigate optimisation (Bidarmaghz 2015,  
408 Bidarmaghz et al. 2012, Bidarmaghz et al. 2016a, 2016b, Narsilio et al. 2012, Narsilio et al. 2018). Using  
409 similar techniques, Ozudogru et al. (2015) also developed a 3D numerical model for simulating vertical  
410 U-tube borehole GHEs.

411 Various authors have also applied 1D line or pipe elements to energy piles, including Choi et al. (2011),  
412 Cecinato & Loveridge (2015), Batini et al. (2015) and Caulk et al. (2016). Rees & He (2013) took an  
413 alternative approach to simplifying the pipe details within a borehole heat exchanger model. They  
414 used a single layer of cells to represent the fluid within the U-tube. The thermal properties of the  
415 material in these cells must be adjusted to make this representation appropriate.

416 Other numerical simulations have considered different physical processes in the soil surrounding  
417 energy piles and geothermal heat exchangers to evaluate coupling between heat transfer and water  
418 flow processes. For example, Wang et al. (2015a) evaluated the impact of coupled heat transfer and  
419 water flow on the behaviour of an energy pile in unsaturated silt and compared results with those  
420 from centrifuge physical modelling tests. Baser et al. (2018) evaluated the roles of enhanced vapour  
421 diffusion and phase change in the coupled heat transfer and water flow in unsaturated soils  
422 surrounding a borehole heat exchanger and found that consideration of these two variables leads to  
423 a faster heating response and larger zone of influence of the heat exchanger. Further, heating of  
424 unsaturated soil was found to lead to permanent drying that may cause changes in the transient  
425 response during cyclic heating and cooling. Specifically, the drying effect leads to a decrease in thermal  
426 conductivity and specific heat capacity of the unsaturated soil.

#### 427 2.1.2.6 Hybrid Models

428 The Duct Storage Model (DST) was developed to consider an underground thermal store constructed  
429 of many identical vertical GHE installed within a cylindrical area (Hellstrom 1989). The model  
430 superimposes three solutions: a finite difference model for the long-term heat transfer between the  
431 thermal store and the surrounding ground, a second finite difference model for the heat transfer  
432 between GHEs and the ground within the store and finally an analytical model for the steady heat  
433 transfer within the heat exchangers. Despite numerical implementation the model runs fast enough  
434 for routine application. It has been implemented in the building energy software TRNSYS for borehole  
435 applications and as a standalone application called PILESIM (Pahud 2007). PILESIM is commercially  
436 available and one of the few tools validated for use with piles. The validation is based on the Zurich  
437 Airport case study (Pahud & Hubbach 2007). However, many of the assumptions in the DST are not



438 appropriate for piles, which are typically installed on an irregular grid and may comprise different sizes  
439 and lengths. The DST also assumes a steady state resistance which has been shown to overestimate  
440 temperature changes.

441 Another technique which has proved successful is that of simulating the energy pile and the ground  
442 as a series of resistances and capacitances using an electrical analogy. This approach has been  
443 adopted by Zarrella et al. (2013) who initially developed a model for boreholes (De Carli et al. 2010,  
444 Zarrella & De Carli 2013) and then extended it to be applicable to energy piles. The pile version uses  
445 an equivalent U-tube simulation to account for a larger number of U-pipes connected in parallel. The  
446 “electrical” circuit is 3D to include axial effects and is computed numerically but is dependent on input  
447 parameters in term of values of the resistances that depend on the pile and pipe geometry. These  
448 needed to be determined separately in advance and is usually done by application of a discretised  
449 model based on the finite difference or finite element methods. A similar approach is presented for  
450 piles with four pipes, without the U-tube simplification, by Maragna & Loveridge (2019).

#### 451 2.1.2.7 Pipe Arrangements and Pile Geometry

452 Numerical simulation is a productive tool for sensitivity analysis and several authors have addressed  
453 the issues of pipe arrangements and pile geometry (e.g., Makasis et al. 2018a, 2018b). Initial studies  
454 (e.g. by Gao et al. 2008) focused on the relative efficiency of U, UU (parallel connection) or W (series  
455 connection) shaped pipes being installed within the piles. However, more recent work by Cecinato &  
456 Loveridge (2015) shows that the most important factor for maximising energy exchange in piles is to  
457 install a greater number of pipes, hence either UU or W shaped arrangements will always be  
458 preferable to a single U tube. The authors showed that following pipe numbers, the pile length was  
459 the next most influential factor, followed by the pile thermal properties. The importance of pile length  
460 is consistent with work by Batini et al. (2015), who also studied the influence of aspect ratio and other  
461 factors on thermal and mechanical performance.

462 Recently there has been significant interest in the use of helical (or “spiral coil”) pipe arrangements  
463 rather than standard vertical pipe installed as U-tubes (e.g. Park et al. 2013; Go et al. 2014; Man et al.  
464 2011). Comparative studies have shown helical pipe arrangements to potentially offer greater heat  
465 transfer rates compared to standard energy pile arrangements (Zarrella et al. 2013; Yoon et al. 2015).  
466 At least some of this advantage is due to the greater pipe lengths that can be accommodated within  
467 the pile using the spiral arrangement.

468 Contiguous flight auger (CFA) piles with short steel cages which prevent full depth installation of heat  
469 transfer pipes have also given rise to an alternative pipe layout. In these cases, to permit a full depth  
470 pipe installation U-tubes are attached to a separate steel bar and plunged centrally into the concrete  
471 following insertion of the short cage (Amis et al. 2014). However, due to the closer proximity of the  
472 pipes such central arrangements of pipes will always be less energy efficient than a standard  
473 arrangement (Loveridge & Cecinato 2016).

474 Further discussion of pile types and pipe arrangements is considered from a field data perspective in  
475 Section 3.1.1.1.

## 476 2.1.3 Energy Walls

### 477 2.1.3.1 Overview

478 The last five years has seen an increased interest in energy retaining walls. These are most typically  
479 diaphragm walls, but also include piled walls. These embedded retaining walls may be constructed to  
480 support building basements, metro stations or shallow cut and cover tunnels. Depending on the end  
481 use of the excavation space in front of the wall, their thermal behaviour may vary and consequently  
482 it is important to correctly understand the nature of this space and what boundary conditions it may  
483 impose on the energy wall. This additional boundary condition is the most important difference when  
484 considering the thermal performance of energy walls as opposed to piles which are surrounded by the  
485 ground. Consequently, some consideration is given to determining this condition before looking  
486 specifically at analytical and numerical methods applied to thermal analysis for energy walls.

### 487 2.1.3.2 The Excavation Space

488 Building basements may be subject to damped seasonal variations if they are not temperature  
489 controlled, or they could approximate constant temperature environments if they are subject to  
490 climate conditioning. On the other hand, metro stations or shallow tunnels may exhibit strong  
491 convective conditions due to the movement of trains or other vehicles, and there might be sources of  
492 heat, like train braking or passengers. When undertaking such an analysis, the excavation space  
493 therefore needs thermal characterisation. The space may be represented by one of three boundary  
494 conditions. An adiabatic condition suggests that there is no heat transfer to this space and is  
495 potentially conservative in the long term if the space is considered a positive source of energy.  
496 However, the space can also be a sink and reduce efficiency due to heat losses, in which case this  
497 assumption may not be conservative. The alternative extreme is a constant (or time varying)  
498 temperature boundary condition. This will give the highest heat transfer rates. Finally, a convective  
499 condition may be assumed, with use of a heat transfer coefficient to determine the magnitude of the  
500 heat transfer occurring within the excavation space. Very high heat transfer coefficients, applicable to  
501 scenarios with high air flow conditions, will approximate a temperature boundary.

502 Bourne-Webb et al. (2016b) studied the difference between a temperature and a convective boundary  
503 using a 2D steady state finite difference simulation. They showed a potential four-fold difference in  
504 heat transfer rates from  $20 \text{ W/m}^2$  to  $80 \text{ W/m}^2$  between the extreme conditions. However, the steady  
505 state analysis may not be representative of long-term behaviour. Transient analysis over two months  
506 by Piemontese (2018) showed a much smaller discrepancy between these conditions, generally less  
507 than  $5 \text{ W/m}^2$ .

508 Current experience shows a variety of approaches taken to the excavation space boundary condition.  
509 Many analyses have assumed a constant (or time varying) temperature condition, for example the  
510 basement applications considered by Kürten et al. (2015a), Kürten (2014) and Sterpi et al. (2017), and  
511 the metro stations studied by Soga et al. (2014), Rui & Yin (2018) and Rammal et al. (2018). Heat  
512 transfer coefficients representing a convective boundary have been used more rarely, notably by  
513 iCConsulten (2005) when assessing metro stations and tunnels and by Bourne-Webb et al. (2016b) in  
514 their sensitivity study. More recently, adiabatic conditions have been assumed for metro station  
515 studies in Torino (Barla et al. 2018) and Melbourne (Narsilio et al. 2016a, 2016b).

516 Field data with which to validate analysis approaches remain relatively rare (see also Section 3).  
517 Angelotti & Sterpi (2018) used data from a diaphragm wall forming a basement wall in northern Italy  
518 to validate their numerical simulations. They found that a time varying temperature boundary was  
519 appropriate over the four months of data available. To provide the best fit they applied a damping  
520 coefficient to reduce the fluctuations of air temperature in the locality to an appropriate value to  
521 approximate conditions within the basement. The constant temperature approach used by Kurten et  
522 al. (2015a) during numerical simulation was also validated, but this time with reference to model test  
523 data (refer to Section 4). No longer-term validations are available.

#### 524 2.1.3.3 Numerical Simulations

525 Numerical simulation is the most common approach for analysis of the thermal capacity of energy  
526 walls. Several different approaches have been applied. Bourne-Webb et al. (2016b) used 2D steady  
527 state finite difference analysis with fixed temperature values on the pipe boundary conditions.  
528 Rammal et al. (2018) approximated the heat transfer process by assuming a constant temperature in  
529 the energy wall in the 3D finite difference analysis. More common, however, is the use of 1D line  
530 elements to simulate the heat transfer pipes within a 3D finite element analysis, for example in the  
531 studies of Sterpi et al. (2017), Di Donna et al. (2016a), Narsilio et al. (2016a, 2016b) and Barla et al.  
532 (2018). 3D finite volume analysis was carried out by Shafagh & Rees (2018), including meshed pipe  
533 detail.

534 Not all the approaches are fully validated by field data. Di Donna et al. (2016a) used the published  
535 short-term thermal performance test data from Xia et al. (2012) to validate their model. Sterpi et al.  
536 (2018) and Shafagh & Rees (2018) both use longer data sets. The former from 4 months of monitoring  
537 from a real case in Italy and the latter from a 38-day multi-stage thermal response test in Spain.

#### 538 2.1.3.4 Analytical Methods

539 While numerical simulation is a common research tool, and has also been used by researchers  
540 supporting practice (e.g. Narsilio et al. 2016a, 2016b; Rammel et al. 2018), more accessible analytical  
541 techniques for analysis of energy walls have yet to be fully developed for routine deployment

542 First Sun et al. (2013) proposed the first analytical solution based on heat conduction. The model  
543 contains many familiar assumptions from the analysis of energy piles, with the addition of a convective  
544 heat transfer boundary condition for the inside face of a retaining wall. The model was tested against  
545 full numerical simulation and the thermal performance test data from the Shanghai Museum of  
546 Nature History (Xia et al. 2012). However, poor fit was found at short time periods (<12 hours)  
547 suggesting the details of the heat exchanger are insufficiently well captured.

548 Subsequently, Kurten et al. (2015b) used an electrical analogy to develop a thermal resistance model  
549 for energy walls. They took account of pipe positioning and used a numerical model to compute the  
550 resistance. The approach was then validated against full numerical simulation and model scale  
551 laboratory tests. More recently Shafagh & Rees (in review) have developed a more general resistance  
552 model for a rectangular shape with an irregular hole. The truly analytical approach, which assumes  
553 either isothermal or convective boundary conditions, would be application to energy wall applications.

554 While the thermal resistance models deal only with the internal heat transfer within the wall, a  
555 composite model has also been developed by Shafagh & Rees (2018) based on the Dynamic Thermal  
556 Network (DTN) approach. The network describes the relationship between temperature and fluxes at

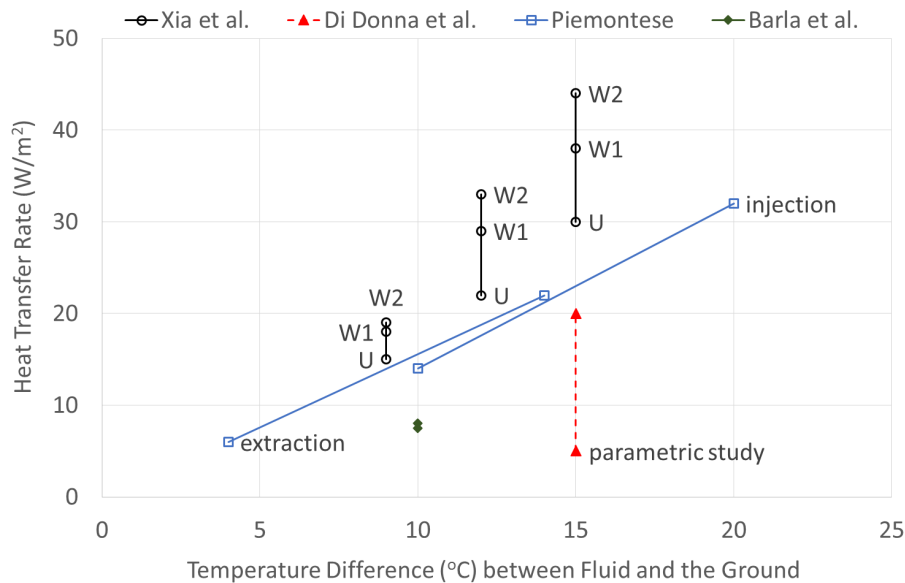
557 surfaces, with these surfaces specified as the ground, the excavations pace and the heat transfer pipes.  
558 DTN is a response factor method and therefore represents transient conduction in terms of the surface  
559 fluxes and temperature variables only. In this approach the current state is expressed entirely in terms  
560 of the current and past temperatures (Rees & Fan, 2013). Each transient heat flux is dependent on  
561 weighed averaged nodal temperatures which are calculated using weighting factors. Shafagh & Rees  
562 (2018) calculated these weighting factors using their finite difference model. However, once the  
563 weighting factors are pre-determined based on the geometry then the run time is fast. The model was  
564 then validated against a long-term thermal response test.

#### 565 2.1.3.5 Pipe Arrangements

566 Various sensitivity analyses have shown the benefit of W as opposed to U shaped pile installations  
567 within the walls (Xia et al. 2012, Barla et al. 2018) based on field and numerical testing (Figure 6).  
568 However, slinky-like arrangements, where many turns are made to maximise the amount of pipe  
569 included in the wall are also popular in some countries, and analyses show these may have the  
570 greatest benefit in terms of heat transferred (Sterpi et al. 2017). Reducing the pipe spacing or  
571 increasing the length of pipe attached to a given wall panel will also often increase energy efficiency  
572 (Kurten 2011, Di Donna et al. 2016a, Barla et al. 2018). However, pipe length alone is an insufficient  
573 measure and pipe arrangement must also be considered in combination (Sterpi et al. 2017).

574 The above pipe optimisation studies were mostly are short-term analyses. The statistical based  
575 parametric analysis by Di Donna et al. (2016a), on the other hand, suggests that the importance of  
576 pipe spacing and arrangement will decrease in the longer term. As more time progresses, the  
577 temperature difference between the ground and the excavation space becomes of prime significance  
578 instead. This is consistent with the steady-state analysis of Bourne-Webb et al. (2016b) and the long-  
579 term transient analyses of Narsilio et al. (2016a). Again, this highlights that the temperature response  
580 of the structure (and hence the energy exchanged) to be highly dependent on this internal excavation  
581 space boundary condition. Finally, the temperature difference between the heat transfer fluid and the  
582 soil is key for determining the heat transfer rate (Xia et al. 2012, Piemontese 2018), Figure 6. This  
583 confirms the importance of balancing thermal loads to maintain maximum temperature differences  
584 during operation (e.g., Narsilio et al. 2016a).

585



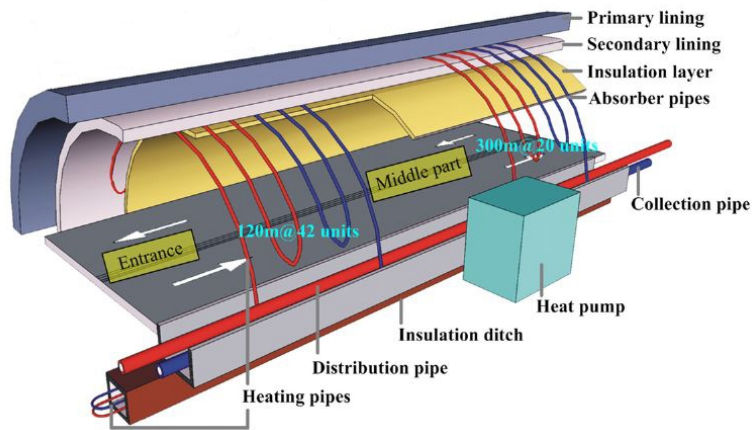
586

587 **Figure 6 Effect of pipe arrangements and temperature difference between fluid and the ground on**  
 588 **the heat transfer rate obtained from energy walls. (U = single U tube; UU = two U-tubes connected**  
 589 **in parallel; W1 or W2 = two U-tubes connecting in series; parametric study includes both U and UU**  
 590 **arrangements).**

591 2.1.4 Energy Tunnels

592 2.1.4.1 Overview

593 Like retaining walls acting as heat exchangers, tunnel linings equipped with heat transfer pipes are  
 594 relatively rare and there is still no routinely adopted design and analysis practice, although some  
 595 guiding principles have been offered in the literature (e.g., Frodl et al. 2010, Nicholson et al. 2014a,  
 596 Tinti et al. 2017). Figure 7 shows a schematic example of an energy tunnel. However, there is an  
 597 increasing interest on the potential use of energy tunnels, driven by sustainability and innovation  
 598 requirements found in large infrastructure projects. Pilot and trial tunnel sections are most typically  
 599 encountered in metro rail projects, with pipe heat exchangers embedded on the tunnel linings shortly  
 600 after shotcreting or in tunnel segments. Depending on the primary intended end-use of the tunnel  
 601 heat exchangers, that is, to exchange heat with the ground or to exchange heat with the tunnel air  
 602 space (i.e., providing heating or cooling to the tunnel space), their thermal behaviour may vary and  
 603 consequently it is also important to correctly understand the nature of this use and the boundary  
 604 conditions that are to be prescribed on the energy tunnels models. Like with energy walls, the  
 605 boundary condition against the air space of the tunnel is the most important difference with borehole  
 606 ground heat exchangers and energy piles, and due consideration must be given in any analytical or  
 607 numerical analysis for energy tunnels. The role of groundwater flow and its predominant direction  
 608 also impact on the thermal energy yield.



609

610 **Figure 7 Schematic view of a energy tunnel. Absorber pipes are embedded into the tunnel lining**  
 611 **(adapted from Zhang et al. 2013, reproduced with permission)**

**Commented [1]:** Reproduced with permission  
 Licence Number 4585510080214.

612 2.1.4.2 *The Tunnel Space*

613 Like with energy walls, the tunnel space needs careful thermal characterisation. The environmental  
 614 conditions of the tunnel air space vary on a case by case basis. They are typically not subjected to  
 615 climate conditioning; however, ventilation is common in metro and vehicle tunnels. Unventilated or  
 616 “hot” tunnels also exist, such as those in the London Underground (Nicholson et al., 2013; Stephen,  
 617 2016, Mortada et al. 2018). These conditions are important when considering thermally activating the  
 618 tunnels. Even in hot tunnels, convective conditions may exist due to the movement of trains or other  
 619 vehicles, and additional sources of heat arising from train braking or passengers may also exists. In  
 620 sewage tunnels (liquid as oppose to gas, air) convection is also important.

621 The tunnel space may be represented by one of three boundary conditions. When there is no heat  
 622 exchange with this space, an adiabatic condition shall be considered. This boundary condition implies  
 623 thermal insulation has been incorporated in the tunnel lining, which is not typically the case for tunnels  
 624 and carries additional material and construction costs (and in the case of metro, passengers and cargo  
 625 tunnels, materials must be fire resistant as well). For the common case of no thermal insulation, the  
 626 tunnel air space can also be a heat sink or source, and the analysis can be carried either modelling the  
 627 space air convective-conductive heat transfer (most comprehensive) or by (un-conservatively)  
 628 prescribing a constant or time varying temperature boundary condition. The latter approach under-  
 629 or over-estimate the heat transfer of the thermally activated tunnel lining, scenarios with high  
 630 air/sewage flow convection, will approximate a temperature boundary.

631 2.1.4.3 *Numerical Simulations*

632 Full scale data with which to validate analysis approaches remain relatively rare (see also Section 3).  
 633 Bidarmaghz et al. (2017) and Bidarmaghz and Narsilio (2018) used data from an energy tunnel pilot  
 634 project in Germany summarised in Buhmann et al. (2016) to validate their numerical simulations. Lee  
 635 at al. (2016) and Zhang et al (2013, 2016a, 2017) performed field scale and laboratory scale thermal

636 performance tests to validate and extend their own numerical and analytical models respectively.  
637 They found that a constant or time varying temperature boundary was appropriate for highly  
638 ventilated tunnels or for short term testing, but this is an area of active research in which longer-term  
639 validations and representativeness of the boundary conditions adopted are still under investigation.  
640 Numerical Simulations

641 While the published literature on energy tunnels is still quite limited, one can see that numerical  
642 modelling has been adopted to undertake technical feasibility studies and or better understand results  
643 from laboratory and field testing (e.g., Nicholson et al 2014a, Narsilio et al. 2016a, 2016b, Barla et al.  
644 2016, Baralis et al. 2018). Numerical simulations are used to assess temperature changes in the ground  
645 and the tunnel space, and heat transfer rates. Studies have been conducted in both two (Franzius &  
646 Pralle 2011) and three dimensions (Nicholson et al. 2014a). Again, the structure internal boundary  
647 condition is very important. Zhang et al. (2014) have observed the importance of the air inside the  
648 tunnel as a heat source, with subsequent analysis linking tunnel air speed and heat transfer rates  
649 (Zhang et al. 2016a, 2017). This is reflected in the study of Nicholson et al. (2014a) where the trains  
650 running within the tunnel were positively taken as a source of heat. However, Franzius & Pralle (2011)  
651 neglected heat transfer into the tunnel which is a significant over simplification. Di Donna & Barla  
652 (2016), Barla et al. (2016), Lee et al. (2016), Bidarmaghz et al. (2017) and Bidarmaghz and Narsilio  
653 (2018) have also used 3D numerical simulations with 1D pipes to reduce computational effort to  
654 perform parametric studies, including the effect of ground and groundwater conditions on the energy  
655 efficiency of energy tunnels.

#### 656 2.1.4.4 Analytical Methods

657 An analytical solution has also been proposed by Zhang et al. (2013) based on a model in radial  
658 coordinates. This accounted for the internal boundary condition via a sinusoidal varying temperature  
659 condition determined from monitoring of road tunnels. The model was successfully validated against  
660 field data, but only over a limited time frame. In addition, empirical models have been used by Tinti  
661 et al. (2017) for high level estimations of thermal yields for sections of tunnels linking Italy and Austria.

662 Analytical methods offer much quicker alternatives for the analysis and design of energy tunnels than  
663 detailed finite element simulations, the most common numerical technique adopted to date for this  
664 purpose (previous section). Clearly, research on analytical techniques for energy tunnels is  
665 underdeveloped at present.

#### 666 2.1.4.5 Pipe Arrangements

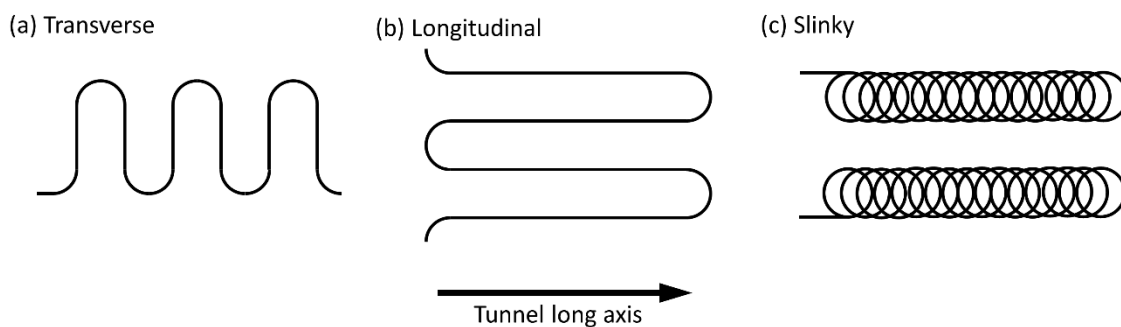
667 As it is the case for other types energy geostructures, pipe arrangements must suit constructability  
668 and minimise or avoid overall construction program delays. Currently, there are three main means to  
669 embedded absorber pipes into tunnels, with similar pipe configuration arrangements. These are also  
670 reflective of the excavation method:

- 671 • Installation of absorber pipes between the outer and inner (shortcrete or other) lining or in  
672 the inner lining. This solution is best suited to be used in drill and blast or punctual mechanised  
673 excavation systems. Examples included the pilot geothermal system of Stuttgart's Fasanenhof  
674 underground station in Germany (Geimer, 2013, Buhmann et al 2016) and of Yakeshi's  
675 Linchang tunnel in Inner Mongolia (Zhang et al. 2014).

- 676 • Installation of precast energy textile or energy fleece, also suitable for drill and blast  
677 excavations (Lee et al., 2016). The first application of this type can be found in Vienna's Lainzer  
678 tunnel (2003) in Austria (Adam and Markiewicz, 2009).
- 679 • Installation of absorber pipes within precast lining segments: suitable for Tunnel Boring  
680 Machine (TBM) excavations. The first GSHP system using thermally activated lining segments  
681 was installed in Austria, in the Stuggart-Jenbach tunnel (Frodl et al., 2010; Franzius and Pralle,  
682 2011).

683 In all three cases, absorber pipes are placed in a meandering fashion, with the pipes either  
684 predominately parallel to the main axis of the tunnel (longitudinal meandering) or perpendicular to it  
685 (transverse meandering). The slinky pipe arrangement has only been trialled in precast energy textiles  
686 (see Figure 8).

687 Adam & Markiewicz (2009) and Brandl et al. (2010) placed heat exchanger pipes on a geotextile  
688 between the primary and secondary tunnel lining for a Vienna metro tunnel constructed using the  
689 New Austrian Tunneling Method (NATM), Schneider & Moorman (2010) incorporated geothermal  
690 heat exchangers into panels in a Stuttgart metro tunnel that were connected with coupling joints that  
691 provide both mechanical interlocking and hydraulic connections, and Nicholson et al. (2014a)  
692 incorporated heat exchanger tubing into segmental panels for the London Crossrail tunnel.



693  
694 **Figure 8 Typical layout of absorber pipes in energy tunnels: (a) longitudinal meandering pipe, (b)**  
695 **transverse, and (c) slinky (only found in energy textiles to date).**

#### 696 2.1.5 Other Geotechnical Structures

697 Energy ground anchors have been suggested and in one case successfully trialled (Adam & Markiewicz  
698 2009, Mimouni et al. 2014). Analysis to date appears to be mainly based on numerical simulations,  
699 although their axisymmetric nature would mean they are well suited to similar design approaches  
700 applied to energy piles. Energy base slabs have also been constructed (e.g. Brandl 2006) and design  
701 approaches would be similar to retaining walls. However, because slabs do not have the benefit of the  
702 embedded part of retaining walls, which are surrounded by soil on both sides, they will always have  
703 lower rates of heat transfer. Recent in situ monitoring of walls and slabs by Angelotti & Sterpi (2018)  
704 show almost three times lower heat transfer rates for the slabs, in the range 3 - 9 W/m<sup>2</sup>. This  
705 compares well to the average rate of 5 W/m<sup>2</sup> reported from various sites by Kipry et al. (2009).

706 Excavations for shallow foundations have also been utilised for ground heat transfer and storage. In  
707 Korea, heat transfer pipes have been trialled at the base of concrete shallow foundations, with  
708 subsequent numerical simulation validated against experimental data (Nam & Chae 2014). In the



709 United States, Oak Ridge National Laboratory led a project to place horizontal pipes within the  
710 excavations already being made for shallow foundations for domestic house (Hughes & Im 2013), so  
711 called Foundation Heat Exchangers. The project was supported by analysis by Oklahoma State  
712 University and others who developed numerical simulation and implemented the results in the  
713 software EnergyPlus for routine application (Cullin et al. 2014, Xing et al. 2012, Spitler et al. 2011).

714 Shallow geothermal systems can also be used to prevent snow accumulation and/or ice formation on  
715 bridges, roads, sidewalks, and similar structures. For example, geothermal systems for bridge de-icing  
716 generally envisage energy piles for the bridge foundation, loops embedded in the abutment  
717 embankment for additional heat exchange with the ground, and loops in the bridge deck that will  
718 maintain the surface warm to prevent ice formation (e.g. Olgun and Bowers, 2013). A brief review on  
719 geothermal energy for bridge deck and pavement de-icing is presented in Yu et al. (2016). Detailed  
720 numerical analyses and feasibility studies are presented elsewhere (e.g. Ho and Dickson, 2017; and  
721 Han and Yu 2018).

## 722 **2.2 Geomechanical and Structural Analysis**

### 723 2.2.1 Overview

724 The geotechnical design of energy geostructures focuses primarily on both ensuring their ultimate  
725 capacity to safely exceed building loading demands, and their long-term serviceability in terms of  
726 deformation response. In the case of energy piles, depending on the restraints provided by the  
727 overlying superstructure and the mobilised side shear stresses and end bearing stresses specific to the  
728 subsurface stratigraphy, temperature changes associated with geothermal heat exchange may lead to  
729 thermally-induced changes in axial stress and deformations. The thermally-induced changes in axial  
730 stress may increase the building loading demands on the energy pile, while the thermally-induced  
731 deformations may lead to changes in the long-term serviceability. Furthermore, depending on the  
732 magnitude of the axial stress before heat exchange processes commence, cyclic heating and cooling  
733 may lead to permanent deformations that need to be characterised. Accordingly, it is critical to  
734 accurately estimate the thermally-induced changes in axial stress and deformations expected for an  
735 energy pile under the site-specific end-restraint boundary conditions and subsurface stratigraphy. For  
736 other energy geostructures such as tunnels and walls, a similar design philosophy may be adopted,  
737 but it is expected that the restraint boundary conditions will differ from those encountered for energy  
738 piles.

### 739 2.2.2 Piles

740 The two major approaches to predict the thermally-induced axial stresses and deformations in energy  
741 piles are load transfer analysis and FE analysis. Load transfer analysis is a simplified approach to  
742 consider axial soil-structure interaction phenomena that relies upon assumed shapes of the mobilised  
743 side shear stress and end bearing stress versus deformation curves (Coyle & Reese 1966). Although  
744 semi-empirical, this approach permits characterisation of nonlinear soil-structure interaction that may  
745 be difficult to consider in finite element analyses. However, a challenge in this analysis is the definition  
746 of the head restraint boundary conditions and the role of radial stresses. Load transfer analysis has  
747 been used successfully to represent the observed mechanical and thermo-mechanical behaviour of  
748 energy piles in the field and centrifuge by Knellwolf et al. (2011), McCartney (2015) and Chen &  
749 McCartney (2016). It has also been used to evaluate the role of cyclic heating and cooling (Pasten &

750 Santamarina 2014; Suryatriyastuti et al. 2014). It is important to note that there has not been sufficient  
751 experimental data collected to validate these predictions. These studies did identify that piles that are  
752 loaded closer to their ultimate capacity will show greater amounts of permanent deformations due to  
753 ratcheting effects. Ouyang et al. (2011) used a hybrid load transfer analysis that combined the axial  
754 stress-strain response of individual energy piles obtained from a load transfer analysis with an elastic  
755 continuum solution to model interaction between energy piles.

756 Finite element analyses have been widely used to study the thermo-mechanical behaviour of energy  
757 piles, considering a range of different constitutive relationships for the energy pile, soil, and interface,  
758 as well as considering different physical processes such as heat flow and thermally-induced pore water  
759 flow. Although FE analyses can consider the impacts of more complex phenomena, they require more  
760 parameters for the constitutive relationships. Although the focus of many energy pile designs is on  
761 the pile performance considering the soil-pile interface, the behaviour of the surrounding soil may  
762 have long-term implications on the energy pile performance. Laloui et al. (2014) and Coccia &  
763 McCartney (2016a, 2016b) provided a review of different constitutive relationships that can be  
764 considered for the thermo-mechanical behaviour of soils and soil-pile interfaces. Several constitutive  
765 relationships used in FE analyses of soils do not consider thermo-mechanical behaviour but account  
766 for different ways to incorporate soil nonlinearity during mechanical loading. Specifically,  
767 Suryatriyastuti et al. (2016) used a hyperbolic model to represent the behaviour of the soil without  
768 consideration of temperature effects. Saggu & Chakraborty (2015), Olgun et al. (2014) and Ozudogru  
769 et al. (2015) used an elasto-plastic formulation with the Mohr-Coulomb yield criterion, while Ng et al.  
770 (2015) used an incremental nonlinear hypoplastic model specific to sand. On the other hand, fewer  
771 models have incorporated thermo-elasto-plastic soil behaviour. Specifically, Rotta Loria & Laloui  
772 (2016a) used a linear thermo-elastic model for the soil, Laloui et al. (2006) used a thermo-elasto-plastic  
773 model with the Drucker-Prager yield criterion, and Di Donna et al. (2016b) used a thermo-elasto-  
774 plastic model with the Mohr-Coulomb criterion. It was not possible to validate whether the soil  
775 constitutive model influenced the axial soil-structure interaction predictions, but all the constitutive  
776 models used in the previous studies still resulted in good matches in terms of the predicted axial  
777 stresses and strains in the energy piles. Laloui et al. (2006), Laloui and Nuth (2006), and Rotta Loria &  
778 Laloui (2016a) assumed that the pile and soil were rigidly connected (a perfectly rough interface),  
779 Suryatriyastuti et al. (2012) and Ozudogru et al. (2015) used an elastic-perfectly plastic soil-pile  
780 interface element, Saggu & Chakraborty (2015) and Ng et al. (2015) used an interface friction angle  
781 smaller than that of the soil and a refined mesh near the interface, while Suryatriyastuti et al. (2016)  
782 used a bounding surface plasticity formulation for the interface. Gawecka et al. (2016, 2017) used a  
783 full-coupled thermo-hydro-mechanical FE model to model the impact of transient heat transfer and  
784 water flow on soil-structure interaction in energy piles and found that thermally-induced stresses in  
785 energy piles dissipate with time as the surrounding subsurface reacts to the changes in pile  
786 temperature. Cyclic effects have been considered in several finite element analyses, with plastic  
787 deformations obtained through the constitutive model of the soil (Ng et al. 2015) or through the soil-  
788 pile interface constitutive model (Suryatriyastuti et al. 2016). Many of the models mentioned above  
789 were validated using field data from Laloui et al. (2006) or Bourne-Webb et al. (2009), although Rotta  
790 Loria et al. (2015a, 2015b) found that FE analyses could also be validated using centrifuge modelling  
791 results.

792 A significant advantage of FE simulations over load transfer analyses is the ability to consider heat flow  
793 analyses and their impacts on the thermo-hydro-mechanical response of the subsurface surrounding

794 the energy pile. Laloui et al. (2006) was able to predict the deformations of the soil surrounding an  
795 energy pile while Di Donna et al. (2016b) and Rotta Loria & Laloui (2016a) were able to characterise  
796 the thermal and thermo-mechanical interactions between pile groups. Wang et al. (2015a) simulated  
797 the coupled flow of heat and water away from a centrifuge-scale energy pile in unsaturated silt, while  
798 Akrouch et al. (2016) simulated coupled heat and mass transfer in unsaturated soil away from  
799 laboratory-scale energy piles. In both cases, the changes in degree of saturation surrounding the  
800 energy pile will lead to a change in effective stress and a corresponding change in the ultimate side  
801 shear stress at the soil-pile interface, similar to that observed experimentally by Goode and McCartney  
802 (2015). Changes in saturation also lead to changes in the soil thermal properties and heat transfer  
803 from the energy pile.

804 Different methods of analyses have been used to consider the behaviour of energy pile groups than  
805 those used for individual energy piles. Rotta Loria et al. (2016a) used a modified interaction factor  
806 approach to consider group effects, while Suryatriyastuti et al. (2016), Di Donna et al. (2016b), and  
807 Rotta Loria & Laloui (2016b) used FE analyses. The interaction factor approach can be used readily in  
808 design calculations, while finite element analysis requires more in-depth site-specific testing to  
809 determine material properties. The critical variables in the design of energy pile groups are the spacing  
810 and diameter of the energy piles, and the relative stiffness of the pile, soil, and overlying slab which  
811 may lead to changes in thermal and mechanical interaction. Although these studies identify that there  
812 may be differential movements or changes in the stresses in the overlying slab if one of the energy  
813 piles operates while the others do not, this effect is lessened when the temperature changes of the  
814 energy piles are the same. It may not be possible to achieve similar changes in pile temperature in  
815 practice, so some differential displacements or stresses are expected. Thermal interaction may lead  
816 to a decrease in the thermal efficiency of the energy piles in terms of a balanced seasonal heat  
817 exchange, so it is still important to have an adequate spacing between energy piles in groups if  
818 possible.

819 Several analyses have been conducted quite recently focused on the behaviour and performance of  
820 groups of energy piles (i.e. Rotta Loria and Laloui 2016a, 2016b, 2017a, 2017b, 2017c). It was shown  
821 that the vertical displacement of energy piles can increase because of thermally-induced group effects  
822 induced by the interactions among piles (Rotta Loria and Laloui, 2017b; Rotta Loria and Laloui, 2017c).

823 New challenges in the analysis of energy piles may arise when they are applied in soft soil, expansive  
824 soil, or unsaturated soil settings, during lateral loading of energy piles, or when different materials are  
825 used in the construction of energy piles. For example, McCartney & Murphy (2017) presented 6 years  
826 of monitoring results from a pair of energy piles in saturated claystone that may have expansive  
827 characteristics and observed a long-term dragdown effect superimposed atop the thermo-mechanical  
828 behaviour of the energy pile. This dragdown could have been due to the natural settlement of the  
829 soils on site under the building load, but they may also have been induced by the ground temperature  
830 changes. Ghaaowd et al. (2018) evaluated the impact of heating on the pullout response of energy  
831 piles from soft clays and observed an increase in pullout capacity that corresponded with a decrease  
832 in void ratio of the clay surrounding the energy piles. This was attributed to the impact of permanent  
833 contraction during drained heating of the clay on the undrained shear strength, which was  
834 characterized experimentally for the same clay by Samarakoon et al. (2018). Analyses of these new  
835 challenges will undoubtedly require the use of advanced finite element software for the long-term  
836 design of energy piles.

## 837 2.2.3 Other Energy Geostructures

838 The thermo-mechanical response of energy walls is expected to be similar to energy piles, with an  
839 exception that the lateral expansion at the ends of the wall will induce a 3D stress field that may be  
840 more complex to evaluate than in energy piles (Soga et al. 2015). Further, structural restraints in the  
841 case of basement walls may lead to differential thermal volume changes that are not observed in the  
842 1D axial analysis of energy piles. While it may be possible to use load transfer analyses for energy  
843 walls, it is expected that FE analyses would be required to evaluate their thermo-mechanical response.  
844 However, Nicholson et al. (2014a) found that the temperature changes within the space enclosed by  
845 a tunnel have a much greater effect than the temperature changes in the wall due to typical levels of  
846 heat extraction.

847 As described in Section 2.1.4.5, different methods have been proposed to incorporate geothermal  
848 heat exchangers into tunnel linings to extract heat from both the interior of the tunnel as well as from  
849 the surrounding ground, depending on the method of tunnel construction. These different designs  
850 may have different thermo-mechanical performance due to the geometry of the concrete section  
851 surrounding the energy pile. The FE analyses developed for energy piles can be adapted to study  
852 energy tunnels, with the main technical difference expected would be a change in the hoop stresses  
853 and strains in the tunnel during heat extraction along with the tensile stresses around the heat  
854 exchangers and between joints (Nicholson et al. 2014a). The surrounding subsurface may provide a  
855 different restraint to thermal strains than in energy piles, and thermal deformations may affect  
856 arching and stress distributions around the tunnel, although these changes likely already occur in the  
857 tunnels without the incorporation of heat exchangers due to changes in ambient tunnel temperature  
858 (Nicholson et al. 2014b). Sailer et al. (2018b) used FE analyses to compare hydro-mechanical FE  
859 analyses where an energy wall expands and contracts during temperature changes without  
860 temperature effects on the soil, and thermo-hydro-mechanical FE analyses where an energy wall  
861 expands and contracts during temperature changes considering temperature effects on the soil. The  
862 changes in pore water pressure of the soil in the latter analysis were found to have major effects on  
863 the stress state in the soil and led to differences in the axial forces in the wall and the vertical  
864 displacement of the wall. Barla et al. (2018) used FE analyses to study the thermal and thermo-  
865 mechanical behaviour of energy walls and also found that the bending moment and horizontal  
866 displacement increase at the top of an energy walls during heating, but with magnitudes within  
867 acceptable structural limits.

868

## 869 **3 Field Scale Testing**

### 870 **3.1 Pile Thermal Tests**

#### 871 3.1.1 Thermal Performance Tests

872 In this discussion thermal performance tests, which aim at obtaining the energy capacity of a system,  
873 are differentiated from thermal response tests, which have their origin in the need to determine the  
874 soil thermal conductivity in situ. Thermal performance tests have been further subdivided into short  
875 term tests, usually conducted over a few days, and longer-term observations, typically conducted  
876 during full operation of a system. This distinction is important, since short term tests commonly  
877 provide an overestimate of energy capacity compared with operational conditions. Short term tests

878 nonetheless can be useful, especially for making comparisons of design aspects such as pile types and  
 879 configurations.

880 **3.1.1.1 Short Term Tests**

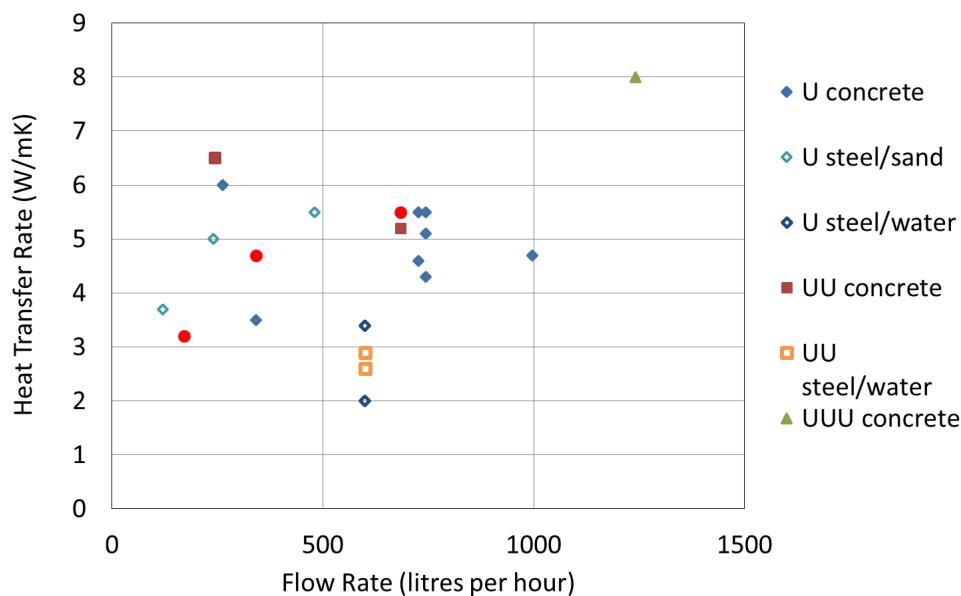
881 In this context short term test are defined as those where the duration of the experiment is no more  
 882 than three months (although typical such tests are less than one week long). The performance of the  
 883 pile heat exchanger is tested by circulating fluid, usually entering the pile at constant temperature,  
 884 through the heat transfer pipes and recording the resulting outlet temperature. From the outlet  
 885 temperature and knowledge of the fluid flow rate and thermal properties it is possible to calculate the  
 886 heat transferred to the heat exchanger and the ground. Seven examples of this type of test have been  
 887 identified for a variety of different piles as summarised in Table 3. The resulting heat exchange rates,  
 888 expressed in W/m, vary substantially and depend on a range of factors including the pile construction,  
 889 the number and arrangements of pipes, the flow rate, the ground conditions, the temperature  
 890 difference between the fluid and the ground and the test duration. Complete information is not  
 891 always available about all these factors, but nonetheless some overarching trends can be identified.

892 **Table 3 Summary of pile thermal performance tests**

Reference	Pile Type	Pile Diameter (mm)	Pipe No & Arrangement*	Flow Rate (L/h)	Temperature Difference+ (°C)	Heat Transfer Rate (W/m)
Jalaluddin et al. (2011)	Steel screw pile, sand filled	140	U	120, 240, 480	10	37 - 55
Hamada et al. (2007)	Hollow pre-cast concrete, mortar filled	300	U, UU	244, 263	9 - 10	54 - 69
Morino & Oka (1994)	Steel, water filled	400	Direct use	1800	15 - 25 5 - 12 (extraction)	120 - 140 70 - 85
Nagano et al. (2005)	Steel, water filled	400	U, UU, direct use	300 - 1800	7 - 14	14 - 95
Gao et al. (2008)	Concrete, cast in situ	600	U, UU, W	171, 342, 684	17	55 - 115
Colls (2013)	Concrete, cast in situ	600	U, UUU	726 - 1242	3 - 16	4 - 8
Katsura et al. (2009)	Hollow steel, water filled	267, 400, 600, 800, 1200	U	480, 960, 1440	9 - 14	70 - 90
Murphy et al. (2015)	Concrete, bored cast in situ	610	U, W, UUU	381 - 1249	1.3 - 8.8	90 - 139
Brettmann & Amis (2011)	Concrete, continuous flight auger (augercast)	300, 450	UU	N.R.	N.R.	73 - 80
Ooka et al. (2007)	Concrete, bored cast in place	1500	8 U	N.R.	N.R.	100 - 120
Singh et al. (2015)	Concrete, bored cast in place	600	U	600	~4	

893 + between the fluid inlet temperature and the undisturbed ground temperature  
 894 \* Notes on pipe arrangements:  
 895 U = single U-tube (2 pipes); UU = two U-tubes in parallel (4 pipes); UUU = three U-tubes in parallel (6 pipes); W = two U-  
 896 tubes in series (4 pipes); Direct use = two open ended pipes inserted into the water filled pile, water infill part of circulation  
 897 system.  
 898 N.R. = Not reported.  
 899

900 Several studies show increasing heat transfer with both increasing flow rate and increasing heat  
 901 exchanger diameter (Gao et al. 2008, Katsura et al. 2009, Jaluddin et al. 2011, Nagano et al. 2005).  
 902 However, when the pile capacity is normalised by temperature difference between the inlet fluid and  
 903 the undisturbed ground, the trends in flow rate are less clear due to scatter relating to other factors  
 904 (Figure 9). The study of Gao et al. (2008) also illustrates how an increasing number of U-tubes in series  
 905 will increase the heat transfer capacity for the same flow rate. This verifies numerical studies by  
 906 Cecinato & Loveridge (2015). However, Gao et al. (2008) also show that using multiple U-tubes in  
 907 parallel is not necessarily advantageous unless the total flow rate to the pile is also increased so that  
 908 the same flow rate to each U-tube can be maintained. The type of heat exchanger is also important.  
 909 The highest rates of heat transfer in Table 3 are both associated with the direct use of infill water in  
 910 steel piles as part of the heat exchanger (Morino & Oka 1994, Nagano et al. 2005). This is not surprising  
 911 since this type of pile will be able to exploit any thermally driven convection within the water  
 912 contained inside the steel pile. What is perhaps more surprising is that the cases of closed loop U-  
 913 tube installations within water filled steel piles also reported by Nagano et al. (2005) have a much  
 914 lower unit extraction rate compared to other installations (Figure 9). Overall, most pile exhibit a heat  
 915 transfer rate in the range of 3 to 6 (W/mK). The effect of intermittent and continuous operating modes  
 916 on the thermal behaviour of a full-scale geothermal energy pile was investigated by Faizal et al. (2016a,  
 917 2016b).



918

919 **Figure 9 Unit heat exchange rates from short term performance tests of piles. Data taken from the**  
 920 **sources listed in Table 3.**

921 3.1.1.2 Long Term Tests and Operation

922 Long term monitoring data for operational energy pile schemes is relatively rare. Six cases where heat  
 923 transfer rates have been recorded over periods of months or years are included in Table 4. One  
 924 notable factor is that most long-term studies consider concrete piles that have been bored and cast in  
 925 situ, whereas many of the thermal performance tests were conducted to examine other types of piles,  
 926 especially steel piles. Four of the case studies (Wood et al. 2010a,2010b; Kipry et al. 2009; Pahud 2007;  
 927 Pahud & Hubbach 2007; Henderson et al. 1998) show significantly lower heat exchange rates than  
 928 shorter term tests, in the range 15 to 35 W/m. This is to be expected and is in line with recommended  
 929 ballpark figures (e.g., SIA, 2005). More surprising are the two studies with higher heat exchange rates  
 930 (Murphy & McCartney 2015; Sekine et al. 2007) of 90 to 220 W/m which fall outside of expected  
 931 ranges. However, it must also be noted that without full information about the thermal loads at all  
 932 the sites, as well as the temperature differences between the fluid and the ground it is not possible to  
 933 make full comparisons between the case studies. Generally enhanced heat transfer rates would be  
 934 expected where the thermal load is highly intermittent and includes a balance of heat injection and  
 935 extraction, where the temperature difference between source and sink is high and where the ground  
 936 has beneficial thermal properties.

937 Other notable observations from the studies include relatively uniform temperature profiles with  
 938 depth down the piles (Murphy & McCartney 2015; McCartney and Murphy 2017) and the favourable  
 939 comparison between piles and boreholes forming part of a combined system (Henderson et al. 1998).  
 940 The first point suggests that largely radial heat flow is occurring (at least within the two-year timescale  
 941 of the study), although the authors do note that the influence of ambient conditions is noticeable for  
 942 the instrumented pile closest to the building edge. In the second study, Henderson et al. (1998) were  
 943 able to compare the energy exchanged by an approximately equal total length of borehole and pile  
 944 heat exchangers. They found the piles beneath their building to be supplying 56% of the heating and  
 945 70% of the cooling, which they attributed to the absence of interaction with ambient conditions due  
 946 to the building positioned above the pile heat exchangers.

947

948 **Table 4 Summary of operational pile performance**

Reference	Pile Type	Pile Diameter (mm)	Pile Length (m)	No Pipes	Monitoring Period	COP / SPF*	Heat Transfer Rate (W/m)
Henderson et al. (1998)	Steel tubes with concrete infill	200	26	2	12 months		16.4 extraction 18.3 injection
Wood et al. (2010a, b)	Bored cast in situ	300	10	2	7 months		26
Murphy and McCartney (2015); McCartney and Murphy (2017)	Bored cast in situ	910	15, 13	4, 8	6 years		91, 95

Pahud & Hubbach (2007)	Bored cast in situ	900 - 1500	26 - 27	10	24 months	2.7 to 3.9 (SPF)	15 extraction 16 rejection
Sekine et al. (2007)	Bored cast in situ	1500	20	8	15 months	3.2 extraction (COP) 3.7 injection (COP)	120 extraction 100 - 220 rejection
Kipry et al. (2009)	Various schemes					3 to 6.5 (SPF)	<30 extraction <35 injection

949 \* COP = coefficient of performance and is the ratio of useable energy to the electricity supplied to the heat pump; SPF =  
950 seasonal performance factor and is the ratio of the useable energy to the electricity supplied to the heat pump and  
951 associated circulation pumps used in the system.

### 952 3.1.2 Thermal Response Tests

953 Thermal response testing is an in-situ technique designed to characterise the thermal properties of  
954 the ground heat exchanger and the surrounding soil or rock to enable appropriate values to be used  
955 in design. The technique as it is commonly deployed now, using mobile tests rigs, was developed for  
956 borehole heat exchangers in the 1990's by two groups working independently, one at Oklahoma State  
957 University (Austin, 1998) and the other at Lulea University of Technology in Sweden (Gehlin 2002).  
958 Both groups developed an idea first proposed by Mogensen (1983) which proposed applying a  
959 constant rate of heating or cooling to a GHE via the circulating fluid and using the resulting  
960 temperature change to determine both the ground thermal conductivity and the borehole thermal  
961 resistance. The test is directly analogous to a pumping test in groundwater engineering to determine  
962 aquifer properties.

963 For the case of borehole heat exchangers, the test has now become relatively routine and there are a  
964 number of relevant national and international standards for its implementation and interpretation  
965 (Sanner et al. 2005; IGSHA 2007, 2009; GSHPA 2011; Banks 2012). Additionally, Spitler & Gehlin  
966 (2015) provide a useful review of the development of the test method and equipment as well as a  
967 review of interpretation methods and uncertainties. The most commonly used analytical model for  
968 interpretation of the test remains the simplified infinite line source. In this model the relationship  
969 between change in temperature and time is log-linear which makes interpretation straight forward.  
970 The thermal conductivity can be determined from the gradient of the straight line and the thermal  
971 resistance from the intercept on the temperature change axis. The thermal conductivity can therefore  
972 be determined independently of the thermal resistance, which is not possible in other more  
973 sophisticated parameter estimation techniques. However, the simplified infinite line source approach  
974 has a key disadvantage when applied to pile heat exchangers. For the log-linear relationship to be  
975 valid a certain amount of time must have elapsed, usually taken as  $5r_b^2/\alpha$  where  $r_b$  is the heat  
976 exchanger radius and  $\alpha$  is the soil thermal diffusivity. This ensures that the mathematical simplification  
977 behind the log-linear relationship is valid, and that the heat exchanger is at a thermal steady state (i.e.  
978 the thermal resistance is constant). While this criterion is typically a few hours for boreholes, it may  
979 be days or weeks for piles given the dependence on the square of the radius. The consequence of this  
980 is that longer test times or different interpretation techniques are required for large diameter piles  
981 (Loveridge et al. 2014a). Longer test times mean greater expense and reliable alternative



982 interpretation techniques for large diameter piles are still under development (e.g. Loveridge et al.  
 983 2015).

984 The following sections summarise the work that has been done on thermal response testing for piles  
 985 in recent years, as well as reporting published test datasets.

986 **3.1.2.1 Case Studies**

987 Seven notable pile thermal response test case studies are highlighted in Table 5 below. Other tests  
 988 have been performed but those summarised in the table are more comprehensively reported and  
 989 contain some alternative measure of the ground thermal conductivity with which to compare the in-  
 990 situ results. In almost all cases the in-situ results for thermal conductivity are higher than those  
 991 measured in the laboratory (Figure 10). There are several factors which may be causing this effect.  
 992 First assuming the inlet temperature is typically higher than the ambient air temperature, thermal  
 993 response tests can lose heat to the atmosphere between the application of the heat input and the  
 994 point at which the circulation fluid enters the ground. This can cause overestimation of the applied  
 995 thermal power and hence over estimation of the thermal conductivity and/or thermal resistance (see  
 996 e.g., Jensen-Page et al. 2018). This effect can be minimised by reducing the distance between the test  
 997 rig and the GHE, by better insulating hoses, and by positioning the fluid temperature sensors as close  
 998 to the ground as possible. Of course, underestimation of the power is also possible when tests are  
 999 conducted in the peak of summer or in particularly warm climates. Secondly, real temperature  
 1000 response functions for piles are expected to have reduced gradients compared with the idealised ILS  
 1001 model (Figure 4). Therefore, fitting of the ILS will lead to artificially low line source gradients and hence  
 1002 overestimations of thermal conductivity.

1003 Furthermore, samples taken from sites will have lost confining stress and also potentially lost moisture  
 1004 before they are tested. Both these factors could result in underestimation of thermal conductivity  
 1005 from laboratory tests. Consequently, quality of thermal response test and quality of soil sample can  
 1006 both affect the accuracy of laboratory – field comparisons. Similar comparisons from borehole thermal  
 1007 response testing have shown that better comparisons can be achieved when appropriate care is taken  
 1008 with respect to quality (Witte et al. 2002, Breier et al. 2011). However, it is likely that the larger  
 1009 diameter and shorter length of piles will contribute to potential errors in thermal response tests  
 1010 results due to additional divergence from line heat source theory. Recently, Akrouch et al. (2015)  
 1011 proposed the ‘thermal cone test’ to determine in-situ the thermal properties of soils. This technique  
 1012 upgrades the well-known cone penetrometer test (CPT), typically used to determine the geotechnical  
 1013 engineering properties of soils to gather their thermal properties as well. Finally, it is also worth  
 1014 highlighting the two orders of magnitude difference in scale between needle probes often used in the  
 1015 laboratory and in situ tests.

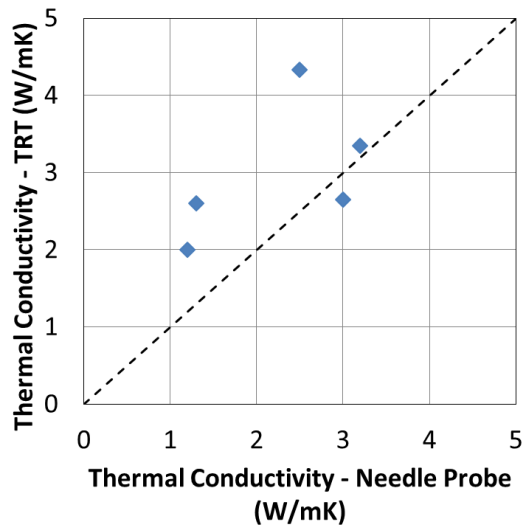
1016 **Table 5 Summary of pile thermal response tests**

Reference	Pile Type	Pile Dia. (mm)	Pile Length (m)	No Pipes	Test Duration	Field Thermal Conductivity (W/mK)	Laboratory Thermal Conductivity (W/mK)	Comments
Hemmingway & Long (2013)	Bored cast in situ	250, 350	14.5	2	13 hours	3.2/3.5 (line source injection & recovery) 5.8 (GPM)	3.2 (needle) ~ 2.3 (literature)	Sands and gravels; tests curtailed due to overheating

Reference	Pile Type	Pile Dia. (mm)	Pile Length (m)	No Pipes	Test Duration	Field Thermal Conductivity (W/mK)	Laboratory Thermal Conductivity (W/mK)	Comments
		300	6	2	20 hours	2.9/2.6 (line source injection & recovery) 2.9 (GPM)	~ 2.2 (literature)	
Alberdi-Pagola et al. (2018)	Square, precast concrete	300	15	2	96 hours	2.4 (simulation) 2.1 (line source)	~ 2.0 (literature)	Two test sites, one in organic clay and sand, one in fill over till.
Loveridge et al. (2014b); Low et al. (2015)	Cast in situ	300	26	2	72 hours	2.5/2.7(line source injection & recovery) 2.4/2.9 (G-function injection & recovery)	1.3 (needle)	London Clay; extended time period between sampling and lab testing
Loveridge et al. (2015)	Bored cast in situ	300, 450	18	2, 4	70 – 100 hours	2.6 – 2.7 (line source) 3.1 ±10% (G-functions)	3.0 (needle)	Silty and sandy clay over dense sand; see also Brettmann et al. 2010, 2011
Park et al. (2015)	Hollow concrete cylinder, grout fill	400	13, 14	4, 6	13 hours	2.2 (simulation)	2.0 (needle)	Residual soil, over weather and unweathered gneiss.
Bouazza et al. (2013)	Bored, cast in situ	600	16	2 6 6	3 days 9 days 52 days	4.2 (line source) 5.0 (line source) 3.8 (line source)	2 to 3 (needle)	Dense sands; power variations may have effected results
Murphy et al. (2014)	Bored cast in situ	610	15	6	20 days	2.0 (line source)	1.2 (needle)	Sandstone; field thermal conductivity corrected for pipe run out length

1017

1018



1019

1020 **Figure 10 Comparison of Thermal Conductivity derived from Laboratory Testing and Thermal**  
 1021 **Response Testing (TRT) on Energy Piles. Laboratory values from the needle probe, using a**  
 1022 **weighted average where different soil units are present. TRT results from line source**  
 1023 **interpretations, average where there are multiple tests or injection and recovery values.**

1024 **3.1.2.2 Recommendations**

1025 Given the test results in Table 5 it is clear that due care is required in the interpretation of pile thermal  
 1026 response tests. Some better results have been obtained from smaller diameter piles and given the  
 1027 costs of long tests on larger diameter piles it is recommended that practical application be restricted  
 1028 to smaller diameters until better interpretation methods are available. Loveridge et al. (2014a) and  
 1029 Loveridge et al. (2015) have suggested that to limit test durations to 100 hours, then pile diameters  
 1030 should be kept to 300mm or possibly 450mm at the most. Routine pile thermal response testing also  
 1031 has project programme implications since time must be provided in the construct schedule for the  
 1032 concrete heat of hydration to dissipate, which will take longer in larger diameter piles. An alternative  
 1033 approach is to use a borehole for thermal response testing at site investigation stage. However, this  
 1034 has its own drawbacks given that the pile lengths are unlikely to be known this early in the project  
 1035 planning. Further research in this area would therefore assist with providing better guidance,  
 1036 especially for larger diameter piles.

1037

1038 **3.2 Pile Geomechanical Tests**

1039 **3.2.1 Single Piles**

1040 Several tests have been performed on full-scale energy piles in the field, including both individual  
 1041 energy pile tests before construction of the building (Laloui et al. 2003; Laloui et al. 2006; Bourne-  
 1042 Webb et al. 2009; Amatya et al. 2012; Akrouch et al. 2014; Wang et al. 2015b; Bouazza et al. 2011;  
 1043 Laloui 2011; Sutman et al. 2014) as well as tests on energy piles beneath constructed buildings (Brandl  
 1044 2006; McCartney & Murphy 2012; Murphy et al. 2015; Murphy & McCartney 2015; Faizal et al. 2018a,  
 1045 2018b). Quantitative observations from these studies have been summarised in recent review papers  
 1046 (e.g., Olgun & McCartney 2014; Bourne-Webb et al. 2019), so this discussion focuses on the range of  
 1047 conditions that were investigated in these studies. Although most of the field-scale pile tests were on

1048 the compression response of bored cast-in place (drilled shaft) energy piles or augercast energy piles,  
1049 Akrouch et al. (2014) investigated the application of tensile loads to energy micropiles. The soil profiles  
1050 in most of the cases were heavily overconsolidated clays or weak rock, which are the best suited for  
1051 bored pile installation. There were not any studies in soft clay, but Akrouch et al. (2014) evaluated the  
1052 response of energy piles in highly expansive clay and observed a pronounced creep effect during  
1053 application of tensile loads. Most of the individual loading tests on energy piles included a loading  
1054 frame at the ground surface using other pipes for reaction support, while Bouazza et al. (2011)  
1055 presented the only study on an energy pile that used an Osterberg cell embedded at the toe to push  
1056 upward and measure side shear stresses and end bearing independently. A wide range in  
1057 instrumentation has been used in the piles, including thermistors and fiberoptic sensors for  
1058 temperature changes, vibrating wire strain gages and fiberoptic sensors for axial and radial strain  
1059 changes, and load cells for axial stress changes. The fiberoptic sensors have a significant advantage of  
1060 being able to monitor continuous profiles of strain and temperature, permitting evaluation of the  
1061 impacts of individual subsurface strata on the axial thermo-mechanical response of energy piles.

### 1062 3.2.2 Pile Groups

1063 Consistent with conventional pile groups, there are relatively few full-scale case histories on energy  
1064 pile groups. Two relevant studies have been performed by Mimouni & Laloui (2015) and Rotta Loria  
1065 and Laloui (2016b). Rotta Loria & Laloui (2016b) assessed the impact of stresses imposed on other  
1066 piles during of a single pile beneath a building load, while Mimouni & Laloui (2015) evaluated the  
1067 response of piles without a head restraint and restrained in a group by a slab, and investigated heating  
1068 of all the piles as a group. Heating all the piles doubled the degree of freedom and led to greater  
1069 upward pile heave during heating. However, this also corresponded to lower differential  
1070 displacements and associated stresses.

1071

## 1072 3.3 Energy Walls

1073 There have now been a number of energy walls constructed around the world. These include at least  
1074 four diaphragm walls for commercial buildings and two other embedded retaining walls for rail  
1075 infrastructure in Austria (Brandl, 1998, 2006), two building basements in the UK (Amis et al, 2010,  
1076 Nicholson et al, 2014b), metro station applications in London and Paris (Soga et al, 2015, Delerablee  
1077 et al, 2018), a public building in Shanghai (Xia et al, 2012) and a recent commercial building in Northern  
1078 Italy (Angelotti & Sterpi, 2018). However, by contrast to piles, few of these case studies report on the  
1079 thermal capacity or performance. Those that are published also tend to be reported with fewer details  
1080 making it harder to learn broader lessons. The sections below identify relevant data that are available.

### 1081 3.3.1 Thermal Performance

1082 The only true short-term thermal performance test for an energy wall is the case of the Shanghai  
1083 Natural History Museum. Xia et al. (2012) present the thermal performance test results for the  
1084 constructed diaphragm wall with heat transfer pipes installed on both the front and rear sides of the  
1085 panel. Three different types of pipe arrangements were tested at three different inlet water  
1086 temperatures. Two of the arrangements involved four pipes with two each on the excavated and  
1087 retained sides, while the third arrangement included only the two pipes on the retained side. The  
1088 experiments also investigated the effects of flow rate and intermittent operation. The results are

1089 presented in terms of energy exchanged per metre of installed heat transfer pipe and range between  
1090 30W/m and 150 W/m depending on the conditions tested. As would be expected the four pipe  
1091 arrangements, intermittent operations, higher temperature differences and higher flow rates all lead  
1092 to greater heat exchange.

1093 Table 6 converts the results of Xia et al. (2012) to exchanged power in  $W/m^2$  and compares them with  
1094 the operational case of Angeloltti & Sterpi (2018) and numerical experiments reported in the  
1095 literature. Angeloltti & Sterpi (2018) present four months of data for heat extraction from a diaphragm  
1096 wall in Tradate in Northern Italy. Each 2.4m wide panel contain a single loop of pipe but arranged in  
1097 three overlapping coils at the back of the wall to maximise pipe lengths. The heat transfer rates for  
1098 this operational case are 12 – 15  $W/m^2$  based on monthly averages and correspond to the lower range  
1099 of data presented by Xia et al. (2012). This is unsurprising since longer term studies would be expected  
1100 to have lower heat transfer rates. The numerical studies also presented in Table 6 have a similar lower  
1101 bound to the field data. However, many studies include the effects of groundwater flow which  
1102 theoretically give a substantial increase in available power.

1103 Total energy obtained from two notable bored pile wall case studies are reported by Brandl (2006)  
1104 and Nicholson et al. (2014b). These operational schemes in are located in Vienna and Oxford  
1105 respectively. In the Vienna scheme the bored pile wall forms part of a railway tunnel, where 59 piles  
1106 of 17 m length are connected to the energy system and used to heat an adjacent school. One heating  
1107 period yielded 214 MWh of thermal energy. In Oxford 61 bored piles of 450mm in diameter were  
1108 equipped with heat transfer pipes. Heating of an associated building was achieved with a COP of 5.8  
1109 for cooling and 3.9 for heating.

**Table 6 Summary of wall thermal performance**

Reference	Approach (Field / Simulation Type /Excavation BC)	Wall Type	Excavation Space	Dimensions	Retained Height	Pipe No & Arrangement t*	Flow Rate (L/h)	Temperature Difference+ (°C)	Duration	Heat Transfer Rate (W/m <sup>2</sup> )
Xia et al. (2012)	Field Thermal Performance Test	Diaphragm wall	Open to air when tested	2.25m long x 1m wide x 38m deep	18.5m	U or W	706	+9 +12 +15	50 hours	15 (U); 18 – 19 (W) 22 (U); 29 – 33 (W) 30 (U); 38 – 44 (W)
Angelotti & Sterpi (2018)	Operational Case	Diaphragm wall	Building basement	0.5m wide x 2.4m long x 15.2mm deep	10.8m	1 loop with 3 overlapping coils in 0.8m width	NR	NR	4 months (Winter)	12 – 15 (extraction)
Bourne-Webb et al. (2016b)	2D steady state FDA; Constant temperature or convection	Diaphragm wall	NR	0.8m wide	Not modelled	U UU	Not modelled	+15	Steady state	13 – 22 20 - 80
Di Donna et al. (2016a)	3D FEA; Constant Temperature	Diaphragm wall	NR	Variable width, 20m deep	Variable	U or UUU	353 - 2121	+8	60 days	5 – 20
Makasis et al. (2018c)	3D FEA & Machine Learning; Varying thermal load; thermally insulated wall	Diaphragm wall	Metro station, basement	13m long x 1m wide x 22m deep	Variable: 5, 10, 20, and 30m	Meandering (W)	330	NR	5 years, monthly analysis	4 – 22 (NR, personal communication)
Piemontese (2018)	3D FEA; Constant Temperature or convection	Diaphragm wall	NR	2.5m long x 1m wide x 20m deep	10m	W	469	+10 to +20 -4 to -14	30 days	14 – 32 (injection) 6 – 22 (extraction) (up to 48 with gw flow)
Rammal et al. (2018)	3D transient FDA; Adiabatic	Diaphragm wall	Metro station	1.2m wide x 32.5m deep	22m	Not modelled	Not modelled	+11 (summer) -5 (autumn) -9 (winter) +7 (spring)	3 year seasonal analysis	12 (100 with gw flow)

Reference	Approach (Field / Simulation Type /Excavation BC)	Wall Type	Excavatio n Space	Dimensions	Retained Height	Pipe No & Arrangemen t*	Flow Rate (L/h)	Temperature Difference* (°C)	Duration	Heat Transfer Rate (W/m <sup>2</sup> )
Barla et al. (2018)	3D transient FEA; Adiabatic	Diaphragm wall	NR	0.8m wide x 15.5m deep	9.5m	W Slinky	706	-10	30 days	7.5 8
Barla et al. (2018)	3D transient FEA; Adiabatic	Diaphragm wall	NR	0.8m wide x 15.5m deep	9.5m	Slinky	291	+13 to -13 (seasonal sinusoidal)	6 years seasonal analysis	7 – 20 (extraction) 10 – 25 (injection) (up to 50 with gw flow)

FEA = finite element analysis; FDA = finite difference analysis; FVA = finite volume analysis.

N.R. = Not reported.

+ between the fluid inlet temperature and the undisturbed ground temperature

\* Notes on pipe arrangements:

U = single U-tube (2 pipes); UU = two U-tubes in parallel (4 pipes); UUU = three U-tubes in parallel (6 pipes); W = two U-tubes in series (4 pipes); Slinky = 1 loop with meandering pipes

Heat transfer rates in absence of groundwater (gw) flow unless stated.

### 1110 3.3.2 Thermal Response Tests

1111 Few thermal response tests have been reported on energy walls. This may be because the absence of easily  
1112 applied analytical solutions for their interpretation means that generating meaningful results from a wall  
1113 thermal response test more challenging. Equally, given these challenges, there may be simpler methods of  
1114 obtaining site specific design parameters, including borehole thermal response tests and laboratory testing.

1115 A number of test have been carried on diaphragm walls constructed as part of the Crossrail project in London,  
1116 although the data is not publicly available. As part of the GEOTECH project, an extended thermal response  
1117 test was carried out on a 17m deep diaphragm wall constructed to support a 6.5m deep basement in Spain.  
1118 Four loops were installed at 0.4m spacing to a depth of 15.6m. Multiple thermal tests were carried out  
1119 consecutively at an applied power of 2kW with pulses of varying durations from a few hours to several days.  
1120 In total the experiment ran for over one month. The data is reported in Shafagh & Rees (2018) where it is  
1121 used for model validation purposes rather than for explicit determination of the ground thermal properties.  
1122 Nonetheless, in the absence of other soil information, fitting their Dynamic Thermal Network model to the  
1123 test data did allow derivation of the wall and ground thermal properties. It is worth noting that the analyses  
1124 used fully transient techniques to capture the thermal behaviour, which, like piles, would be essential for  
1125 avoidance of model errors related to the capacitance of the heat exchanger.

### 1126 3.4 Energy Tunnels

1127 Similarly to energy walls, there have now been a few pilot and testing energy tunnels constructed around the  
1128 world and a few operational energy tunnels. These include notable test sections constructed in Austria and  
1129 Germany at the Katzenburg, Lainzer and Jenbach tunnels (Schneider & Moormann 2010; Adam & Markiewicz  
1130 2009; Franzius & Pralle 2011); a tunnel heat exchanger constructed in Inner Mongolia to transfer heat from  
1131 deeper within the tunnel to the tunnel portal regime where there is a risk of freezing during cold winter  
1132 conditions (Zhang et al. 2013), and a series of energy geotextile installed inside a disused tunnel in Korea (Lee  
1133 et al. 2012).

1134 Typically, thermal performance tests are conducted. Although the construction of the above structures has  
1135 been well reported, details of their thermal performance is just becoming available and complement other  
1136 numerical (or model scale) results being published. The scarcity of published data in this emerging field of  
1137 research makes it hard to generalised broader lessons. Nevertheless, the sections below identify relevant data  
1138 that are available.

#### 1139 3.4.1 Thermal Performance Tests

1140 A number of thermal performance tests have been carried out and reported on a 200 m section of the Linchang  
1141 tunnel in the city of Yakeshi in Inner Mongolia, starting from about 2013. Results have been used by the same  
1142 research group conducting the tests and others to assist with validation of analytical models for heat transfer  
1143 around the tunnel (Zhang et al. 2014) as well as to validate and contrast against results of various numerical  
1144 models (e.g., Barla et al. 2016; Barla and DiDonna 2018). A number of constant temperature inlet tests were  
1145 carried out, each over about two day period. These showed a linear relationship between the inlet  
1146 temperature and the heat exchanged, with resulting rates of 24 to 60 W/m length of the heat exchange pipes,  
1147 depending on the temperature difference and flow rate used. Not surprisingly, these figures are similar to  
1148 those obtained for diaphragm walls.



1149 Longer thermal performance tests were conducted on the Stuttgart's Fasanenhof tunnel, where two blocks of  
1150 10 m each were thermally activated by imbedding meandering absorber pipe between outer and inner  
1151 shotcrete linings. Tests were run for about half a year at constant inlet temperature with flow rates kept  
1152 constant for 5 months and then almost doubled for a further 2 months. The heat transfer rates were found  
1153 to be between 30W/m<sup>2</sup> and 5W/m<sup>2</sup> of activated tunnel depending on operational conditions (Buhmann et al.  
1154 2016, ). These results were used by others to validate numerical models and explore the impact on nearby  
1155 borehole ground heat exchangers (Bidarmaghz et al. 2017) and the impact of groundwater flow (Barla and  
1156 DiDonna 2018, Bidarmaghz and Narsilio 2018). The results from these field scale tests in Fasanenhof are  
1157 consistent with the average heat transfer yield reported for the 54m long energy tunnel segmental lining of  
1158 Stuttgart's Jenbach tunnel, of about 15 W/m<sup>2</sup> on average (Frodl et al., 2010; Buhmann et al. 2016).

1159 Short term and longer-term tests were also performed on six variants of energy geotextiles attached to the  
1160 abandoned tunnel in South Korea, near Seocheon. The pipe arrangement included similar pipe lengths of both  
1161 transverse and longitudinal meandering pipe (see Section 2.1.4.5) and greater lengths of pipe in slinky  
1162 configuration, and also tested proximity of the absorber pipes to the tunnel space. Both constant power and  
1163 varying inlet temperature to represent operational conditions. The heat transfer rates were found to be up  
1164 to around 40W/m<sup>2</sup> of geotextile on average, with higher yield rendered by the slinky configurations. Again,  
1165 this is similar to conditions found for diaphragm walls. The field data gathered from the tunnel lining also  
1166 showed clearly that the air temperature inside the tunnel had a large impact on the temperatures in the  
1167 circulating fluid, emphasising the importance of understanding this boundary condition. This has been also  
1168 flagged by the German-Austrian experienced.

1169 While not explicitly addressed by the current field scale energy tunnel literature, numerical simulations built  
1170 upon these experimental results strongly suggest that the groundwater flow velocity and the degree of tunnel  
1171 air ventilation and thermal insulation have a significant impact on the thermal yield of energy tunnels. Table  
1172 7 summarises such observations and provides more details of field and full scale testing, as well as other means  
1173 to assess the thermal aspects of energy tunnels.

Table 7 Summary of tunnel thermal performance

Reference	Approach	Heat Exchanger Type	Tunnel Location	Dimensions	Equivalent Tunnel Diameter (m)	Pipe No & Arrangement*	Flow Rate (L/h) (per pipeline)	Temperature Difference+ (°C)	Duration	Heat Transfer Rate (W/m <sup>2</sup> )
	(Field Simulation Type / BC)									
Zhang et al. 2014	Field Thermal Performance Test	Cast in situ - Fixed between outer and inner tunnel lining	Linchang tunnel, Yakeshi city, Inner Mongolia	NR (~70 m <sup>2</sup> estimated) (8 m long)	7.7	Longitudinal meandering, 1m and 0.5m pipe spacing	487 to 1250	2 to 6	42 hours	25 to 50
Buhmann et al. 2016	Field Thermal Performance Test	Cast in situ - Fixed to outer tunnel lining	Stuttgart-Fasanenhof, Germany	360 m <sup>2</sup> (20 m long)	9.6	Longitudinal meandering	580 (5 months) to 1085 (2 months) (Re 2400 to 4330)	3.6	6 months (Summer)	30 to 5
Frodl et al., 2010; Buhmann et al. 2016	Field Thermal Performance Test / Operation	Tunnel segmental lining	Stuttgart-Jenbach, Germany	2,200 m <sup>2</sup> (54 m long)	13	Transversal Meandering	500	4.6	2 months (Winter)	15
Lee et al. 2016	Field Thermal Performance Test (and Numerical model)	Cast off site - Fixed on inner tunnel lining	Abandoned railroad tunnel, Seocheon, South Korea	~90 m <sup>2</sup>	NR	6 types: including longitudinal meandering, transverse and slinky	30 to 60 (heating)   90 to 120 (cooling)	4 to 5 (heating) and 12 (cooling)	2.5 months (heating) + 2 months (cooling)	Transverse: 4-6 (Heating) and 24-34 (Cooling) Longitudinal: 5-10 (Heating) and 24-28 (Cooling) Slinky: 11 (Heating) and 37 (Cooling)

Reference	Approach	Heat Exchanger Type	Tunnel Location	Dimensions	Equivalent Tunnel Diameter (m)	Pipe No & Arrangement*	Flow Rate (L/h) (per pipeline)	Temperature Difference+ (°C)	Duration	Heat Transfer Rate (W/m <sup>2</sup> )
	(Field Simulation Type / BC)									
Zhang et al. 2016a; Zhang et al. 2017	Laboratory TRT	Cast in situ - external to outer lining	Laboratory study (1/20th scale)	NR (~20 m <sup>2</sup> estimated scaled up) (18 m long scaled up)	8 (scaped up, 0.4 m in model)	Longitudinal and transverse meandering, 1m (scaled up) pipe spacing	360 to 1800 (estimated equivalent)	7, 12, 17	1 to 4 days	30 to 60
Zhang et al. 2013	Analytical model	Cast in situ - Fixed between outer and inner tunnel lining	Linchang tunnel, Yakeshi city, Inner Mongolia	NR (~3,500 m <sup>2</sup> estimated) (200 m long)	12	Meandering	290 to 1470 (750 recommended)	varies	2 to 90 days	~12 (average, estimated)
Tinti et al. 2017	Analytical (empirical) model	Cast in situ - Fixed between outer and inner tunnel lining	Mules Access Tunnel of the Brenner Base Tunnel (BBT) system, Eastern Alps, Italy	~37,000 m <sup>2</sup> (1,265 m long)	9.5	Meandering	800	10 (varies)	NR	11 to 32
Nicholson et al. (2014a)	FEM Numerical model	Within tunnel lining	Cross-rail London, UK	~4800 m <sup>2</sup> (33 rings) (250 m long)	6.3	Longitudinal Meandering	216 to 432	2 to 10 (varies)		10 to 30
Barla et al. 2016; DiDonna and Barla 2016; Barla and DiDonna 2018	3D FEM Numerical model	Tunnel segmental lining	Metro Torino line 1, Italy	~30,000 m <sup>2</sup> (1350 m long)	7.4	Transversal Meandering	600	3 to 4	1 month	53 (Winter) to 74 (Summer)

Reference	Approach	Heat Exchanger Type	Tunnel Location	Dimensions	Equivalent Tunnel Diameter (m)	Pipe No & Arrangement*	Flow Rate (L/h) (per pipeline)	Temperature Difference+ (°C)	Duration	Heat Transfer Rate (W/m <sup>2</sup> )
	(Field Simulation Type / BC)									
Bidarmaghz and Narsilio 2018; Bidarmaghz et al. 2017	3D FEM Numerical model	Within tunnel lining	Stuttgart–Fasanenhof, Germany	240 m <sup>2</sup> (10 m long)	10	Longitudinal meandering, 0.4m pipe spacing	560	NR	5 years	12 to 40

### 1176 **3.5 Other Energy Geostrutures**

1177 The use of basement slabs as heat exchangers is well known from the literature (e.g. Adam & Markiewicz,  
1178 2009, Katzenbach et al., 2014), but there are few details of well recorded case studies providing details of  
1179 thermal performance. Katzenbach et al., 2014 suggest that slabs are less thermally effective compared to  
1180 other geostrutures, but that they nonetheless remain attractive due to their low installation costs. These  
1181 points are supported by recent in situ monitoring of walls and slabs by Angelotti & Sterpi (2018), who show  
1182 almost three times lower heat transfer rates for the slabs, in the range 3 – 9 W/m<sup>2</sup>. This compares well to the  
1183 average rate of 5 W/m<sup>2</sup> reported from various sites by Kipry et al. (2009).

1184 Large diameter sewer pipes adapted as energy geostrutures have also been successfully trialled at full scale.  
1185 As reported by Adam & Markiewicz (2009), the heat transfer pipes are placed in the material of the base of  
1186 the pipe. Initial results of a trial section showed dependency of the peak power obtained on the effluent level  
1187 in the sewer, its flow rate and temperature.

## 1188 **4 Model Scale Testing**

1189 Although field-scale testing of energy piles permits consideration of the effects of actual construction  
1190 techniques and real soil conditions, there are limitations to this type of testing. In addition to issues with  
1191 expense, time, and site coordination, there are many uncertainties in the field that may not permit a  
1192 comprehensive understanding of the thermal or thermo-mechanical process of interest. Model testing in  
1193 either laboratory-scale or centrifuge-scale provides an opportunity to understand the mechanisms of energy  
1194 pile behaviour under carefully controlled conditions (material properties, geometric features), and dense  
1195 instrumentation arrays can be used to detect heat transfer, water flow, and changes in stress or strain.  
1196 Furthermore, boundary conditions can play a critical role in both the thermal and thermo-mechanical  
1197 evaluation of energy piles and other energy geostrutures. From a thermal perspective, boundary conditions  
1198 at the surface, far field, and within the embedded heat exchangers can affect the heat transfer process and  
1199 should be well-characterised. From a geomechanical perspective, the restraint provided at the head and toe  
1200 of the structure have major effects on the magnitude and location of the thermally-induced stresses. In the  
1201 field, it is often difficult to ensure that the toe of the foundation is completely clean, which may result in a  
1202 softer restraint at the toe than expected from the characteristics of the intact material (Murphy et al. 2015).  
1203 In addition, it is difficult to assess the restraint provided to the top of the foundation by an overlying slab or  
1204 beam. For example, the head deformations of energy piles will affect the response of other energy piles in a  
1205 group. The thermal and mechanical boundary conditions in laboratory-and centrifuge-scale testing can be  
1206 carefully controlled, which provides them with a major advantage over field testing. Finally, the parameters  
1207 governing the failure of a foundation may play an important role in the prediction of the thermo-mechanical  
1208 soil-structure interaction behaviour. Axial or lateral loading tests to failure are relatively simple to perform in  
1209 the laboratory or centrifuge (e.g., McCartney & Rosenberg 2011; Wang et al. 2011, 2012a; Yavari et al. 2014a;  
1210 Goode et al. 2014a; Goode and McCartney 2015), while they may be very complex in the field.

1211 Due to the advantages mentioned above, the information gained for model scale testing can potentially be  
1212 used to provide trust-worthy calibration or validation data for numerical or analytical models describing  
1213 energy geostruture behaviour. Of these model testing options, laboratory-scale testing permits realistic  
1214 simulation of heat transfer processes and can potentially be used to study thermo-mechanical effects for some  
1215 soil types. Centrifuge testing is more suited for evaluation of thermo-mechanical soil-structure interaction due  
1216 to scaling issues with heat flow that will be discussed later. However, some thermo-hydro-mechanical

1217 processes that depend on the stress state such as thermally-induced excess pore water pressure during  
1218 undrained heating may be considered in centrifuge testing.

1219 All the model scale testing conducted by researchers so far has been limited to energy piles except for the  
1220 work by Kurten (2011) to assess the thermal behaviour of energy walls and the experimental study of tunnel  
1221 linings by Zhang et al. (2016b).

## 1222 **4.1 Model Test on Piles**

### 1223 4.1.1 Laboratory Scale Tests (1-g)

#### 1224 4.1.1.1 Overview

1225 Laboratory-scale testing in tanks permits both careful control of the preparation of soil layers, use of different  
1226 heating sources and loading mechanisms for energy piles, and potentially visualisation of different  
1227 phenomena. A summary of the different laboratory-scale tests that will be discussed in this section is  
1228 presented in Table 8. Most laboratory-scale experiments on energy piles have been performed on reduced-  
1229 scale models, typically  $\frac{1}{4}$  to  $\frac{1}{2}$  scale systems. In many cases the scaled diameter of the model energy pile can  
1230 be similar to energy piles in the field, but the length is typically shorter than in the field. Although there has  
1231 not been a detailed evaluation of scaling relationships for reduced-scale energy piles tested under self-weight  
1232 conditions (1-g), there have been studies in the earthquake engineering field that may provide some insight  
1233 into potential scaling relationships. Most work on this topic has built upon the scaling relationships of Rocha  
1234 (1957) and Lai (1988). The main concept of their relationships is that the constitutive relationship that governs  
1235 the mechanical response of the soil should be scaled, and thus both stresses and strains (strain which is already  
1236 dimensionless) in the model are linearly related through a scalar scaling parameter. This approach was  
1237 proposed because many soils when tested under low effective stresses will exhibit dilative, strain softening  
1238 behaviour. By using a looser soil in the scaled model, the stress strain curve under lower effective stresses will  
1239 have a closer shape to that expected in the full-scale model. They found that their scaling relationships work  
1240 well for small-strain behaviour where the soil can be considered as an elastic body. A similar scaling conflict  
1241 for heat flow to that encountered in centrifuge modelling, which will be discussed later, may be encountered  
1242 as the length is scaled in their approach. Nonetheless, the scaling conflict may have less of an effect than in  
1243 centrifuge tests. Further research is needed to evaluate scaling relationships for laboratory testing of energy  
1244 piles, either through re-interpretation of available data or through numerical modelling of physical models (Ko  
1245 1988).

#### 1246 4.1.1.2 Evaluation of Heat Transfer in Laboratory-scale Tests

1247 One of the earliest laboratory-scale tests to consider the role of heat flow around an energy pile was  
1248 performed by Ennigkeit & Katzenbach (2001), who evaluated heat flow processes. They developed a solution  
1249 to the heat equation assuming that the primary mode of heat transfer is conduction and were able to obtain  
1250 a good match to their data. Their work showed the utility of incorporating dense instrumentation arrays  
1251 around a carefully prepared soil layer to validate analytical models. Thermal tests on scale-model energy piles  
1252 have since been performed by Kramer and Basu (2014a, 2014b) and Kramer et al. 2015), who processed their  
1253 heat flow results to interpret the heat flux from the energy pile into the soil. Akrouch et al. (2016) performed  
1254 a coupled heat transfer and water flow analysis for energy piles in unsaturated clay and found that heating of  
1255 the energy pile results in a drying effect of the soil surrounding the energy pile. This drying effect also served  
1256 to lead to a slight reduction in the thermal conductivity of the soil. An innovative technique to study heat flow

1257 in laboratory-scale models developed by Black & Tatari (2015) involves the use of transparent soils and digital  
1258 image analysis. Transparent soils consist of particles saturated with a fluid having a compatible refractive index  
1259 that leads to transparent conditions and have been used together with lasers and digital image analysis to  
1260 study deformation problems in geotechnical engineering. Black & Tatari (2015) found that temperature  
1261 changes led to a change in the refractive index and a loss of optical clarity of the fluid, which can be used as a  
1262 beneficial attribute of transparent soil to study heat transfer processes around energy piles.

#### 1263 4.1.1.3 Evaluation of Soil-structure Interaction in Laboratory-scale Tests

1264 Several studies have been performed on energy piles in laboratory-scale tanks. Wang et al. (2011, 2012a)  
1265 performed tests at various temperatures on small-scale steel energy piles, with an innovative setup that  
1266 permits the pile to be loaded upward from the base after heating. This approach permits the role of the side  
1267 shear stress to be isolated. They evaluated the behaviour of the model energy piles in loosely-compacted, dry  
1268 N50 fine sand, partially saturated N50 fine sand, and partially saturated 300WQ silica flour. During heating,  
1269 the authors observed no change in shaft resistance with the dry sand and a decrease in shaft resistance with  
1270 the partially saturated sand and with the partially saturated 300WQ silica flour. The changes in shaft resistance  
1271 may be due to some mobilisation of side friction during the thermal expansion of the steel, which led to less  
1272 additional axial stress required to reach the ultimate capacity of the energy pile during mechanical loading.

1273 Kalantidou et al. (2012) performed a thorough evaluation of a multi-stage test on an aluminium model-scale  
1274 energy pile in a dry sand layer. They tracked the head displacement of the energy pile during heating-cooling  
1275 cycles, and during mechanical loading after heating to different temperatures. They observed a hysteretic  
1276 response during heating and cooling, which indicates that some plastic deformations occurred at the soil-pile  
1277 interface during the temperature changes. This effect is likely overemphasised due to the relatively large  
1278 thermal expansion of the aluminium, which has a coefficient of thermal expansion that approximately double  
1279 that of most soils and reinforced concrete. Tang et al. (2014) performed similar tests to Kalantidou et al. (2012)  
1280 but focused on the role of the applied load on the foundation head. Application of a greater foundation load  
1281 will lead to a greater initial mobilisation of side shear resistance and end bearing, which can influence the  
1282 subsequent thermo-mechanical response. However, the magnitude of thermal stress will depend on the  
1283 restraint provided by the overlying structure (i.e., the head stiffness) more than the applied load on the  
1284 foundation head. Yavari et al. (2014a) performed complimentary tests to those of Kalantidou et al. (2012)  
1285 using similar a similar dry sand, but incorporated strain gages to infer soil-structure interaction behaviour.  
1286 They were able to measure strain profiles that are consistent with those measured in full-scale energy piles.  
1287 Subsequently, Yavari et al. (2014b) performed a simplified finite element analysis of the energy pile tests and  
1288 found good agreement between the calibrated model and the laboratory-scale results. Marto & Amaludin  
1289 (2015) performed tests on aluminium energy piles in compacted Kaolinite and observed similar compression  
1290 curves for different temperatures. However, their model scale energy pile and soil container were relatively  
1291 small compared to other laboratory-scale tests.

1292 The characteristics of the energy pile can have a major effect on the soil-structure interaction response  
1293 because the displacement required to mobilise the side shear resistance may be relatively small. Accordingly,  
1294 tests on reinforced concrete will provide closer response to actual energy piles in the field. Kramer & Basu  
1295 (2014b) and Kramer et al. (2015) reported results from small-scale tests on a precast concrete pile tested  
1296 under 1-g using F50 Ottawa sand and observed a slight increase in pile capacity at increased temperatures.  
1297 Although a relatively large layer of sand must be prepared in their tank-scale tests, their results permit the  
1298 evaluation of the failure conditions of energy piles in addition to their thermal response. Di Donna et al. (2015)  
1299 performed direct shear tests under different temperatures to evaluate the effects of cyclic temperature

**Commented [2]:** John  
Do you mean Kramer et al 2015?

1300 changes on soil-structure interaction mechanisms. They found that a sand-concrete interface was affected  
 1301 by cyclic degradation (i.e., deformations induced by temperature changes) but not affected directly by  
 1302 temperature. Conversely, the response of a clay-concrete interface changed at different temperatures. They  
 1303 observed an increase of interface strength with increasing temperature because of clay volume changes  
 1304 associated with the changes in temperature.

1305 Laboratory-scale tests have provided interesting insight into energy pile behaviour in some settings, which  
 1306 have also matched well with modelling results. However, the scaling relationships of Rocha (1957) have not  
 1307 been considered when extrapolating the trends from laboratory-scale (low stress) conditions to full-scale piles  
 1308 that are also influenced by installation effects. Although 1-g tests have not been performed on saturated clays,  
 1309 pore water pressure development and thermal consolidation in saturated clays can alter the stress state and  
 1310 result in deformations around a heat exchanger pile. In energy piles, the rate of heating and the rate of  
 1311 dissipation of excess pore water pressures must be carefully considered. Fast heating may lead to undrained  
 1312 heating and pore water pressure increases that may cause a decrease in pile capacity. Slow heating may lead  
 1313 to drained heating and thermal consolidation that may cause an increase in pile capacity. The role of the initial  
 1314 effective stress state is an important issue to consider in these conditions (Ghaaowd et al. 2017), which may  
 1315 not be completely captured in a tank scale test.

1316 A different approach was followed Eslami et al. (2017) to study the effect of the temperature on the variation  
 1317 on the bearing capacity of thermo-active piles. A mini-pressuremeter test was conducted in the laboratory in  
 1318 in a container with controlled temperatures ranging from 1 to 40 C. It was observed that as temperature  
 1319 increased, the pressuremeter modulus ( $E_p$ ) slight decreased, and both, the limit pressure ( $p_l$ ) and creep ( $p_r$ )  
 1320 significantly decreased. Murphy and McCartney (2014) developed a thermal borehole shear device to evaluate  
 1321 the impact of temperature on the soil-concrete interface shear behaviour in-situ and found negligible effect  
 1322 of temperature on the frictional behaviour of the interface with a sandy soil. This negligible impact of  
 1323 temperature on the drained interface shear strength in cohesionless is consistent with the negligible increase  
 1324 in ultimate capacity of energy piles in sands with increasing pile temperature observed by Goode and  
 1325 McCartney (2015).

1326

1327

**Table 8 Summary of laboratory-scale tests on energy piles**

Study	Tank dimensions	Pile/heater material	Pile type	Soil type	Purpose
Ennigkeit and Katzenbach (2001)	1 m diameter, 2.4 m height	Aluminum	Heating rod	Dry sand	Heat flow analysis
Wang et al. (2011, 2012a)	0.272 m diameter, 0.15 m height	Steel	End-bearing	Moist sand, silica flour	Upward loading for side shear evaluation
Kalantidou et al. (2012), Tang et al. (2014)	0.57 m diameter, 0.85 m height	Aluminum	Semi-floating	Dry sand	Cyclic heating and cooling, loading to failure
Yavari et al. (2014a)		Aluminum	Semi-floating	Dry sand	Cyclic heating and cooling



Study	Tank dimensions	Pile/heater material	Pile type	Soil type	Purpose
Kramer and Basu (2014a, 2014b); Kramer et al. (2015)	1.83 m × 1.83 m square, 2.13 m height	Reinforced concrete	Semi-floating	Dry sand	Heating, effect of temperature of load-settlement curve
Black & Tatari (2015)	0.6 m × 0.5 m rectangle, 0.4 m height	Aluminum	Semi-floating	Transparent soil	Heat flow visualization
Marto and Amaludin (2015)	0.27 m diameter, 0.25 m height	Metal	Semi-floating	Compacted clay	Effect of temperature on pile head displacement

1328

#### 1329 4.1.2 Centrifuge Tests on Energy Piles (N-g)

##### 1330 4.1.2.1 Overview

1331 Because soil properties are very sensitive to self-weight conditions, laboratory-scale tests may not accurately  
 1332 capture the soil behaviour that may affect the thermo-mechanical response of a full-scale energy pile. This is  
 1333 particularly the case in sands, where a change in the mean effective stress can change the shape of the shear  
 1334 stress-strain curve and volumetric strain response significantly, potentially converting from contractive, strain-  
 1335 hardening behaviour at high mean effective stress to a dilative, strain-softening behaviour at low mean  
 1336 effective stress. Accordingly, a geotechnical centrifuge can be used to increase the self-weight of a soil layer,  
 1337 and more accurately consider the role of mean effective stress in the soil layer. A summary of the different  
 1338 centrifuge tests that will be discussed in this section is presented in Table 9.

1339 Centrifuge physical modelling is based on the concept of geometric similitude. In this case, the lengths of  
 1340 geometric features in a model  $L_m$  can be scaled down from the lengths of geometric features in a full-scale  
 1341 prototype  $L_p$ , as follows:

$$L_m = \frac{L_p}{N} \quad (7)$$

1342 where  $N$  is the acceleration ratio, defined as follows:

$$N = \frac{\omega^2 r}{g} \quad (8)$$

1343 where  $g$  is the acceleration due to earth's gravity,  $\omega$  is the angular velocity of the centrifuge, and  $r_e$  is the  
 1344 effective radius (typically at the centre of the energy pile). Using the concept of geometric similitude, the  
 1345 effective stresses in a centrifuge-scale model  $\sigma_m$  can be shown to be the same as those in a prototype  $\sigma_p$ , as  
 1346 follows:

$$\sigma_m = \rho g N z_m = \rho g N \left( \frac{z_p}{N} \right) = \rho g z_p = \sigma_p \quad (9)$$

1347 where  $\rho$  is the density of the soil and  $z_m$  and  $z_p$  are the depths from the surface of the soil layer in the model  
 1348 or prototype. Similarly, the strains in a centrifuge-scale model  $\epsilon_m$  are also equal to those in a prototype  $\epsilon_p$ , as  
 1349 follows:

$$\varepsilon_m = \frac{\Delta L_m}{L_m} = \frac{\Delta L_m N}{N L_m} = \frac{\Delta L_p}{L_p} = \varepsilon_p \quad (10)$$

1350

1351 Accordingly, the stress and strains in a centrifuge-scale model are expected to be the same as those in a  
 1352 prototype. This also includes the thermal axial strains in an energy pile, as the coefficient of thermal expansion  
 1353 of an energy pile is not expected to depend on self-weight.

1354 Although the centrifuge is effective at increasing the self-weight of the soil layer, and thus affecting any aspect  
 1355 of soil behaviour that is stress-dependent, it is not effective at scaling other features that do not depend on  
 1356 self-weight, such as heat flow and diffusion-based flow processes. Experimental evaluations of heat flow in  
 1357 the centrifuge will be discussed in the next section, but an implication of the fact that heat flow does not scale  
 1358 is that the zone of influence of heat flow in the centrifuge will be greater than that in the prototype. Another  
 1359 way of considering this is that during heating for a certain time period, heat will have travelled over a greater  
 1360 scaled distance in the centrifuge model than in the prototype. Accordingly, most engineers use a scaling factor  
 1361 for the time in the centrifuge scale model  $t_m$  compared with the time for heat flow in the prototype  $t_p$ . This  
 1362 scale factor can be assessed using Fick's law as follows:

1363

$$\frac{dT_m}{dt_m} = \alpha_m \frac{d^2T_m}{dz_m^2} \quad (11)$$

1364 where  $T_m$  is the temperature in model scale,  $z_m$  is the length in model scale, and  $\alpha_m$  is the thermal diffusivity.  
 1365 Using a similar equation for the prototype, the following relationships between the times in model and  
 1366 prototype scales can be derived:

1367

$$t_m = \left(\frac{z_m}{z_p}\right)^2 t_p = N^2 t_p \quad (12)$$

1368 where  $z_p$  is the length in prototype scale. Accordingly, when scaling results from a centrifuge model to  
 1369 prototype scale, heat will be transferred  $N^2$  times faster than in the actual prototype soil layer.

1370 An implication of temperature scaling is that a greater volume of soil surrounding the model-scale foundation  
 1371 will be affected by changes in temperature. Soils change in volume with temperature, so if a greater zone of  
 1372 soil around the foundation is affected then the effects of differential volume change of the foundation and  
 1373 soil may be emphasised. From this perspective, centrifuge modelling will provide a worst-case scenario. A  
 1374 solution to address the scaling issue is to calibrate numerical simulations of the tests using the data from  
 1375 model scale. However, if the goal of testing is to evaluate the impact of temperature on the load-settlement  
 1376 curve of the foundations, time should be provided to reach steady-state conditions. However, if the goal is to  
 1377 evaluate the impact of temperature on the axial strain distribution in the foundation, tests can be performed  
 1378 until strains stabilize while the foundation temperature is held constant. This amount of time depends on the  
 1379 soil type.

#### 1380 4.1.2.2 Evaluation of Heat Transfer and Water Flow in Centrifuge-scale Tests

1381 One of the earliest uses of centrifuge modelling for the evaluation of the thermo-hydro-mechanical response  
 1382 of soil surrounding a heat source was performed by Maddocks & Savvidou (1984), who were interested in the

1383 disposal of nuclear waste canisters in soft clay deposits offshore. The study was complimented by an  
1384 assessment of scaling relationships for heat and water flow in the centrifuge by Savvidou (1988) and the  
1385 development of an analytical solution for coupled heat flow and thermal consolidation by Booker & Savvidou  
1386 (1984; 1985). Although this experimental situation is perhaps the most complex setting that can be  
1387 encountered by an energy pile in the field, the lessons learned from these studies are still useful for  
1388 understanding different processes that may occur in soil surrounding an energy pile. As the study was focused  
1389 on soft clay soils, it was found that heating of a cylindrical source will lead to diffusive heat flow due to  
1390 conduction, which is affected by the scaling issue mentioned in the previous section. However, they also  
1391 observed the generation of excess pore water pressures during undrained heating. These will dissipate with  
1392 time leading to volume changes. Furthermore, Savvidou (1988) observed that for soils with high Rayleigh  
1393 numbers (i.e., soils with relatively high hydraulic conductivity) such as saturated sand, convective heat flow  
1394 may occur due to buoyancy driven flow of water in the soil layer, this phenomenon has been also observed in  
1395 numerical simulations (Bidarmaghz & Narsilio 2016; Diao et al. 2004b). Because convective heat flow is  
1396 associated with the flow of water, this process can lead to non-similar conditions between a model and  
1397 prototype. This behaviour is not expected for dry sands or lower permeability soils (i.e., clays or unsaturated  
1398 soils). Because of complexities that may be encountered in some soil layers (e.g. because of volume change or  
1399 convection), the approach suggested by Ko (1988) can be used to confirm the scaling relationships proposed  
1400 by Savvidou (1988) when conducting tests in the centrifuge involving heat transfer. Specifically, soil layers  
1401 having different thicknesses and energy piles with different diameters can be tested in the centrifuge  
1402 container at different g-levels so that each model represents the same prototype system. As each model is  
1403 theoretically similar to the same prototype, they should have the same behaviour in prototype scale if the  
1404 scaling relationships are valid.

1405 The geotechnical centrifuge is an ideal setting for the evaluation of the change in pore water pressure  
1406 encountered during undrained heating of saturated soils. Centrifuge modelling not only permits formation of  
1407 a NC clay deposit that has a similar stress state to a prototype soil layer in the field (zero effective stress at the  
1408 surface and increasing effective stress with depth), but also permits a dense instrumentation array to  
1409 characterize the heat transfer and water flow processes and extensive in-situ characterization to evaluate  
1410 thermo-hydro-mechanical processes. Because studies such as Ghaaowd et al. (2017) showed that the  
1411 magnitude of excess pore water pressures induced in saturated soils is closely linked with the initial effective  
1412 stress, the effective stress profile in the centrifuge model will ensure that the pore water pressures that  
1413 develop with depth will be closer to those expected in the field than in laboratory-scale consolidation  
1414 chambers under constant mean stress.

1415 Several centrifuge studies have been performed on energy piles in dry sand. In these soil layers, the heat flow  
1416 is expected to be insensitive to the g-level. This was confirmed by the study of Krishnaiah & Singh (2004) who  
1417 performed spatial and temporal measurements of temperature in dry quartz sand surrounding a cylindrical  
1418 heat source during centrifugation at different g-levels. Their results confirm that centrifugation does not lead  
1419 to a change in the heat flow process, and that application of geometric similitude to the model measurements  
1420 will lead to a greater zone of influence of the heat source. However, dry sands are not expected to undergo a  
1421 significant thermal volume change during heating and cooling, so this greater zone of influence may not have  
1422 a major effect. Rosenberg (2010) presented results from heat flow around an energy pile in unsaturated silt,  
1423 and subsequent analyses by Kaltreider et al. (2015) using model-scale dimensions confirm that conduction  
1424 was the primary mode of heat transfer.

#### 1425 4.1.2.3 *Evaluation of Soil-Structure Interaction in Centrifuge-Scale Tests*

1426 There are several experimental studies which investigated the temperature effects on the load-displacement  
1427 curve and soil-structure interaction response of centrifuge-scale energy piles. McCartney et al. (2010) and  
1428 McCartney & Rosenberg (2011) performed early centrifuge-scale on reinforced-concrete, semi-floating energy  
1429 piles in unsaturated, compacted silt, focusing on changes in the load settlement curve after a heating-cooling  
1430 cycle and after monotonic heating to steady-state conditions, respectively. McCartney et al. (2010) found that  
1431 the capacity of the energy pile after a heating-cooling cycle was greater than that of an unheated energy pile.  
1432 McCartney & Rosenberg (2011) found that the capacity of the energy pile increased with temperature.  
1433 Although the observations of McCartney & Rosenberg (2011) were initially proposed to be due to radial  
1434 expansion of the energy pile, leading to a change in normal stress on the sides of the pile, later tests found  
1435 that heating of the energy pile led to thermally-induced water flow in the unsaturated silt and a corresponding  
1436 increase in effective stress. The compaction of the soil around the foundations may have led to an initially high  
1437 radial stress that may not be representative of energy piles in the field.

1438 A later series of centrifuge tests were performed in a layer of the same compacted silt but with an end-bearing  
1439 energy pile having embedded strain gages (Stewart & McCartney 2012, 2014). Stewart & McCartney (2014)  
1440 provided an interpretation of the thermally induced strains, stresses, and displacements in the energy pile.  
1441 Although, the concrete mix design of the energy pile evaluated by Stewart & McCartney (2012, 2014) led to a  
1442 relatively low Young's modulus and coefficient of thermal expansion, the trends in the results corresponded  
1443 well with those observed in full-scale energy piles (McCartney 2013). Stewart & McCartney (2014) also  
1444 observed a reduction in water content near the test pile due to thermally induced water flow. McCartney  
1445 (2013) reported the results from a semi-floating energy pile having the same Young's modulus as that of  
1446 Stewart & McCartney (2014) and observed lower compressive stresses in the energy pile due to the lower  
1447 restraint provided by the relatively compressible soil at the toe of the semi-floating pile. Small-scale testing  
1448 also presents opportunities to evaluate different technologies to assess soil-structure interaction effects. For  
1449 example, Khosravi et al. (2012) performed non-destructive load-response tests on the scale-model, end-  
1450 bearing energy pile developed by Stewart & McCartney (2014) in compacted silt and found that a slight  
1451 increase in the speed of a compressive wave was observed due to the greater restraint of a heated energy  
1452 pile.

1453 Goode et al. (2014), Goode & McCartney (2014) and Goode & McCartney (2015) developed a new pair of end-  
1454 bearing and semi-floating energy piles with a slightly larger diameter than that evaluated by Stewart and  
1455 McCartney (2014) that permitted a stiffer concrete mix design that had thermo-mechanical properties close  
1456 to that expected in an energy pile in the field. The centrifuge tests performed by Goode et al. (2014) and  
1457 Goode & McCartney (2015) on semi-floating energy piles in dry Nevada sand indicate that the shape of the  
1458 compression curve does not change significantly with temperature. They also observed that the thermal axial  
1459 strains in the pile were close to the free-expansion strain due to the relatively low restraint provided by the  
1460 medium-dense sand. A null point near the centre of the energy pile was observed from an integration of the  
1461 strains with depth. Goode and McCartney (2014) evaluated the role of head restraint (load control and  
1462 stiffness control) for an end-bearing energy pile in dry Nevada sand, and found that stiffness control conditions  
1463 lead to higher thermal axial stresses due to the greater restraint provided for the energy pile. Goode &  
1464 McCartney (2015) also compared the behaviour of semi-floating and end-bearing energy piles in dry sand and  
1465 compacted silt and found that higher stresses were observed in the compacted silt. The strain distributions in  
1466 the energy piles in compacted silt were more nonlinear with depth, likely due to greater side shear stresses.  
1467 Goode and McCartney (2015) also performed loading-unloading tests on an end-bearing energy pile in dry

1468 sand after heating to different temperatures and did not observe a noticeable change in the slope of the  
 1469 recompression curve.

1470 Ng et al. (2014) and Ng et al. (2015) performed centrifuge tests on aluminium energy piles in saturated clay  
 1471 and saturated sand layers, respectively, focusing both on the impact of cyclic heating and cooling and on the  
 1472 role of temperature on the compression curve. Different from the observations of Goode et al. (2014) for  
 1473 semi-floating energy pile tests in dry sand, Ng et al. (2015) observed an increase in the ultimate bearing  
 1474 capacity of semi-floating energy piles in saturated sand heated to higher temperatures.

1475 The effect of cyclic temperature-induced changes in energy pile performance is another area of research.  
 1476 During its lifetime, an energy pile is exposed to daily and seasonal temperature changes which result in  
 1477 expansion and contraction of the pile itself. These relative deformations between the soil and the pile can  
 1478 induce slip at the soil-pile interface which can affect the shear stress transfer between the soil and the pile.  
 1479 Further, ratcheting mechanisms may occur for semi-floating foundations that lead to continued thermally-  
 1480 induced settlements or heave after multiple cycles. In addition, the soil surrounding the energy pile is exposed  
 1481 to temperature changes which can induce excess pore pressures, volume changes and degradation of the  
 1482 strength of the soil at the pile interface. Progressive migration away from energy piles in unsaturated soils can  
 1483 reduce the thermal conductivity and cause desaturation of the soil at the pile interface. The role of cyclic  
 1484 heating and cooling has been studied by Stewart and McCartney (2014) and Ng et al. (2014). Little  
 1485 permanent head displacements were noted by Stewart and McCartney (2014) for an end-bearing energy pile  
 1486 in compacted silt. However, Ng et al. (2014) observed that continued downward displacements were observed  
 1487 for a semi-floating energy pile in saturated clay, albeit approaching a shakedown behaviour after several  
 1488 cycles. Further tests need to be performed to evaluate whether ratcheting conditions may occur during cyclic  
 1489 heating of energy piles in over-consolidated clay or dense sand.

1490 In addition to help clarify the role of different variables (soil type, saturation conditions, cyclic loading, restraint  
 1491 at the head or toe of the energy pile), the results from the centrifuge modelling are also useful to calibrate  
 1492 and validate numerical simulations. Wang et al. (2012b, 2015) used a coupled thermo-hydro-mechanical  
 1493 model to evaluate the thermal axial stresses and strains in the energy pile results presented by Stewart and  
 1494 McCartney (2014). A good match between the calibrated model and the experimental results was obtained  
 1495 when the model was performed using model-scale results. Rotta Loria et al. (2015) used a finite element model  
 1496 with the Mohr-Coulomb failure criterion to evaluate the centrifuge results for semi-floating energy piles in  
 1497 sand presented by Goode et al. (2014), and a good match between the model and experimental results was  
 1498 obtained. The promising match between the observations from centrifuge data and numerical simulations  
 1499 emphasizes the usefulness of centrifuge modelling in the development of new numerical simulation tools.

1500

**Table 9 Summary of centrifuge-scale tests on energy piles**

<b>Study</b>	<b>Pile/heater material</b>	<b>Pile/heater type</b>	<b>Soil type</b>	<b>Purpose</b>
Maddocks & Savvidou (1984)	Steel	Thin heating rod	Saturated clay	Thermo-hydro-mechanical process characterization
Krishnaiah & Singh (2004)	Steel	Thin heating rod	Dry sand	Heat flow evaluation at different g-levels
McCartney et al. (2010)	Reinforced concrete	Semi-floating	Compacted silt	Temperature effects on load-settlement curve
McCartney & Rosenberg (2011)	Reinforced concrete	Semi-floating	Compacted silt	Temperature effects on load-settlement curve

Study	Pile/heater material	Pile/heater type	Soil type	Purpose
Stewart and McCartney (2012, 2014)	Reinforced sand-cement	End-bearing	Compacted silt	Soil-structure interaction, cyclic effects
Khosravi et al. (2012)	Reinforced sand-cement	End-bearing	Compacted silt	Dynamic load-response test
McCartney (2013)	Reinforced sand-cement	Semi-floating	Compacted silt	Soil-structure interaction
Goode et al. (2014)	Reinforced concrete	Semi-floating	Dry sand	Soil-structure interaction, temperature effects on load-settlement curve
Goode & McCartney (2014)	Reinforced concrete	End-bearing	Dry sand	Role of head restraint
Goode & McCartney (2015)	Reinforced concrete	Semi-floating and end-bearing	Dry sand and compacted silt	Soil-structure interaction, temperature effects on load-settlement curve
Ng et al. (2014)	Aluminum	Semi-floating	Saturated clay	Soil-structure interaction, cyclic effects
Ng et al. (2015)	Aluminum	Semi-floating	Saturated sand	Soil-structure interaction, temperature effects on load-settlement curve
Ghaaowd et al. (2018)	Aluminum	End-bearing anchor	Saturated clay	Temperature effects on load-settlement curve

1501

## 1502 4.2 Model Scale Tests on Other Energy Geostructures

1503 Kurten et al. (2015a) present results of energy performance testing carried on a model energy wall.  
 1504 Constructed within a sand box of dimensions 3m x 3m x 2m the model walls contained both U and W shaped  
 1505 pipe arrangements. It was possible to control the temperature conditions on both sides of the wall. The results  
 1506 showed the overall pipe length to be more important than the actual pipe arrangements, with heat exchange  
 1507 rates of between 20 W/m and 100 W/m of pipe. These short-term results are compatible with the full-scale,  
 1508 short-term tests performed by Xia et al. (2012). Overall energy outputs from the model tests were quoted as  
 1509 36 W/m<sup>2</sup> to 150 W/m<sup>2</sup>.

1510 Zhang et al. (2016b) completed a model scale sand box experiment on a geothermal tunnel lining subjected  
 1511 to cross flow of groundwater (see Table 7). The experiment was 1/20<sup>th</sup> scale and construction within a 1.4 m  
 1512 x 1.2 m x 1.2 m tank. The authors investigated both the spacing and nature of the arrangement of the heat  
 1513 transfer pipes, the temperature difference between the inlet temperature and the ground and the role of  
 1514 groundwater based on sensitivity to Darcy velocity. The issue of scaling was not addressed in detail, but it was  
 1515 noted that the groundwater flow velocity in the model is 20 times that in the prototype and hence values were  
 1516 chosen with this factor in mind. Overall the results showed that significant groundwater flow both lowers the  
 1517 temperature change at the tunnel and spreads the temperature increment over a wider area. It also reduces  
 1518 the time to steady state and increases the degree of recovery during intermittent operation. Instrumentation  
 1519 within the tunnel also showed the significant heat transfer occurring between the model geostructure and the  
 1520 air within the tunnel, again showing the importance of this boundary condition. It is commented that the  
 1521 results of the model test are consistent with those from the full-scale tests carried out by the same authors  
 1522 (Zhang et al. 2016b, Zhang et al. 2014).

## 1523 5 Discussion

1524 It follows from the preceding material that geoprofessionals indeed contribute to the development of GSHP  
1525 technology and the dual use of geostructures as load bearing and as heat exchanger elements (as well as the  
1526 thermal optimisation of borehole GHEs). By doing so, peak energy demand is lowered and/or flattened via this  
1527 efficient heating and cooling of residential, commercial and industrial buildings. Moreover, using  
1528 geostructures remove the need for construction of (or minimise the number of) special purpose GHEs, further  
1529 contributing to reduce capital costs for shallow geothermal energy systems.

1530 The GSHP technology has been primarily driven by colleagues specialising in Mechanical Engineering and the  
1531 Heating, Ventilation and Air Conditioning (HVAC) industry with limited input from Geotechnical Engineering.  
1532 This situation is rapidly changing. While there is still further research and development opportunities for the  
1533 design and installation of borehole GHEs, there exist today a swathe of thermal design approaches developed  
1534 for boreholes. In contrast, much fewer guidelines are available for the design and construction of energy piles  
1535 and for other energy geostructures such as retaining walls or tunnel linings. When it comes to thermal  
1536 analyses for geostructures, particularly for energy piles, a number of lessons can be imported, albeit with  
1537 limitations, from existing knowledge for GSHP systems that use boreholes, as highlighted in Section 2.1.2.  
1538 However, regarding thermo-geomechanical considerations, the existing GSHP literature developed for  
1539 boreholes is of limited use.

1540 For thermal analysis and design of energy piles (and other geostructures) appropriate analytical models are  
1541 still required. An analytical solution which is solved transiently in radial coordinates has been proposed by  
1542 Javed & Claesson (2011). The model was developed for boreholes but is potentially suitable for adaption for  
1543 piles. One aspect which would require reconsideration is the simplification of the pipe details to an annulus  
1544 to permit adoption of radial coordinates. In addition, the model has a uniform surface boundary temperature  
1545 and assumes homogeneous and isotropic ground conditions which for 'short' piles (relative to typical deeper  
1546 boreholes) poses issues. Regardless of the model employed, in energy piles analytical models dealing with the  
1547 short term transient behaviour are yet to be effectively developed. Numerical simulations (Section 2.1.2.5),  
1548 hybrid models (Section 2.1.2.7) or other novel techniques such as Machine Learning (Makasis et al. 2018c,  
1549 2018d) may guide these analytical developments in the view of the current limited access to full scale and  
1550 model scale testing data.

1551 For the thermo-geomechanical analysis of energy piles (and other geostructures), ensuring that their ultimate  
1552 bearing capacity is not exceeded by the combined building and thermally induced forces, and that their long-  
1553 term serviceability is maintained have driven the core of the research by geoprofessionals. Although published  
1554 long term experimental data is lacking in general, Sections 2.2, 3 and 4 and the long-term experience from  
1555 Switzerland and Austria (e.g., Brandl's work) suggest negligible or manageable thermo-mechanical effects  
1556 arising from GSHP system operations. However, special attention and further research is needed when dealing  
1557 with soft, normally consolidated and/or unsaturated soils.

1558 In all cases, there has not been sufficient experimental data collected to validate predictions. This situation is  
1559 also changing. The largest field instrumented program in shallow geothermal research is believed to be  
1560 running in Australia (Johnston et al. 2014, Narsilio et al. 2014, Aditya et al. 2018), but it mostly accounts for  
1561 borehole GHEs and the GSHP industry there is not as developed as in other parts of the world. Although not  
1562 in a systematic and coordinated manner as in the Australian case, a number of other isolated monitored full  
1563 scale tests were conducted and are being conducted around the globe, particularly in North America, parts of  
1564 Europe (e.g., Switzerland, UK, Spain) and parts of Asia (e.g., Korea, China). These testing account for borehole  
1565 GHEs and energy piles mostly. Not only a larger dataset is still needed, but also other energy geostructures

1566 are required to be tested to advance knowledge and validate and calibrate numerical and analytical models,  
1567 alongside constructability. The absence of standard thermal performance testing makes generalisations hard  
1568 to be derived, which is also compounded by the incomplete site characterisation and knowledge of soil  
1569 conditions.

1570 Similar limitations and difficulties arise in *in situ* thermal response testing for determining soil conditions.  
1571 Perhaps more importantly are the limitations of the test itself, initially developed for slender boreholes, when  
1572 attempted on energy piles or retaining walls, with vastly different geometrical ratios and more subjected to  
1573 influences from the elements (e.g. Bidarmaghz et al. 2016b, Jensen-Page et al. 2018). For the log-linear  
1574 relationship to derive *in situ* thermal parameters at steady state conditions to be valid, it may be days or weeks  
1575 for energy piles (as oppose to 1-2 days for boreholes), or different interpretation techniques are still required,  
1576 with a few currently just under development (e.g. Loveridge et al. 2015).

1577 Model scale testing offer good opportunities to overcome the disadvantages of field scale testing as  
1578 highlighted in Section 4. However, there still exist scaling issues and scaling compatibility amongst the different  
1579 physical processes involved. Materials' thermo-mechanical mismatches with prototypes, for example on the  
1580 materials used for energy pile centrifuge models, have been generally overlooked, and while still providing  
1581 useful information, there are opportunities to perform more realistic model testing (e.g. Minto et al. 2016).

1582 Clearly practical tools for geoengineers and practitioners are still required. GSHP technology and energy  
1583 geostructures are starting to be implemented more widely and seriously considered in large scale  
1584 infrastructure projects (e.g. Cross Rail in London, Metro extensions in Melbourne, Paris and Torino). Tools for  
1585 design as well as for management and constructability of energy geostructure are desperately required  
1586 alongside guidelines, which would eventually lead to standards. While some solid research bases have been  
1587 already developed perhaps for a first generation 'practical' design tool, there is still much to learn for a routine  
1588 application of GSHP technology. Even more so, when larger scale implementation of the technology is sought  
1589 (see for example, Nicholson et al. 2013, Ryżyński and Bogusz 2016, Mortada et al. 2018). The development  
1590 and implementation of guidelines for the structural and geotechnical design of energy geo- structures is  
1591 another critical component of this activity that need more work. Perhaps the first effort in this area  
1592 corresponds to the SIA-D0190 (2005) Swiss guide that deals with the design of energy piles. A similar standard  
1593 was developed in the United Kingdom by the Ground Source Heat Pump Association (GSHPA, 2012). Most  
1594 recently the 'CFMS/SYNTEC INGENIERIE/SOFFONS-FNTP' (2017) was proposed in France. Following the  
1595 Eurocodes, the French guidelines consider a performance-based design approach, which is a significant  
1596 difference respect to the Swiss and British standards, which are basically prescriptive approaches.  
1597 Undoubtedly more effort and advances are necessary in this area as well.

## 1598 **6 Summary**

1599 An overview on the most relevant and recent advances on energy geo-structures was presented in this paper.  
1600 Aspects covering the design and analysis of thermo-active geostructures were discussed in this contribution  
1601 with particular attention to the influence of temperature changes on pile, surrounding soils and other  
1602 components of the system. Analytical functions and approaches (e.g. G-functions, thermal resistances)  
1603 generally used in the design of energy piles were presented and analysed in detail together with numerical  
1604 solution typical used to tackle this type of problem. The discussion did not limit to energy piles, because other  
1605 energy geostructures were also considered, including, retaining walls, tunnels and bridges (i.e. deck de-icing).  
1606 The paper also reviews recent developments in terms of laboratory and field testing associated with thermo-  
1607 active structures, encompassing, lab 1-g tests, centrifuge experiments; and large-scale/field tests. Finally, the  
1608 discussion focused on highlighting the main findings and progress in the last few years in this very active area,



1609 as well as on identifying present and future challenges related to the interaction between energy  
1610 geostructures and the ground.

1611

## 1612 **References**

1613 Adam, D. & Markiewicz, R. (2009) Energy from earth-coupled structures, foundations, tunnels and sewers,  
1614 *Geotechnique*, 59 (3), 229-236.

1615 Aditya, G. R., Narsilio, G. A. & Johnston, I. W. (2018) Full-scale instrumented ground source heat pump  
1616 experiments in Melbourne, Australia. Symposium of Energy Geotechnics in Switzerland in September 2018,  
1617 185-191, doi:10.1007/978-3-319-99670-7\_24

1618 Akrouch, G., Sánchez, M., & Briaud, J-L. (2014) Thermo-mechanical behaviour of energy piles in high plasticity  
1619 clays. *Acta Geotechnica*, 9(3), 399-412.

1620 Akrouch, G.A., Briaud, J-L., Sánchez, M., and Yilmaz, R. (2015) Thermal Cone Test to Determine Soil Thermal  
1621 Properties. *Journal of Geotechnical and Geoenvironmental Engineering* 10.1061/(ASCE) GT.1943-  
1622 5606.0001353, 04015085

1623 Akrouch, G.A., Sanchez, M.A., and Briaud, J-L. (2016) An experimental, analytical, and numerical study on the  
1624 thermal efficiency of energy piles in unsaturated soils. *Computers and Geotechnics* 71, 207-220.

1625 Akrouch, G.A., Sanchez, M.A., and Briaud, J-L. (2018) Performance of a Shallow Geothermal Energy System  
1626 under Cooling-Dominated Conditions". *Renewable Energy* (under review).

1627 Alberdi-Pagola M; Erbs Poulsen S; Loveridge F; Madsen S; Lund Jensen R (2018) Comparing heat flow models  
1628 for interpretation of precast quadratic pile heat exchanger thermal response tests. *Energy*, 145, 721-733.

1629 Amatya, B.L., Soga, K., Bourne-Webb, P.J., Amis, T., and Laloui, L. (2012) Thermo-mechanical behaviour of  
1630 energy piles. *Géotechnique*, 62(6), 503-519.

1631 Amis, T., Robinson, C. & Wong, S. (2010) Integrating Geothermal Loops into the Diaphragm Walls of the  
1632 Knightsbridge Palace Hotel Project. *EMAP – Basements and Underground Structures 2010*, 10p.

1633 Amis, T. & Loveridge, F. (2014) Energy piles and other thermal foundations for GSHP – Developments in UK  
1634 practice and research, *The REHVA European HVAC Journal*, January, 32 – 35.

1635 Amis, T., McCartney, J.S., Loveridge, F., Olgun, C. G., Bruce, M.E. & Murphy, K. (2014) Identifying Best Practice,  
1636 Installation, Laboratory Testing, and Field Testing, *DFI Journal*, 8 (2), 74-83.

1637 Angelotti, A. & Sterpi, D. (2018). On the performance of energy walls by monitoring assessment and numerical  
1638 modelling. *ICE Environmental Geotechnics*. <https://doi.org/10.1680/jenge.18.00037>.

1639 Arulrajah, A., Narsilio G., Kodikara, J., and Orense, R. (2015), "Key issues in environmental geotechnics:  
1640 Australia–New Zealand", *Environmental Geotechnics*, 2 (6), 326-330.

1641 Austin, W.A. (1998) Development of an in situ system for measuring ground thermal properties. Masters  
1642 Thesis. Oklahoma State University. Stillwater, OK.

1643 Banks, D. (2012) *An Introduction to Thermogeology, Ground Source Heating and Cooling*, 2<sup>nd</sup> Edition, Wiley  
1644 Blackwell, Chichester, UK.

- 1645 Baralis, M, Barla, M., Bogusz, W., Di Donna, A., Ryżyński, G. & Žeruń, M. (2018) Geothermal potential of the  
 1646 NE extension Warsaw (Poland) metro tunnels. *Environmental Geotechnics*, 2018 (in press, Published Online:  
 1647 August 17), 1-13. <https://doi.org/10.1680/jenge.18.00042>
- 1648 Barla, M., Di Donna, A. & Perino, A. (2016) Application of energy tunnels to an urban environment.  
 1649 *Geothermics*. 61, 104-113.
- 1650 Barla, M. & Di Donna, A. (2018) Energy tunnels, concepts and design aspects, *Underground Space*, 3(4), 268-  
 1651 276.
- 1652 Barla, M., Di Donna, A. & Santi, A. (2018). Energy and mechanical aspects on the thermal activation of  
 1653 diaphragm walls for heating and cooling. *Renewable Energy*. <https://doi.org/10.1016/j.renene.2018.10.074>.
- 1654 Başer, T., Dong, Y., Moradi, A.M., Lu, N., Smits, K., Ge, S., Tartakovsky, D., and McCartney, J.S. (2018) Role of  
 1655 water vapor diffusion and nonequilibrium phase change in geothermal energy storage systems in the vadose  
 1656 zone. *Journal of Geotechnical and Geoenvironmental Engineering*. 144(7), 04018038.
- 1657 Batini, N., Rotta Loria, A. F., Conti, P., Testi, D., Grassi, W. & Laloui, L. (2015) Energy and geotechnical behaviour  
 1658 of energy piles for different design solutions, *Applied Thermal Engineering*, 85, 199-213.
- 1659 Black, J., & Tatari, A. (2015) Transparent soil to model thermal processes: An energy pile example. *ASTM*  
 1660 *Geotechnical Testing Journal*. 38 (5), GTJ20140215.
- 1661 Bennet, J., Claesson, J., Hellstrom, G., 1987. Multipole method to compute the conductive heat flow to and  
 1662 between pipes in a composite cylinder. Report. University of Lund, Department of Building and Mathematical  
 1663 Physics. Lund, Sweden.
- 1664 Bernier, M. (2001) Ground Coupled Heat Pump System Simulation, *ASHRAE Transactions*, 107 (1), 605-616.
- 1665 Bidarmaghz, A. (2015) 3D numerical modelling of vertical ground heat exchangers, PhD Thesis, University of  
 1666 Melbourne.
- 1667 Bidarmaghz, A., Narsilio, G.A. (2016), Shallow geothermal energy: emerging phenomena in permeable  
 1668 saturated soils, *Geotechnique Letters*, Proceedings of the Institution of Civil Engineers ICE (UK), 6(2), pp. 119-  
 1669 123. DOI: 10.1680/jgele.15.00167
- 1670 Bidarmaghz, A., Narsilio G. A., and Johnston, I. W. (2012), Numerical modelling of ground loop configurations  
 1671 for direct geothermal applications", In Narsilio, G. A., Arulrajah, A., and Kodikara, J. (eds.), Proceedings of the  
 1672 11<sup>th</sup> Australia New Zealand Conference on Geomechanics (ANZ-2012). ISBN 978-0-646-54301-7. Melbourne,  
 1673 Australia, July 15-18, 614-619.
- 1674 Bidarmaghz, A, Makasis, N, Narsilio, G.A., Francisca, F.M., and Carro Pérez, M.E. (2016a), "Geothermal Energy  
 1675 in Loess", *Environmental Geotechnics*, Proceedings of the Institution of Civil Engineers ICE (UK), 3(4), 225-236.
- 1676 Bidarmaghz, A., and Narsilio G., (2018). "Heat exchange mechanisms in energy tunnel systems." *Geomechanics*  
 1677 *for Energy and the Environment*, 16(December), 83-95.
- 1678 Bidarmaghz, A., Narsilio, G. A., Johnston, I.W. & Colls, S. (2016b) The importance of surface air temperature  
 1679 fluctuations on long-term performance of vertical ground heat exchangers, *Geomechanics for Energy and the*  
 1680 *Environment*, 6, 35-44.
- 1681 Bidarmaghz, A., Narsilio G., Buhmann P., Moormann C., and Westrich B. (2017) Thermal interaction between  
 1682 tunnel ground heat exchangers and borehole heat exchangers. *Geomechanics for Energy and the*  
 1683 *Environment*. 10(June), 29-41. Doi: 10.1016/j.gete.2017.05.001

- 1684 Booker, J.R. & Savvidou, C. (1984) Consolidation around a spherical heat source. *Int J Solids Struct.* 20(11-12):  
1685 1079-1090.
- 1686 Booker, J.R. & Savvidou C. (1985) Consolidation around a point heat source. *Int J Numer Anal Meth.* 9(2): 173-  
1687 184.
- 1688 Bouazza, A., Wang, B. & Singh, R.M. (2013) Soil effective thermal conductivity from energy pile thermal tests.  
1689 Coupled Phenomena in Environmental Geotechnics: Proceedings of the International Symposium, Torino,  
1690 Italy, 1-3 July 2013, Taylor & Francis, London, pp. 211-219.
- 1691 Bouazza, A., Singh, R.M., Wang, B., Barry-Macaulay, D., Haberfield, C., Chapman, G., Baycan, S. & Carden, Y.  
1692 (2011) Harnessing on site renewable energy through pile foundations. *Australian Geomech. J.*, 46(4), 79-90.
- 1693 Bouazza. A., Wang, B. & Singh B. M. (2013) Soil effective thermal conductivity from energy pile thermal tests,  
1694 In: Coupled Phenomena in Environmental Geotechnics, Manessero et al. (Eds), Taylor and Francis Group,  
1695 London. 211-219pp.
- 1696 Bourne-Webb, P.; Burlon, S.; Javed, S.; Kürten, S.; Loveridge, F. (2016) Analysis and design methods for energy  
1697 geostructures. *Renewable and Sustainable Energy Reviews*, 65, 402-419
- 1698 Bourne-Webb, P.J., Bodas Freitas, T.M. & da Costa Gonçalves, R.A. (2016) Thermal and mechanical aspects of  
1699 the response of embedded retaining walls used as shallow geothermal heat exchangers. *Energy and Buildings*.  
1700 doi: 10.1016/j.enbuild.2016.04.075.
- 1701 Bourne-Webb, P., Amatya, B., Soga, K. & Payne, P. (2009) Energy pile test at Lambeth College, London:  
1702 geotechnical and thermodynamic aspects of pile response to heat cycles, *Géotechnique* 59(3), 237-248.
- 1703 Bourne-Webb, P.J., Freitas, T.M.B., Assunção, R.M.F. (2019) A review of pile-soil interactions in isolated,  
1704 thermally-activated piles. *Computers and Geotechnics* 108, 61-74.
- 1705 Brandl, H. (2006) Energy foundations and other thermo active ground structures, *Geotechnique*, 56 (2), 81 -  
1706 122.
- 1707 Brandl, H., Adam, D., Markiewicz, R. Unterberger, W. & Hofinger, H. (2010) Massivabsorbertechnologie zur  
1708 Erdwärmennutzung bei der Wiener U-Bahnlinie U2, Osterr. Ingenieur- und Architekten- Zeitschrift, 155, Heft  
1709 7-9/2010 und Heft 10-12/2010, 1-7.
- 1710 Breier, R.A., Smith, M.D. & Spitler, J.D. (2011) Reference data sets for vertical boreholes ground heat exchanger  
1711 models and thermal response tests analysis, *Geothermics*, 40, 79 - 85.
- 1712 Brettmann, T. and Amis, T. (2011) Thermal conductivity evaluation of a pile group using geothermal energy  
1713 piles, *Proc. Geo-Frontiers 2011 Conf.*, Dallas, TX, USA, March, ASCE, 499-508.
- 1714 Buhmann, P., Moormann, C., Westrich, B., Pralle, N. & Friedemann, W. (2016) Tunnel geothermics—A German  
1715 experience with renewable energy concepts in tunnel projects. *Geomechanics for Energy and the Environment*  
1716 8, 1-7. DOI: 10.1016/j.gete.2016.10.006
- 1717 Carslaw HS and Jaeger JC (1959) *Conduction of Heat in Solids*. Second Edition, Oxford University Press.
- 1718 Caulk, R., Ghazanfari, E., & McCartney, J.S. (2016) Parameterization of a calibrated geothermal energy pile  
1719 model. *Geomechanics for Energy and the Environment*. 5(3), 1-15.
- 1720 Cecinato, F. & Loveridge, F. (2015) Influences on the thermal efficiency of energy piles. *Energy*, 82, 1021-2023.

1721 Chen, D. & McCartney, J.S. (2016) Calibration parameters for load transfer analysis of energy piles in uniform  
1722 soils. *ASCE International Journal of Geomechanics*. 1-17. 10.1061/(ASCE)GM.1943-5622.0000873. 04016159.

1723 Choi, J.C., Lee, S.R. & Lee, D.S. (2011) Numerical simulation of vertical ground heat exchangers: Intermittent  
1724 operation in unsaturated soil conditions, *Computers and Geotechnics*, 38, 949-958.

1725 CIBSE (2013) *Ground Source Heat Pumps TM51:2013*, Chartered Institute of Building Services Engineers,  
1726 London, UK.

1727 Claesson, J. & Javed, S. (2011) An analytical method to calculate borehole fluid temperatures for time-scales  
1728 from minutes to decades. *ASHRAE Transactions*, 117(2), 279-288.

1729 Claesson, J. & Hellström, G. (2011) Multipole method to calculate borehole thermal resistances in a borehole  
1730 heat exchanger. *HVAC & R Research*, 17(6), 895-911.

1731 Claesson, J. & Javed, S. (2012) A load aggregation method to calculate extraction temperatures of borehole  
1732 heat exchangers, *ASHRAE Trans*, 118(1), 530-9.

1733 Coccia, C.J.R. & McCartney, J.S. (2016a) Thermal volume change of poorly draining soils I: Critical assessment  
1734 of volume change mechanisms. *Computers and Geotechnics*. 80: 26-40. 10.1016/j.compgeo.2016.06.009.

1735 Coccia, C.J.R. & McCartney, J.S. (2016b) Thermal volume change of poorly draining soils II: Constitutive  
1736 modelling. *Computers and Geotechnics*. 80(December), 16-25. 10.1016/j.compgeo.2016.06.010.

1737 Colls, S. (2013) *Ground heat exchanger design for direct geothermal energy systems*, PhD Thesis, University of  
1738 Melbourne, Australia.

1739 Coyle, H.M. & Reese, L.C. (1966) Load transfer for axially loaded piles in clay. *J. Soil Mech. Found. Div.*, 92(2),  
1740 1-26.

1741 CFMS/SYNTec INGENIERIE/SOFFONS-FNTP (2017) *Recommandations pour la conception, le dimensionnement  
1742 et la mise en oeuvre des géostructures thermiques*. Version 1; pp 120.

1743 Cullin J. R., Spitler J. D., Montagud C. et al. (2015) Validation of vertical ground heat exchanger design  
1744 methodologies. *Science and Technology for the Built Environment*, 21(2), 137-149

1745 Cullin, J. R., Spitler, J. D., & Gehlin, S. E. A. (2014) Suitability of foundation heat exchangers for ground source  
1746 heat pump systems in European Climates, *REHVA Journal*, January 2014, 26-40.

1747 De Carli, M., Tonon, M., Zarrella, A. & Zecchin, R. (2010) A computational capacity resistance model (CaRM)  
1748 for vertical ground-coupled heat exchangers, *Renewable Energy*, 35 (7), 1537-1550.

1749 Delerabee, Y. & Rammal, D., Mroueh, H., Burlon, S., Habert, J. & Froitier, C. (2018). Integration of  
1750 Thermoactive Metro Stations in a Smart Energy System: Feedbacks from the Grand Paris Project.  
1751 *Infrastructures*. 3. 56.

1752 Di Donna, A. & Barla, M. (2016) The role of ground conditions on energy tunnels' heat exchange,  
1753 *Environmental Geotechnics*, 3 (4), 214 - 224. <http://dx.doi.org/10.1680/jenge.15.00030>

1754 Di Donna, A., Cecinato, F., Loveridge, F. & Barla, M. (2016a) Energy performance of diaphragm walls used as  
1755 heat exchangers, *Proceedings of the Institution of Civil Engineers, Geotechnical Engineering*.

1756 Di Donna, A., Rotta Loria, A.F., Laloui, L. (2016b) Numerical study of the response of a group of energy piles  
1757 under different combinations of thermo-mechanical loads. *Computers and Geotechnics*. 72, 126-142

1758 Di Donna, A., Ferrari, A. & Laloui, L. (2015), Experimental investigations of the soil–concrete interface: physical  
1759 mechanisms, cyclic mobilization, and behaviour at different temperatures. *Can. Geotech. J.*, 53(4), 659-672

1760 Diao, N. R., Zeng, H. Y. & Fang, Z. H. (2004a) Improvements in modelling of heat transfer in vertical ground  
1761 heat exchangers, *HVAC&R Research*, 10 (4), 459-470.

1762 Diao, N., Li, Q. & Fang, Z. (2004b) Heat transfer in ground heat exchangers with groundwater advection. *Int. J.*  
1763 *Therm. Sci.* 43, No. 12, pp. 1203–1211.

1764 Do, S.L. & Haberl, J.S. (2010) A Review of Ground Coupled Heat Pump Models Used in Whole-Building  
1765 Computer Simulation Programs. Energy Systems Laboratory (<http://esl.tamu.edu>). Available electronically  
1766 from <http://hdl.handle.net/1969.1/93221>.

1767 Dupray, F., Laloui, L. & Kazangba (2014) Numerical analysis of seasonal heat storage in an energy pile  
1768 foundation, *Computers and Geotechnics*, 55, 67-77.

1769 Ennigkeit, A., & Katzenbach, R. (2001) The double use of piles as foundation and heat exchanging elements.  
1770 *Soil Mechanics and Geotechnical Engineering. Proc. 14<sup>th</sup> International Conference on Soil Mechanics and*  
1771 *Geotechnical Engineering. Taylor and Francis. London. Vol. 2. 893-896.*

1772 Eskilson, P. (1987) *Thermal analysis of heat extraction boreholes*. Doctoral Thesis, Department of  
1773 Mathematical Physics, University of Lund, Sweden.

1774 Eskilson, P. & Claesson, J. (1988) Simulation model for thermally interacting heat extraction boreholes.  
1775 *Numerical Heat Transfer*, 13, pp. 149-165.

1776 Eslami, H., Rosin-Paumier, S., Abdallah, A. & Masrouri, F. (2017) Pressuremeter test parameters of a  
1777 compacted illitic soil under thermal cycling. *Acta Geotechnica*:1-14.

1778 Faizal M, Bouazza A, Singh RM. (2016a) Heat transfer enhancement of geothermal energy piles. *Renewable*  
1779 *and Sustainable Energy Reviews* 57: 16–33. <http://dx.doi.org/10.1016/j.rser.2015.12.065>.

1780 Faizal M, Bouazza A, Singh RM. (2016b) An experimental investigation of the influence of intermittent and  
1781 continuous operating modes on the thermal behaviour of a full scale geothermal energy pile. *Geomechanics*  
1782 *for Energy and the Environment*, 8: 8-29. <https://doi.org/10.1016/j.gete.2016.08.001>.

1783 Faizal, M., Bouazza, A., McCartney, J.S., & Haberfield, C. (2018a) Axial and radial thermal responses of an  
1784 energy pile under a 6-storey residential building. *Canadian Geotechnical Journal*. [https://doi.org/10.1139/cgj-](https://doi.org/10.1139/cgj-2018-0246)  
1785 [2018-0246](https://doi.org/10.1139/cgj-2018-0246).

1786 Faizal, M., Bouazza, A., Haberfield, C., & McCartney, J.S. (2018b) Axial and radial thermal responses of a field  
1787 scale energy pile under monotonic and cyclic temperatures. *Journal of Geotechnical and Geoenvironmental*  
1788 *Engineering*. 144(10), 04018072.

1789 Fadejev, J., Simson, R., Kurnitski, J. & Haghghat, F. (2017). A review on energy piles design, sizing and  
1790 modelling. *Energy* 122, 390-407

1791 Fisher, D.E., Rees, S.J., Padhmanabhan, S.K. & Murugappan, A. (2006) Implementation and validation of  
1792 ground-source heat pump system models in an integrated building and system simulation environment,  
1793 *HVAC&R Research*, 12 (1), 693-710.

1794 Franzius, J.N. & Pralle, N. (2011) Turning segmental tunnels into sources of renewable energy, *Proceedings of*  
1795 *the ICE Civil Engineering*, 164, 35-40.

1796 Frodl, S. , Franzius, J. N. and Bartl, T. (2010). Design and construction of the tunnel geothermal system in  
1797 Jenbach /. Geomechanik Tunnelbau | Geomechanics and Tunnelling, 3(5),, 658-668.  
1798 doi:10.1002/geot.201000037

1799 Gao, J., Zhang, X., Liu, J., Li, K. & Yang, J. (2008). Numerical and experimental assessment of thermal  
1800 performance of vertical energy piles: an application, Applied Energy, 85, 901-910.

1801 Garber, D., Choudhary, R. & Soga, K. (2013) Risk based lifetime costs assessment of a ground source heat pump  
1802 (GSHP) system design: Methodology and case study, Building and the Environment, 60, 66 – 80.

1803 Gawecka et al. (2016), Effects of transient phenomena on the behaviour of thermo-active piles. Proc. 1st Int.  
1804 Conf. Energy Geotechnics, ICEGT 2016, 71-78

1805 Gawecka et al. (2017), Numerical modelling of thermo-active piles in London Clay, ICE Geotechnical  
1806 Engineering, 170, 201-219

1807 Gehlin, S. (2002) Thermal response test, model development and evaluation, Doctoral Thesis, Lulea Technical  
1808 University.

1809 Gehlin & Hellstrom (2003) Influence on thermal response test by groundwater flow in vertical fractures in hard  
1810 rock. Renewable Energy 28(14): pp. 2221-2238.

1811 Geimer, C., 2013. Metro tunnels enable geothermal-air conditioning – BINE information service, Projektinfo  
1812 09/2013, FIZ Karlsruhe – Leibniz Institute for Information Infrastructure, Germany (ISSN 0937-8367)

1813 Ghaaowd, I., Takai, A., Katsumi, T., and McCartney, J.S. (2017) Pore water pressure prediction for undrained  
1814 heating of soils. Environmental Geotechnics. 4(2), 70-78.

1815 Ghaaowd, I., McCartney, J.S., Huang, X., Saboya, F., & Tibana, S. (2018) Issues with centrifuge modeling of  
1816 energy piles in soft clays. 9<sup>th</sup> International Conference on Physical Modelling in Geotechnics. London, England.  
1817 Jul. 17-20. 1-6.

1818 Glassley, W. (2010) Geothermal energy: renewable energy and the environment. 2010, Florida, USA: CRC  
1819 Press. 320 Pages. ISBN 9781420075700

1820 Go, G-H., Lee, S-R., Yoon, S., Kang, H-B. (2014) Design of spiral coil PHC energy pile considering effective  
1821 borehole thermal resistance and groundwater advection effects, Applied Energy, 125, 165-178.

1822 Goode, J.C., III, Zhang, M. & McCartney, J.S. (2014) Centrifuge modeling of energy foundations in sand. Physical  
1823 Modeling in Geotechnics: Proc. 8<sup>th</sup> International Conference on Physical Modelling in Geotechnics. Perth,  
1824 Australia. Jan. 14-17. C. Gaudin & D. White, eds. Taylor and Francis. London. 729-736.

1825 Goode, J.C., III, & McCartney, J.S. (2014) Evaluation of head restraint effects on energy foundations. Proc.  
1826 GeoCongress 2014 (GSP 234), M. Abu-Farsakh & L. Hoyos, eds. ASCE. Pp. 2685-2694.

1827 Goode, J.C., III, & McCartney, J.S. (2015) Centrifuge modeling of boundary restraint effects in energy  
1828 foundations. ASCE Journal of Geotechnical and Geoenvironmental Engineering. 141(8), 04015034-1-13.

1829 GSHPA (2012) *Thermal pile design installation and materials standards*, Issue 1.0. Ground Source Heat Pump  
1830 Association, Milton Keynes, UK, p. 85.

1831 GSHPA (2011) *Closed-loop Vertical Borehole Design, Installation & Materials Standards Issue 1.0*, September  
1832 2011. Ground Source Heat Pump Association, Milton Keynes, UK.

1833 Habert, J., El'Mejahed, M. & Bernard J-B. (2016) Lessons learned from mechanical monitoring of a  
1834 thermoactive pile, In: *Energy Geotechnics: Proceedings of the 1st International Conference on Energy*  
1835 *Geotechnics*, F. Wuttke, S. Bauer, M. Sanchez, eds. ICEGT 2016, Kiel, Germany, 29-31 August 2016.

1836 Hamada, Y., Saitoh, H., Nakamura, M., Kubota, H., & Ochifuji, K. (2007) Field performance of an energy pile  
1837 system for space heating, *Energy and Buildings*, 39, 517-524.

1838 Hellstrom, G. (1989) *Duct Ground Heat Storage Model, Manual for Computer Code*. Department of  
1839 Mathematical Physics, University of Lund, Sweden.

1840 Hellstrom, G., 1991. *Ground Heat Storage, Thermal Analysis of Duct Storage Systems, Theory*. Department of  
1841 Mathematical Physics, University of Lund, Sweden.

1842 Hemmingway, P. & Long, M. (2013) Energy piles: site investigation and analysis, *Proc. Inst. Civil. Eng.*  
1843 *Geotechnical Engineering* 166(6), 561-575.

1844 Henderson, H.I., Carlson, S.W. & Walburger, A.C. (1998) North American monitoring of a hotel with room sized  
1845 GSHPs, *Proc IEA Room Size Heat Pump Conference*, Canada, 1998.

1846 Han C. & Yu X. (2018) An innovative energy pile technology to expand the viability of geothermal bridge deck  
1847 snow melting for different United States regions: Computational assisted feasibility analyses, *Renew. Energy*  
1848 123: 417-427.

1849 Ho I.H. & Dickson M. (2017) Numerical modeling of heat production using geothermal energy for a snow-  
1850 melting system, *Geomech. Energy Environ.* 10: 42-51.

1851 Hughes, P. & Im, P. (2013) Foundation heat exchanger final report: demonstration, measured performance,  
1852 and validated model and design tool, Oak Ridge National Laboratory, Available online  
1853 [http://web.ornl.gov/sci/ees/etsd/btrc/publications/ORNL-](http://web.ornl.gov/sci/ees/etsd/btrc/publications/ORNL-FHX%20Final%20Report_Jan%202012%20for%20Distribution_rev_01152013.pdf)  
1854 [FHX%20Final%20Report\\_Jan%202012%20for%20Distribution\\_rev\\_01152013.pdf](http://web.ornl.gov/sci/ees/etsd/btrc/publications/ORNL-FHX%20Final%20Report_Jan%202012%20for%20Distribution_rev_01152013.pdf)

1855 ICConsulten (2005) *Wirtschaftliche optimierung von tunnelthermieabsorberanlagen,*  
1856 *grundlagenuntersuchung und planungsleitfaden*, 23.12.2005. Rev 1, 84 pp.

1857 IGSHPA (2009) *Ground Source Heat Pump Residential and Light Commercial Design and Installation Guide*,  
1858 Oklahoma State University, Stillwater, USA.

1859 IGSHPA (2007) *Closed-loop/geothermal heat pump systems: Design and installation standards*, International  
1860 Ground Source Heat Pump Association/Oklahoma State University.

1861 Ingersoll, L.R., Zobel, O.J. & Ingersoll, A.C. (1954) *Heat Conduction with Engineering and Geological*  
1862 *Applications*. 3<sup>rd</sup> Edition, McGraw-Hill, New York.

1863 Jalaluddin, Miyara, A., Tsubaki, K., Inoue, S., & Yoshida, K. (2011) Experimental study of several types of ground  
1864 heat exchanger using a steel pile foundation, *Renew Energy*, 36, 764-771.

1865 Javed S and Claesson J (2011) New analytical and numerical solutions for the short-term analysis of vertical  
1866 ground heat exchangers. *ASHRAE Transactions*, 117(1), 3-12.

1867 Jensen-Page, L., Narsilio G., Bidarmaghz, A., and Johnston, I., (2018). Investigation of the effect of seasonal  
1868 variation in ground temperature on Thermal Response Tests *Renewable Energy*, 125, 609-619.

1869 Johnston, I.W., Narsilio, G.A., Colls, S., Valizadeh Kivi, A., Payne, D., Wearing-Smith, M. & Noonan, G. (2014)  
1870 Direct geothermal energy demonstration projects for Victoria, Australia *IPENZ Transactions (NZ)* (ISSN 1179-  
1871 9293) 41, pp. 1-10.

- 1872 Kakaç, S. & Yener, Y. 2008. Heat conduction, 4rd Edition, Taylor and Francis Group, Boca Raton FL, USA,
- 1873 Kalantidou, A., Tang, A.M., Pereira, J.-M., & Hassen, G. (2012) Preliminary study on the mechanical  
1874 behaviour of heat exchanger pile in physical model." *Géotechnique*. 62 (11), 1047-1051.
- 1875 Kaltreider, C., Krarti, M. & McCartney, J.S. (2015) Heat transfer analysis of thermo-active foundations. *Energy*  
1876 *and Buildings*. 86, 492-501.
- 1877 Katsura, T., Nakamura, Y., Okawada, T., Hori, S. & Nagano, K. (2009) Field test on heat extraction or injection  
1878 performance of energy piles and its application, *Proceedings of EFFSTOCK*, 2009.
- 1879 Katzenbach, R., Olgun, C.G., Loveridge, F., Suttman, M., Bowers, G. A., McCartney, J.S., Laloui, L., Mimouni, T.,  
1880 Dupray, F., Spitler, J. D., Clauss, F., Meyer, L. L. & Akrouch, G. (2014) New Technologies and Applications;  
1881 *Materials and Equipment in Near Surface Geothermal Systems*, *DFI Journal*, 8 (2), 93-107.
- 1882 Khosravi, A., Abdelrahman, S., & McCartney, J.S. (2012) Evaluation of thermal soil-structure interaction in  
1883 energy foundations using an impulse-response test. *Proc. GeoCongress 2012 (GSP 225)*. R.D. Hryciw, A.  
1884 Athanasopoulos-Zekkos, & N. Yesiller, eds. ASCE. 4466-4475.
- 1885 Kipry, H., Bockelmann, F., Plessner, S. & Fisch, M.M. (2009) Evaluation of optimisation of UTES system of energy  
1886 efficient buildings, *Proceedings of EFFSTOCK*, 2009.
- 1887 Knellwolf, C., Peron, H., & Laloui, L. (2011) Geotechnical analysis of heat exchanger piles. *J. Geotech*  
1888 *Geoenviron Eng.* 137(10):890-902.
- 1889 Ko, H-Y. (1988) Summary of the state-of-the-art in centrifuge model testing. *Centrifuges in Soil Mechanics*.  
1890 W.H. Craig, R.G. James, & A.N. Schofield, eds., Balkema, Rotterdam, Netherlands, 11-18.
- 1891 Kramer, C.A. & Basu, P. (2014a) Experimental characterization of energy output from a model geothermal pile.  
1892 *Proc. GeoCongress 2014*. ASCE, Reston, VA. 3703-3712.
- 1893 Kramer, C.A. & Basu, P. (2014b) Performance of a model geothermal pile in sand. *Proceedings of 8<sup>th</sup>*  
1894 *International Conference on Physical Modelling in Geotechnics*. Perth, Australia. Jan. 14-17. C. Gaudin & D.  
1895 White, eds. Taylor and Francis. London. 771-777.
- 1896 Kramer, C.A., Ghasemi-Fare, O. & Basu, P. (2015) Laboratory thermal performance tests on a model heat  
1897 exchanger pile in sand. *Geotechnical and Geological Engineering*. 33 (2), 253-271.
- 1898 Krishnaiah, S., & Singh, D.N. (2004) Centrifuge modelling of heat migration in soils. *International Journal on*  
1899 *Physical Modeling in Geotechnics*. 4 (3), 39-47.
- 1900 Kurten, S. (2011) Use of geothermal energy with thermo-active seal panels, *Geotechnical Engineering: New*  
1901 *Horizons*, *Proc 21<sup>st</sup> European Young Geotechnical Engineers Conference*, Rotterdam, 2011.
- 1902 Kurten, S., Mottaghy, D. & Ziegler, M. (2015a) Design of plane energy geostructures based on laboratory tests  
1903 and numerical modelling. *Energy and Buildings*, 107, 434 - 444.
- 1904 Kurten, S., Mottaghy, D. & Ziegler, M (2015b) A new model for the description of the heat transfer for plane  
1905 thermo-active geotechnical systems based on thermal resistances. *Acta Geotechnica*, 10 (2), 219 - 229.
- 1906 Lai, S. (1988) Similitude for Shaking Table Tests on Soil-Structure-Fluid Model in 1G Gravitational Field. Report  
1907 to the Port and Harbour Research Institute. Report 27.3. 3-24.
- 1908 Laloui, L., Olgun, C.G., Sutman, M., McCartney, J.S., Coccia, C.J.R., Abuel-Naga, H.M., and Bowers, G.A. (2014)  
1909 *Issues involved with thermo-active geotechnical systems: Characterization of thermo-mechanical soil*



1910 behaviour and soil-structure interface behaviour. *The Journal of the Deep Foundations Institute*. 8(2), 107-  
1911 119.

1912 Laloui, L., Nuth, M., and Vulliet, L. (2006) Experimental and numerical investigations of the behaviour of a heat  
1913 exchanger pile. *Int. J. Numer. Anal. Methods Geomech.*, 30(8), 763–781.

1914 Laloui & Di Donna. (2013) *Energy geostructures*. John Wiley & Sons.

1915 Laloui, L. (2011) In-situ testing of heat exchanger pile. *GeoFrontiers 2011, Geotechnical special publication*  
1916 211, J. Han and D. E. Alzamora, eds., ASCE, Reston, VA, 410–419.

1917 Laloui, L., Moreni, M., and Vulliet, L. (2003) Comportement d'un pieu bifonction, fondation et échangeur de  
1918 chaleur. *Can. Geotech. J.*, 40(2), 388–402.

1919 Laloui, L., and Nuth, M. (2006) Numerical modeling of some features of heat exchanger pile. *Foundation*  
1920 *Analysis and Design: Innovative Methods*. Geotechnical Special Publication 153. R.L. Parsons, L. Zhang, W. D.  
1921 Guo, K.K. Phoon, and M. Yang, eds., ASCE, Reston, VA. 189–195.

1922 Lamarche L, & Beauchamp B (2007) A new contribution to the finite line-source model for geothermal  
1923 boreholes. *Energy and Buildings*, 39(2), 188-198.

1924 Lamarche, L., Kajl, S. & Beauchamp, B. (2010) A review of methods to evaluate borehole thermal resistance in  
1925 geothermal heat pump systems, *Geothermics*, 39, 187-200.

1926 Lazzari, S., Priarone, A. & Zanchini, E. (2010) Long-term performance of BHE (borehole heat exchanger) fields  
1927 with negligible groundwater movement. *Energy*, 35, pp. 4966-4974.

1928 Lee, C., Park, S., Choi, H.-J., Lee, I.-M. & Choi, H. (2016) Development of energy textile to use geothermal  
1929 energy in tunnels. *Tunnelling and Underground Space Technology* 59, 105-113.

1930 Lee, C., Park, S., Won, J., Jeoung, J., Sohn, B. & Choi, H. (2012) Evaluation of thermal performance of energy  
1931 textile installed in tunnel, *Renewable Energy*, 42, 11-22.

1932 Li, M. & Lai, A.C.K. (2012) New temperature response functions (g-functions) for pile and borehole ground  
1933 heat exchangers based on composite-medium-line-source theory. *Energy*, 38(Feb), 255-263

1934 Loveridge, F. & Cecinato, F. (2016) Thermal performance of thermo-active CFA piles, *Proceedings of the*  
1935 *Institution of Civil Engineers, Environmental Geotechnics*, 3(4), 265-279.

1936 Loveridge, F. & Powrie, W. (2014) On the thermal resistance of pile heat exchangers, *Geothermics*. 50, 122 -  
1937 135.

1938 Loveridge, F. & Powrie, W. (2013a) Pile heat exchangers: thermal behaviour and interactions, *Proceedings of*  
1939 *the Institution of Civil Engineers Geotechnical Engineering*, 166 (2), 178 - 196.

1940 Loveridge, F., Powrie, W. and Nicholson, D. (2014b) Comparison of two different models for pile thermal  
1941 response test interpretation, *Acta Geotechnica*, 9 (3), 367-384

1942 Loveridge, F. & Powrie, W. (2013b) Temperature response functions (G-functions) for single pile heat  
1943 exchangers, *Energy*, 57, 554 - 564.

1944 Loveridge, F., Brettmann, T., Olgun, G. & Powrie, W. (2014a) Assessing the applicability of thermal response  
1945 testing to energy piles, *DFI-EFFC International Conference on Piling and Deep Foundations*, Stockholm,  
1946 Sweden, 20-21 May 2014.

- 1947 Loveridge, F., Olgun, C.G., Brettmann, T. & Powrie, W. (2015) The thermal behaviour of three different auger  
1948 pressure grouted piles used as heat exchangers, *Geotechnical and Geological Engineering*, 33 (2), 273 – 289.
- 1949 Loveridge F. A., Amis T & Powrie W (2012) Energy Pile Performance and Preventing Ground Freezing,  
1950 Proceedings of the 2012 International Conference on Geomechanics and Engineering (ICGE'12), Seoul, August,  
1951 2012.
- 1952 Low, J., Loveridge, F., Nicholson, D. & Powrie, W. (2015) A comparison of laboratory and in situ methods to  
1953 determine soil thermal conductivity for energy foundations applications, *Acta Geotechnica*, 10, 209-218.
- 1954 Maddocks, D.F. & Savidou, C. (1984) The effects of heat transfer from a hot penetrometer installed in the  
1955 ocean bed. Application of Centrifuge Modeling to Geotechnical Design. W.H. Craig, ed. Balkema, Rotterdam.  
1956 337-356.
- 1957 Lu, Q. & Narsilio, G.A. (2019) Economic analysis of utilising energy piles for residential buildings. *Renewable*  
1958 *Energy*; under review.
- 1959 Makasis, N., Narsilio G., Bidarmaghz, A. and Johnston, I.W., (2018a). "Ground-source heat pump systems: The  
1960 effect of variable pipe separation in ground heat exchangers", *Computers and Geotechnics*, 100 (August), 97-  
1961 109.
- 1962 Makasis, N., Narsilio G., Bidarmaghz, A. and Johnston, I.W., (2018b). "Carrier fluid temperature data in vertical  
1963 ground heat exchangers with a varying pipe separation", *Data in Brief*, 18 (June), 1466-1470.
- 1964 Makasis, N., Narsilio G., and Bidarmaghz, A. (2018c). "A robust prediction model approach to energy geo-  
1965 structure design", *Computers and Geotechnics*, 104 (December), 140-151.
- 1966 Makasis, N., Narsilio G., and Bidarmaghz, A. (2018d) A machine learning approach to energy pile design,  
1967 *Computers and Geotechnics*, 97 (May), 189-203.
- 1968 Man, Y., Yang, H., Diao, N., Cui, P., Lu L. & Fang, Z. (2011) Development of a spiral heat source model for novel  
1969 pile ground heat exchangers, *HVAC&R Research*, 17 (6), 1075-1088.
- 1970 Man Y, Yang H, Diao N, Liu J and Fang Z (2010) A new model and analytical solutions for borehole and pile  
1971 ground heat exchangers. *Intl. J. of Heat and Mass Transfer*, 53(13-14), 253-2601
- 1972 Maragna C; Loveridge F (2019) A resistive-capacitive model of pile heat exchangers with an application to  
1973 thermal response tests interpretation. *Renewable Energy*, **138**, pp. 891-910
- 1974 Marcotte, D. & Pasquier, P. (2008) On the estimation of thermal resistance in borehole thermal conductivity  
1975 test. *Renewable Energy*, 33, pp. 2407-2415.
- 1976 Marcotte, D., Pasquier, P., Sheriff, F. & Bernier, M. (2010) The importance of axial effects for borehole design  
1977 of geothermal heat-pump systems. *Renewable Energy*, 35, pp. 763-770.
- 1978 Marto, A. & Amaludin, A. (2015) Response of shallow geothermal energy pile from laboratory model tests.  
1979 *International Symposium on Geohazards and Geomechanics (ISGG2015)*. 1-9.
- 1980 McCartney, J.S. (2015) Structural performance of thermo-active foundations. In: *Advances in Thermo-Active*  
1981 *Foundations*. M. Krarti, ed. ASME Press. New York. pp. 1-44. ISBN: 9780791861059.
- 1982 McCartney, J.S., and Murphy, K.D. (2012) Strain distributions in full scale energy foundations. *J. Deep Found.*  
1983 *Inst.*, 6(2), 28–36.

- 1984 McCartney, J. S., Sánchez, M., & Tomac, I. (2016) Energy geotechnics: Advances in subsurface energy recovery,  
1985 storage, exchange, and waste management, *Computers and Geotechnics*, 75, 244-256.
- 1986 McCartney, J.S. (2013) Centrifuge modeling of energy foundations. *Energy Geostructures: Innovation in*  
1987 *Underground Engineering*, L. Laloui & A. Di Donna, eds., Wiley-ISTE, London, 99-115.
- 1988 McCartney, J.S., Rosenberg, J.E., & Sultanova, A. (2010) Engineering performance of thermo-active foundation  
1989 systems. *GeoTrends: The Progress of Geological and Geotechnical Engineering in Colorado at the Cusp of a*  
1990 *New Decade (GPP 6)*. C.M. Goss, J.B. Kerrigan, J. Malamo, M.O. McCarron, M.O. & R.L. Wiltshire, eds. 27-42.
- 1991 McCartney, J.S. & Rosenberg, J.E. (2011) Impact of heat exchange on side shear in thermo-active foundations.  
1992 *GeoFrontiers 2011 (GSP 211)*. J. Han & D.E. Alzamora, eds. ASCE, Reston VA. 488-498.
- 1993 McCartney, J.S. & Murphy, K.D. (2017) Investigation of potential dragdown/uplift effects on energy piles.  
1994 *Geomechanics for Energy and the Environment*. 10(June), 21-28. DOI: 10.1016/j.gete.2017.03.001.
- 1995 Menezes, C., Cripps, A., Bouchlaghem, D. & Russel, R., (2012) Predicted vs actual energy performance on non-  
1996 domestic buildings: using post occupancy evaluation data to reduce the performance gap, *Applied Energy*, 97,  
1997 355-364.
- 1998 Mikhaylova, O., Johnston, I.W., and Narsilio, G.A. (2016a) Uncertainties in the Design of Ground Heat  
1999 Exchangers, *Environmental Geotechnics*, Themed issue on energy geostructures, *Proceedings of the*  
2000 *Institution of Civil Engineers ICE (UK)*, 3 (4), August 2016, 253-264. DOI: 10.1680/jenge.15.00033.
- 2001 Mikhaylova O., Soga K., Choudhary R., Johnston I. (2016b) Utilisation of Urban Open Spaces for Sustainable  
2002 Heating and Cooling: A City-Scale Perspective. in Wuttke, F., Bauer, S. & Sanchez, M. (eds.). *Energy*  
2003 *Geotechnics: Proceedings of the 1st International Conference on Energy Geotechnics, ICEGT 2016*. CRC  
2004 Press/Balkema, p. 37-44 8 p. Kiel, Germany, 29-31 August 2016
- 2005 Mikhaylova, O., Johnston I.W., & Narsilio, G.A. (2016c) Ground thermal response to borehole ground heat  
2006 exchangers, In: *Energy Geotechnics: Proceedings of the 1st International Conference on Energy Geotechnics*,  
2007 F. Wuttke, S. Bauer, M. Sanchez, eds. ICEGT 2016, Kiel, Germany, 29-31 August 2016.
- 2008 Minto, A., Leung, A. K., Vitali, D. & Knappett, J. A. (2016) Thermomechanical properties of a new small-scale  
2009 reinforced concrete thermo-active pile for centrifuge testing in Wuttke, F., Bauer, S. & Sanchez, M.  
2010 (eds.). *Energy Geotechnics: Proceedings of the 1st International Conference on Energy Geotechnics, ICEGT*  
2011 *2016*. CRC Press/Balkema, p. 37-44 8 p.
- 2012 Mimouni, T. & Laloui, L. (2014) Towards a secure basis for the design of geothermal piles, *Acta Geotechnica*,  
2013 9 (3), 355-366.
- 2014 Mimouni, T., Dupray, F. & Laloui, L. (2014) Estimating the geothermal potential of heat-exchanger anchors on  
2015 a cut-and-cover tunnel, *Geothermics*, 51, 380-387.
- 2016 Mimouni, T., & Laloui, L. (2015) Behaviour of a group of energy piles. *Canadian Geotechnical Journal*. 52, 1913-  
2017 1929.
- 2018 Mogensen P. (1983) Fluid to duct wall heat transfer in duct system heat storages. In: *International conference*  
2019 *on subsurface heat storage in theory and practice*, Stockholm, Sweden: Swedish Council for Building Research,  
2020 p. 652-57.
- 2021 Morino, K. & Oka, T. (1994) Study on heat exchanged in soil by circulating water in a steel pile, *Energy Build.*,  
2022 21 (1), 65-78.

- 2023 Mortada, A., Choudhary, R. & Soga, K. (2018) Multi-dimensional simulation of underground subway spaces  
2024 coupled with geoenergy systems. *Journal of Building Performance Simulation* 11(5), 517-537.
- 2025 Muraya, N.K., O'Neal, D.L. & Heffington, W.M. (1996) Thermal interference of adjacent legs in a vertical U-  
2026 tube heat exchanger for a ground-coupled heat pump. *ASHRAE Transactions*, 102, pp. 12-21.
- 2027 Murphy, K.D., Henry, K.S., & McCartney, J.S. (2014) Impact of horizontal run-out length on the thermal  
2028 response of full-scale energy foundations. *Proceedings of GeoCongress 2014 (GSP 234)*, M. Abu-Farsakh and  
2029 L. Hoyos, eds. ASCE. pp. 2715-2714.
- 2030 Murphy, K.D. & McCartney, J.S. (2014) Thermal borehole shear device. *ASTM Geotechnical Testing Journal*.  
2031 37(6), 1040-1055.
- 2032 Murphy, K.D., and McCartney, J.S. (2015) Seasonal response of energy foundations during building operation.  
2033 *Geotech. Geol. Eng.*, 33(2), 343-356.
- 2034 Murphy, K.D., McCartney, J.S., and Henry, K.S. (2015) Evaluation of thermo-mechanical and thermal behaviour  
2035 of full-scale energy foundations. *Acta Geotechnica*, 10(2), 179-195.
- 2036 Nagano, K., Katsura, T., Takeda, S., Saeki, E., Nakamura, Y., Okamoto, A. & Narita, S. (2005) Thermal  
2037 characteristics of steel foundation piles as ground heat exchangers, *Proc. 8th IEA Heat Pump Conference 2005*,  
2038 Las Vegas, P6-12.1-9.
- 2039 Nam, Y. & Chae, H-B. (2014) Numerical simulation for optimum design of ground source heat pump system  
2040 using building foundation as horizontal heat exchanger, *Energy*, 73, 933 - 942.
- 2041 Narsilio G. A., Johnston, I. W., Colls, S., Bidarmaghz, A., Valizadeh-kivi, A., and Neshastehriz, S. (2012) Direct  
2042 geothermal energy research and demonstration projects for Victoria, Australia. In Choi, Chang-Koon (ed.),  
2043 *Proceedings of the 2012 World Congress on Advances in Civil, Environmental, and Materials Research*  
2044 *(ACEM'12)*. ISBN 978-89-89693-34-5 98530. Seoul, Korea, July 26-29, 2433-2446.
- 2045 Narsilio, G. A., Johnston, I. W., Bidarmaghz, A., Colls, S., O. Mikhaylova, O., Kivi, A. and Aditya, R. (2014)  
2046 *Geothermal energy: Introducing an emerging technology*. In: Horpibulsuk, S., Chinkulkijniwat, A., and  
2047 Suksiripattanapong, C., eds. *Proceedings of the International Conference on Advances in Civil Engineering for*  
2048 *Sustainable Development (ACESD 2014)*, Suranaree University of Technology, Nakhon Ratchasima, Thailand,  
2049 27-29 August. Volume 1 of 2, pp. 141-154.
- 2050 Narsilio, G.A., Bidarmaghz, A., Johnston, I.W., and Colls, S. (2018) Detailed numerical modelling of ground heat  
2051 exchangers based on first principles. *Computers and Geotechnics*, ( accepted).
- 2052 Narsilio, G., Bidarmaghz, A., Disfani, M., Johnston, I. and Makasis, N. (2016a) Geo-exchange feasibility study -  
2053 Phase 1: Parkville and Domain metro stations, Melbourne (Vic), Australia. MMRA (Part of Report MMR-AJM-  
2054 PWAA-RP-MM- 002505.P3.IFR and MMR-AJM-PWAA-RP-MM-003122.P2.IFR). 66 pages.
- 2055 Narsilio, G., Makasis, N., Bidarmaghz, A., Disfani, M., (2016b) Geo-exchange feasibility study - Phase 2:  
2056 Parkville metro station, Melbourne (Vic), Australia. MMRA. 65 pages.
- 2057 Nicholson, D., Chen, Q., de Silva, M., Winter, A. & Winterling, R. (2014a) The design of thermal tunnel energy  
2058 segments for Crossrail, UK, *Proc ICE Sustainability*, 167 (3), 118-134.
- 2059 Nicholson, D., Smith, P., Bowers, G. A., Cuceoglu, F., Olgun, C. G., McCartney, J. S., Henry, K., Meyer, L. L. &  
2060 Loveridge, F. A. (2014b) Environmental impact calculations, life cycle cost analysis, *DFI Journal*, 8 (2), 130-146.

2061 Nicholson, DP, Chen, Q, Pillai, A, Chendorain, M. (2013), Developments in thermal pile and thermal tunnel  
2062 linings for city scale GSHP systems. In: Thirty-eighth workshop on geothermal reservoir engineering, Stanford  
2063 University, Stanford, California SGPTR-198; February 11-13, 2013. p. 8.

2064 Ng, C.W.W., Shi, C., Gunawan, A., Laloui, L., & Liu, H.L. (2015) Centrifuge modelling of heating effects on energy  
2065 pile performance in saturated sand. *Canadian Geotechnical Journal*. 52(8): 1–13.

2066 Ng, C.W.W., Shi, C., Gunawan, A., & Laloui, L. (2014) Centrifuge modelling of energy piles subjected to heating  
2067 and cooling cycles in clay. *Géotechnique Letters* 4: 310–316.

2068 Olgun, C. G., Ozudogru, T. Y., Abdelaziz, S. L., and Senol, A. (2014) Long-term performance of heat exchanger  
2069 pile groups. *Acta Geotechnica*. 10(5), 553–569.

2070 Olgun, C.G. and McCartney, J.S. (2014) Outcomes from the International Workshop on Thermoactive  
2071 Geotechnical Systems for Near-Surface Geothermal Energy: From Research to Practice. *The Journal of the  
2072 Deep Foundations Institute*. 8(2), 58-72.

2073 Olgun, C. G. and Bowers, G. A. (2013) Numerical modeling of ground source bridge deck deicing. *International  
2074 Workshop on Geomechanics and Energy–The Ground as Energy Source and Storage*, Lausanne, Switzerland,  
2075 26-28

2076 Ooka, R., Sekine, K., Mutsumi, Y., Yoshiro, S. & SuckHo, H. (2007) Development of a ground source heat pump  
2077 system with ground heat exchanger utilizing the cast-in place concrete pile foundations of a building. *EcoStock  
2078 2007*. 1-8.

2079 Oschner, K. (2008) *Geothermal Heat Pumps, A Guide for Planning and Installation*. Earthscan, London, UK.

2080 Ouyang, Y., Soga, S., and Leung, Y.F. (2011) Numerical back-analysis of energy pile test at Lambeth College,  
2081 London. *GeoFrontiers 2011 (GSP 211)*. J. Han & D.E. Alzamora, eds. ASCE, Reston VA. 440-449.

2082 Ozudogru, T., Olgun, C.G., & Arson, C. (2015) Analysis of friction induced thermo-mechanical stresses on a heat  
2083 exchanger pile in isothermal soil. *Geotechnical and Geological Engineering*. 33, 357-371.

2084 Pahud, D. (2007) *PILESIM2, Simulation Tool for Heating/Cooling Systems with Heat Exchanger Piles or Borehole  
2085 Heat Exchangers*, User Manual, Scuola Universitaria Professionale della Svizzera Italiana, Lugano, Switzerland.

2086 Pahud, D. & Hubbach, M. (2007) Measured Thermal Performances of the Energy Pile System of the Dock  
2087 Midfield at Zürich Airport, *Proceedings European Geothermal Congress 2007*, Unterhaching, Germany, 30  
2088 May-1 June 2007.

2089 Park, H., Lee, S.R., Yoon, S. & Choi, J.C. (2013) Evaluation of thermal response and performance of PHC energy  
2090 pile: field experiments and numerical simulation, *Appl. Energy*, 103 (3), 12–24.

2091 Park S, Sung C, Jung K, Sohn B, Chauchois A, & Choi H (2015) Constructability and heat exchange efficiency of  
2092 large diameter cast-in-place energy piles with various configurations of heat exchange pipe. *Applied Thermal  
2093 Engineering*. 90:1061-1071.

2094 Pasten, C., and Santamarina, J. (2014) Thermally induced long-term displacement of thermoactive piles. *J.  
2095 Geotech. Geoenviron. Eng.*, 10.1061/(ASCE)GT.1943-5606.0001092, 06014003.

2096 Paul, N.D. (1996). The effect of grout thermal conductivity on vertical geothermal heat exchanger design and  
2097 performance. Mechanical Engineering Dept., South Dakota State University.

2098 Piemontese, M. (2018) Sensitivity Analysis on the Geothermal Potential of Energy Walls. Master's Thesis.  
2099 Politecnico di Torino.

- 2100 Rammal, D., Mroueh, H., & Burlon, S. (2018) Thermal behaviour of geothermal diaphragm walls: Evaluation of  
2101 exchanged thermal power. *Renewable Energy*. <https://doi.org/10.1016/j.renene.2018.11.068>.
- 2102 Raymond, J., Therrien, R. and Gosselin, L. (2011). Borehole temperature evolution during thermal response  
2103 tests, *Geothermics*, 40, (2011), pp. 69-78
- 2104 Rees, S.J. & Fan, D. (2013) A numerical implementation of the Dynamic Thermal Network method for long time  
2105 series simulation of conduction in multi-dimensional non-homogeneous solids. *International Journal of Heat  
2106 and Mass Transfer*, 61. pp. 475-489.
- 2107 Rees, S.J. & He, M. (2013) A three-dimensional numerical model of borehole heat exchanger heat transfer and  
2108 fluid flow. *Geothermics*. 46, 1-13.
- 2109 Rocha, M. (1957) The possibility of solving soil mechanics problems by the use of models. Proc. 4<sup>th</sup>  
2110 international Conference on Soil Mechanics and Foundation Engineering. Taylor and Francis. London. Vol. 1.  
2111 183-188.
- 2112 Rosenberg, J.E. (2010) Centrifuge Modeling of Soil Structure Interaction in Thermo-Active Foundations. M.S.  
2113 Thesis. University of Colorado at Boulder.
- 2114 Rotta Loria, A. F., Gunawan, A., Shi, C., Laloui, L., and Ng, C. W. W. (2015a) Numerical modelling of energy piles  
2115 in saturated sand subjected to thermo-mechanical loads. *Geomech. Energy Environ.*, 1, 1-15.
- 2116 Rotta Loria, A.F., Di Donna, A., & Laloui, L. (2015b) Numerical study on the suitability of centrifuge testing for  
2117 capturing the thermal-induced mechanical behaviour of energy piles. *ASCE Journal of Geotechnical and  
2118 Geoenvironmental Engineering*. 141 (10), 04015042-1-10.
- 2119 Rotta Lora, A. & Laloui, L. (2016a) The interaction factor method for energy pile groups, *Computers and  
2120 Geotechnics*, 80, 121-137.
- 2121 Rotta Loria, A.F. & Laloui, L. (2016b) Thermally induced group effects among energy piles. *Géotechnique*.  
2122 <http://dx.doi.org/10.1680/jgeot.16.P.039>.
- 2123 Rotta Loria, A.F. & Laloui, L. (2017a) The equivalent pier method for energy pile groups. *Geotechnique*  
2124 67(8):691-702.
- 2125 Rotta Loria, A.F. & Laloui, L. (2017b) Group action effects caused by various operating energy piles.  
2126 *Geotechnique*: 10.1680/jgeot.17.P.213.
- 2127 Rotta Loria, A.F. & Laloui, L. (2017c) Thermally induced group effects among energy piles. *Geotechnique*  
2128 67(5):374-393
- 2129 Rui, Y. & Yin, M. (2018) Thermo-hydro-mechanical coupling analysis of a thermo-active diaphragm wall. *Can.  
2130 Geotech. J.*, 55, 720-735.
- 2131 Ryżyński, G. & Bogusz, W. (2016) City-scale perspective for thermoactive structures in Warsaw. *Environmental  
2132 Geotechnics* 3(4), 280-290. <https://doi.org/10.1680/jenge.15.00031>
- 2133 Saggiu, R. & Chakraborty, T. (2015) Cyclic thermo-mechanical analysis of energy piles in sand. *Geotechnical and  
2134 Geological Engineering*. 33, 321-342.
- 2135 Sailer E, Taborda DMG, Zdravkovic L, 2018a, A new approach to estimating temperature fields around a group  
2136 of vertical ground heat exchangers in two-dimensional analyses, *Renewable Energy*, 118, 579-590.

- 2137 Sailer E, Taborda DMG, Zdravkovic L, Potts DM, 2018b, Factors affecting the thermo-mechanical response of  
 2138 a retaining wall under non-isothermal conditions, London, 9th European Conference on Numerical Methods  
 2139 in Geotechnical Engineering, Publisher: Taylor Francis Group, Pages: 741-749
- 2140 Samarakoon, R., Ghaaowd, I. & McCartney, J.S. (2018) Impact of drained heating and cooling on undrained  
 2141 shear strength of normally consolidated clay. *Energy Geotechnics: SEG-2018. Proceedings of the 2nd*  
 2142 *International Symposium on Energy Geotechnics. Lausanne, Switzerland. Sep. 26-28. A. Ferrari, L. Laloui, eds.*  
 2143 *Springer, Vienna. 243-249.*
- 2144 Sanchez, M., Falcão, F., Mack, M., Pereira, J-M., Narsilio, G., and Guimarães, L. (2017) Salient Comments from  
 2145 an Expert Panel on Energy Geotechnics. *Environmental Geotechnics, 4 (EG2): 135-142*
- 2146 Sanner, B., Hellstrom, G., Spitler, J. & Gehlin S.E A. (2005) Thermal Response Test – Current Status and World-  
 2147 Wide Application, In: *Proceedings World Geothermal Congress, 24-29th April 2005 Antalya, Turkey.*  
 2148 *International Geothermal Association.*
- 2149 Savidou, C. (1988) Centrifuge modelling of heat transfer in soil. *Proc., Centrifuge 88, J.-P. Corté, ed., Balkema,*  
 2150 *Rotterdam. 583-591.*
- 2151 Schneider, M. & Moormann, C. (2010) GeoTU6 – a geothermal tesearch project for tunnels. *Tunnel. 2/2010,*  
 2152 *14-21.*
- 2153 Sekine, K., Ooka, R., Yokoi, M., Shiba, Y. & Hwang, S. (2007) Development of a ground-source heat pump  
 2154 system with ground heat exchanger utilizing the cast-in-place concrete pile foundations of buildings, *ASHRAE*  
 2155 *Trans, January 2007, 558-566.*
- 2156 Shafagh, I. & Rees, S. (2018) A foundation wall heat exchanger model and validation study. *Proc. IGSHPA*  
 2157 *Research Conf., Stockholm, 336-344.*
- 2158 Shafagh, I. & Rees, S. (In Review) Conduction shape factors in rectangular sections with circular eccentric inner  
 2159 boundaries. *International Journal of Thermal Sciences. In Review.*
- 2160 Sharqawy, M.H., Mokheimer, E.M. & Badr, H.M. (2009) Effective pipe-to-borehole thermal resistance for  
 2161 vertical ground heat exchangers. *Geothermics 38, 271-277.*
- 2162 Shonder, J.A. & Beck, J.V. (1999) Determining effective soil formation thermal properties from field data using  
 2163 a parameter estimation technique. *ASHRAE Trans. 105, pp. 458-466.*
- 2164 Shonder, J.A., & Beck, J.V. (2000) Field test of a new method for determining soil formation thermal  
 2165 conductivity and borehole resistance. *ASHRAE Trans. 106, 843-850.*
- 2166 SIA-D0190 (2005) *Utilisation de la chaleur du sol par des ouvrages de fondation et de soutènement en béton,*  
 2167 *D 0190, Swiss Society of Engineers and Architects, Zurich, Switzerland.*
- 2168 Signorelli, S., Bassetti, S., Pahud, D. & Kohl, T. (2007) Numerical evaluation of thermal response tests,  
 2169 *Geothermics, 36, 141-166.*
- 2170 Singh, R., Bouazza, A., and Wang, B. (2015). Near-field ground thermal response to heating of a  
 2171 geothermal energy pile: observations from a field test. *Soils and Foundations*
- 2172 Soga, K. & Rui. (2016) *Energy geostructures. A chapter in Advances in ground-source heat pump systems (ed.*  
 2173 *S.J. Rees). Elsevier.*
- 2174 Soga, K, Yi, R., & Nicholson, D. (2015), Behaviour of a thermal wall installed in the Tottenham Court Road  
 2175 station box. *Proc. Crossrail Conf., Crossrail Ltd & Federation of Piling Specialists, City Hall, London, 112-119*

- 2176 Soga, K., Qi, H., Rui, Y. & Nicholson, D. (2014) Some considerations for designing GSHP coupled geotechnical  
 2177 structures based on a case study. 7th International Congress on Environmental Geotechnics (7ICEG2014),  
 2178 Melbourne, 10-14<sup>th</sup> November, 2014.
- 2179 Spitler, J.D. & Gehlin, S.E.A. (2015) Thermal response testing for ground source heat pump systems – An  
 2180 historical review, *Renewable and Sustainable Energy Reviews*, 50, 1125-1137.
- 2181 Spitler, J.D., Fisher, D.E., Cullin, J. R., Xing, L. Lee, E., Rees, S.J. & Fan, D. (2011) Foundation heat exchanger  
 2182 model and design tool development and validation, final report to Oak Ridge National Laboratory. Available  
 2183 online [http://temp-hvac.okstate.edu/sites/default/files/pubs/reports/01-FHX\\_2013.pdf](http://temp-hvac.okstate.edu/sites/default/files/pubs/reports/01-FHX_2013.pdf).
- 2184 Stephen, P. <https://www.railmagazine.com/infrastructure/stations/cooling-thetube>. Rail Magazine  
 2185 (February), 2016.
- 2186 Sterpi, D., Coletto, A., & Mauri, L. (2017), Investigation on the behaviour of a thermo-active diaphragm wall by  
 2187 thermo-mechanical analyses. *Geomech. for Energy and Environ.*, 9, 1-20.
- 2188 Sterpi, D., Tomaselli, G., Angelotti, A. (2018) Energy performance of ground heat exchangers embedded in  
 2189 diaphragm walls: Field observations and optimization by numerical modelling. *Renewable Energy*.  
 2190 <https://doi.org/10.1016/j.renene.2018.11.102>
- 2191 Stewart, M.A. & McCartney, J.S. (2012). Strain distributions in centrifuge model energy foundations.” *Proc.*,  
 2192 *GeoCongress 2012 (GSP 225)*, R.D. Hryciw, A. Athanasopoulos-Zekkos, & N. Yesiller, eds., ASCE, Reston, VA,  
 2193 4376–4385.
- 2194 Stewart, M.A. & McCartney, J.S. (2014) Centrifuge modeling of soil-structure interaction in energy  
 2195 foundations. *ASCE Journal of Geotechnical and Geoenvironmental Engineering*. 140 (4), 04013044-1-11.
- 2196 Sun, M., Xia, C. & Zhang, G. (2013) Heat transfer model and design method for geothermal heat exchange  
 2197 tubes in diaphragm walls, *Energy and Buildings*, 61, 250 – 259.
- 2198 Suryatriyastuti, M.E., Mroueh, H., & Burlon, S. (2014) A load transfer approach for studying the cyclic  
 2199 behaviour of thermo-active piles. *Computers and Geotechnics*. 55, 378-391.
- 2200 Suryatriyastuti, M.E., Mroueh, H., & Burlon, S. (2012) Understanding the temperature-induced mechanical  
 2201 behaviour of energy pile foundations. *Renewable and Sustainable Energy Reviews*. 16, 3344-3354.
- 2202 Suryatriyastuti, M.E., Burlon, S. & Mroueh, H., (2016) On the understanding of cyclic interaction mechanisms  
 2203 in an energy pile group. *Int. J. Numer. Anal. Meth. Geomech.* 40(1), 3-24.
- 2204 Sutman, M., Brettmann, T., and Olgun, C. G. (2014) Thermo-mechanical behaviour of energy piles: Full-scale  
 2205 field test verification. *DFI 39th Annual Conf. on Deep Foundations*, Deep Foundations Institute. 1-10.
- 2206 Tang, A.M., Kalantidou, A., Pereira, A., Hassen, G., & Yavari, N. (2014). Mechanical behaviour of energy piles  
 2207 in dry sand. *Geotechnical Engineering Journal of the SEAGS & AGSSEA*. 4 (3), 86-89.
- 2208 Tinti, F., Boldini, D., Ferrari, M., Lanconelli, M., Kasmaee, S., Bruno, R., Egger, H., Voza, A. & Zurlo, R. (2017)  
 2209 Exploitation of geothermal energy using tunnel lining technology in a mountain environment. A feasibility  
 2210 study for the Brenner Base tunnel – BBT. *Tunnelling and Underground Space Technology* 70, 182-203. Doi:  
 2211 10.1016/j.tust.2017.07.011
- 2212 TRNSYS. (2018) Available on the web at: <http://sel.me.wisc.edu/trnsys/index.html>.



- 2213 Wang, B., Bouazza, A., & Haberfield, C. (2011) Preliminary observations from laboratory scale model  
 2214 geothermal pile subjected to thermal-mechanical loading. *Geo-Frontiers 2011 (GSP 211)*. J. Han & D.E.  
 2215 Alzamora, eds. ASCE, Reston VA. 430-439.
- 2216 Wang, B., Bouazza, A., Barry-Macaulay, D., Singh, M.R., Webster, M., Haberfield, C., & Chapman, G. (2012a)  
 2217 Field and laboratory investigation of heat exchanger pile. *GeoCongress 2012*. Oakland, CA. 4396-4405.
- 2218 Wang, W., Regueiro, R., Stewart, M.A., & McCartney, J.S. (2012b) Coupled thermo-poro-mechanical finite  
 2219 element analysis of a heated single pile centrifuge experiment in saturated silt. *Proc., GeoCongress 2012 (GSP*  
 2220 *225)*, R. D. Hryciw, A. Athanasopoulos-Zekkos, & N. Yesiller, eds., ASCE, Reston, VA. 4406-4415.
- 2221 Wang, W., Regueiro, R. & McCartney, J.S. (2015a) Coupled axisymmetric thermo-poro-elasto-plastic finite  
 2222 element analysis of energy foundation centrifuge experiments in partially saturated silt. *Geotechnical and*  
 2223 *Geological Engineering*. 33 (2), 373-388.
- 2224 Wang, B., Bouazza, A., Singh, R., Haberfield, C., Barry-Macaulay, D. & Baycan, S. (2015b). Posttemperature  
 2225 effects on shaft capacity of a full-scale geothermal energy pile. *J. Geotech. Geoenviron. Eng.* 141 (4): 04014125.  
 2226 [https://doi.org/10.1061/\(ASCE\)GT.1943-5606.0001266](https://doi.org/10.1061/(ASCE)GT.1943-5606.0001266).
- 2227 Wagner, V., Bayer, P., Kübert, M., Blum, P. (2012) Numerical sensitivity study of thermal response tests,  
 2228 *Renewable Energy*, 41(0), pp. 245-253, doi: 10.1016/j.renene. 2011.11.001.
- 2229 Witte, H.J.L., van Gelder, G.J. & Spitler, J.D. (2002) In situ measurement of ground thermal conductivity: a  
 2230 Dutch perspective. *ASHRAE Transactions*, 108 (1), 263 – 272.
- 2231 Wood, C.J., Liu, H. & Riffat, S.B. (2010a) Comparison of a modelled and field tested piled ground heat  
 2232 exchanger system for a residential building and the simulated effect of assisted ground heat recharge. *Intl. J.*  
 2233 *Low Carbon Technologies*, 5(3), 137-143
- 2234 Wood, C.J., Liu, H. & Riffat, S.B. (2010b) An investigation of the heat pump performance and ground  
 2235 temperature of a pile foundation heat exchanger system for a residential building, *Energy*, 35, 3932-4940.
- 2236 Viera A; Alberdi-Paolga M; Christodoulides P; Javed S; Loveridge F; Nguyen F; Cecinato F; Maranha J; Florides  
 2237 G; Prodan I (2017) Characterisation of ground thermal and thermo-mechanical behaviour for shallow  
 2238 geothermal energy applications. *Energies*, **10** (12), 2044.
- 2239 Xia, C., Sun, M., Zhang, G., Xiao, S. & Zou, Y. (2012) Experimental study on geothermal heat exchangers buried  
 2240 in diaphragm walls, *Energy and Buildings*, 5, 50 – 55.
- 2241 Xing, L., Cullin, J. R., Spitler, J. D., Im, P. & Fisher, D. E. (2012) Foundation heat exchangers for residential ground  
 2242 source heat pump systems – numerical modelling and experimental validation, *HVAC&R Research*, 17 (6),  
 2243 1059-1072.
- 2244 Yavari, N., Tang, A. M., Pereira, J.-M. & Hassen, G. (2014a) Experimental study on the mechanical behaviour  
 2245 of a heat exchanger pile using physical modelling. *Acta Geotechnica*. 9 (3), 385-398.
- 2246 Yavari, N., Tang, A. M., Pereira, J.-M. & Hassen, G. (2014b) A simple method for numerical modelling of energy  
 2247 pile's mechanical behaviour. *Géotechnique Letters*. 4, 119–124.
- 2248 Yavuzturk, C., Spitler, J., D. & Rees, S., J. (1999) A Transient Two-Dimensional Finite Volume Model for the  
 2249 Simulation of Vertical U-Tube Ground Heat Exchangers. *ASHRAE Transactions*, 105(2), pp. 465-474.

2250 Yoon, S., Lee, S-R., Xue, J., Zosseder, K., Go, G-H. & Park, H. (2015) Evaluation of the thermal efficiency and a  
2251 cost analysis of different types of ground heat exchangers in energy piles, *Energy Conservation and*  
2252 *Management*, 105, 393-402.

2253 Yu X., Zhang, N., Pradhan, A. & Puppala, A. (2016) Geothermal energy for bridge deck and pavement deicing—  
2254 A brief review. *Geo-Chicago 2016*. ASCE. <https://doi.org/10.1061/9780784480137.057>

2255 Zarrella, A. & De Carli, M. (2013) Heat transfer analysis of short helical borehole heat exchangers, *Applied*  
2256 *Energy*, 102, 1477-1491.

2257 Zarrella, A., De Carli, M. & Galgaro, A. (2013) Thermal performance of two types of energy foundation pile:  
2258 helical pipe and triple U-tube, *Applied Thermal Engineering*, 61, 301-310.

2259 Zeng, H.Y., Diao, N.R. & Fang, Z. (2002) A finite line-source model for boreholes in geothermal heat exchangers.  
2260 *Heat Transfer - Asian Research*, 31(7), 558-567

2261 Zhang, G. Xia, C., Xhao, X. & Zhou, S. (2016a) Effect of ventilation on the thermal performance of tunnel lining  
2262 GHEs, *Applied Thermal Engineering*, 93, 416 - 424.

2263 Zhang, G., Guo, Y., Zhou, Y., Ye, M., Chen, R., Zhang, H., Yang, J., Chen, J., Zhang, M., Lian, Y. & Liu, C. (2016b)  
2264 Experimental study on the thermal performance of tunnel lining GHE under groundwater flow, *Applied*  
2265 *Thermal Engineering*, 106, 784 - 795.

2266 Zhang, G., Liu, S., Zhao, X., Ye, M., Chen, R., Zhang, H., Yang, J. & Chen, J. (2017) The coupling effect of  
2267 ventilation and groundwater flow on the thermal performance of tunnel lining GHEs. *Applied Thermal*  
2268 *Engineering* 112, 595-605.

2269 Zhang, G., Xia, C., Yang, Y., Sun, M. & Zou, Y (2014) Experimental study on the thermal performance of tunnel  
2270 lining ground heat exchangers, *Energy and Buildings*, 77, 149-157.

2271 Zhang, G., Xia, C., Sun, M., Zou, Y. & Xiao, S. (2013) A new model and analytical solution for the heat conduction  
2272 of tunnel lining ground heat exchangers, *Cold Regions Science and Technology*, 88, 59-66.

2273

2274

2275	<b>List of Tables</b>	
2276	Table 1 Main types of G-function for use with piles.....	10
2277	Table 2 Methods for calculating ground heat exchanger steady state thermal resistance.....	11
2278	Table 3 Summary of pile thermal performance tests.....	27
2279	Table 4 Summary of operational pile performance.....	29
2280	Table 5 Summary of pile thermal response tests.....	31
2281	Table 6 Summary of wall thermal performance.....	36
2282	Table 7 Summary of tunnel thermal performance.....	40
2283	Table 8 Summary of laboratory-scale tests on energy piles.....	46
2284	Table 9 Summary of centrifuge-scale tests on energy piles.....	51
2285		
2286		

2287	<b>List of Figures</b>	
2288	Figure 1 Typical arrangement of an energy pile .....	7
2289	Figure 2 Schematic of the classical G-function models: (a) infinite line source (ILS), (b) infinite cylindrical source	
2290	(ICS), (c) finite line source (FLS). $T_{\infty}$ =far field temperature; H=heat exchanger length; h=depth below ground	
2291	surface. Adapted from Bidarmaghz 2015.....	8
2292	Figure 3 Example G-functions showing development of long-term steady state conditions for heat exchangers	
2293	of finite length. Aspect ratio = pile length / pile diameter .....	9
2294	Figure 4 Different G-functions displayed at short time scales. Pile upper and lower bound G-functions after	
2295	Loveridge & Powrie (2013b) .....	9
2296	Figure 5 Example G-functions for different arrangements of boreholes (Bourne-Webb et al. 2016). $t^*$ is the	
2297	ratio of the elapsed time and time to steady state; $r^*$ is the non-dimensional radial coordinate.....	13
2298	Figure 6 Effect of pipe arrangements and temperature difference between fluid and the ground on the heat	
2299	transfer rate obtained from energy walls. (U = single U tube; UU = two U-tubes connected in parallel; W1 or	
2300	W2 = two U-tubes connecting in series; parametric study includes both U and UU arrangements).....	19
2301	Figure 7 Schematic view of a energy tunnel. Absorber pipes are embedded into the tunnel lining (adapted from	
2302	Zhang et el. 2013, reproduced with permission).....	20
2303	Figure 8 Typical layout of absorber pipes in energy tunnels: (a) longitudinal meandering pipe, (b) transverse,	
2304	and (c) slinky (only found in energy textiles to date). .....	22
2305	Figure 9 Unit heat exchange rates from short term performance tests of piles. Data taken from the sources	
2306	listed in Table 3.....	28
2307	Figure 10 Comparison of Thermal Conductivity derived from Laboratory Testing and Thermal Response Testing	
2308	(TRT) on Energy Piles. Laboratory values from the needle probe, using a weighted average where different soil	
2309	units are present. TRT results from line source interpretations, average where there are multiple tests or	
2310	injection and recovery values.....	33
2311		